



TAMPERE UNIVERSITY OF TECHNOLOGY
*International Master's Degree Programme In
Biomedical Engineering*

DHANESH KATTIPPARAMBIL RAJAN

**MASKLESS EXPOSURE DEVICE FOR
PHOTOLITHOGRAPHY**

MASTER OF SCIENCE THESIS

Examiners: Professor Jukka Lekkala, Professor Jari Hyttinen
Subject approved by the Faculty Council on 5th March 2008 by
the Faculty of Science and Environmental Engineering

ABSTRACT

TAMPERE UNIVERSITY OF TECHNOLOGY

International Master's Degree Programme in Biomedical Engineering

KATTIPPARAMBIL RAJAN, DHANESH: Maskless Exposure Device
for Photolithography

Master of Science Thesis, 96 Pages.

May 2008

Major: Medical Physics

Examiners: Professor Jukka Lekkala, Professor Jari Hyttinen

Keywords: lithography, maskless lithography, MEMS production

Photolithography plays a consequential role in transferring patterns from photomasks to substrates and thereby is an important tool in semiconductor, IC, MEMS and many microstructures' production. The photomasks are preprinted prior to the photolithographic procedure with certain layouts, and these layouts are transferred to surfaces of materials like silicon during the lithography and finally these surfaces undergo chemical processes by which three dimensional micro features are formed. Therefore photomasks containing specific layouts are the inevitable components in the entire procedure, but unfortunately those are expensive in its nature together with time consuming production formalities. Some of the successful attempts to remove these difficulties are cost effective photomasks and maskless lithography.

A system named 'Maskless Exposure Device' (MED) is introduced here as my thesis related research and it is intended to replace the expensive photomasks. The device transfers images and layouts created on a computer, easily and effortlessly to different substrate surfaces and can be repeatedly used in photolithography by introducing new drawings on the computer screen and thereby, MED is nothing but a maskless lithographic technique.

The device can be mainly used in research and development applications in MEMS production, microfluidic systems, semiconductor and biosensor designs, patterning of cell culture substrates, electrode structures etc. Research on design of microsensors and microactuators could be confronted extremely cost effectively with maximum time saving considerations.

PREFACE

‘Shoot for the moon. Even if you miss it you will land among the stars.’

Les Brown.

This thesis has been carried out at the Department of Automation Science and Engineering in Tampere University of Technology. I want to gratefully acknowledge the department for providing all facilities and funding to carry out the research for the thesis. I wish to thank the personnel in my home institute - Ragnar Granit Institute - for providing all assistance and support in the development of the thesis.

I wish to express my gratitude to the examiners of the thesis, Professor Jukka Leikkala and Professor Jari Hyttinen. Rendering guidance in complicated situations, Professor Jukka Leikkala has helped me many times in figuring out many practical problems. Also I would like to point out the helping hands of Professor Jouko Halttunen who read and commented on my thesis in a very valuable way.

Also, I express my thanks to Mr. Markus Karjalainen who was a great help in the research for the thesis. Dr. Heikki Jokinen has been helping me a lot and the normal words of gratitude may not be sufficient enough to express my heart, but let me say, I am very lucky to have met him and to have shared the same office with him.

Finally, I would like to thank my parents and my wife Aveline for their help, love and support in my career endeavors and in life.

Tampere, May 2008

Dhanesh Kattipparambil Rajan

Department of Automation Science and Engineering

33720 Tampere

+ 358445373150

FINLAND

CONTENTS

1. INTRODUCTION	8
2. FUNDAMENTALS OF PHOTOLITHOGRAPHY	12
2.1. Wafer and Surface Preparation	12
2.2. Photomask and Exposure.....	13
2.3. The break-down of the costs of photomask manufacturing	14
2.4. A mathematical expression of mask cost and comparison of mask costs for various lithographic methods	15
2.5. Contact, proximity and projection exposure methods and their comparison .	16
2.6. Involvement of Photoresists in Photolithography	18
2.7. Developing and Etching	19
2.8. Post Bake and Processing	21
2.9. List of important subtractive processes	23
2.10.Objective of the thesis work	23
3. MASKLESS PHOTOLITHOGRAPHY	25
3.1. A general outline of Maskless Exposure Device for photolithographic pattern transfer	25
3.2. Maskless Exposure Device experimental set up	26
3.3. Component devices of the Maskless Exposure Device	27
3.3.1. Laptop and layout drawing software.....	27
3.3.2. Projector	28
3.3.3. Trinocular Microscope (TM) - the heart of the device – and its functioning	31
3.3.4. Leaning Screen	34
3.4. Operation and focusing of the Maskless Exposure Device	36
4. PRELIMINARY TESTS USING THE Maskless EXPOSURE DEVICE.....	39
4.1. Processing conditions	39
4.2. Two initial general tests and their details	39
4.3. Bright Field and Dark Field tests	41
4.4. Verification of some test results using profilometer	45
4.5. Pixel size calculations.....	54
4.6. Image intensity compensation.....	54

4.7. Etching of the substrate patterned by the Maskless Exposure Device	57
5. The theory behind the maskless EXPOSURE DEVICE.....	60
5.1. Physics of Optical Lithography.....	60
5.2. Problems faced with the design of the device and their possible solutions. ...	63
5.2.1. Heat and Vibration problems.....	63
6. USE OF POSITIVE PHOTORESIST ma-P 1225 AND OPTIMISATION EXPERIMENTS	65
6.1. Positive Tone Photoresist ma-P 1225.....	65
6.2. Optimisation experiments	67
6.2.1. Brightness or proper shade of blue	67
6.2.2. Exposure time and development time	70
6.2.3. Image size.....	72
6.2.4. Software program and image file saving formats	75
6.2.5. Resolution of the device	76
7. EXPERIMENTS FOR FABRICATION OF A MATRIX ARRAY OF ELECTRODES on gold coated glass plate	83
7.1. Multiple intensity exposure.....	83
7.2. Matrix array of electrodes.....	85
8. Conclusion and Discussion.....	90
9. REFERENCE.....	93

ABBREVIATIONS AND NOTATIONS

<i>A</i>	Exposure dependent absorption (Also called Dill A)
<i>B</i>	Exposure independent absorption (Also called Dill B)
<i>BMP</i>	Bitmap
<i>C</i>	Sensitivity of the photoresist (Also called Dill C)
<i>C₁</i>	Polymer concentration in grams per 100 ml solution
<i>CD</i>	Compact disc
<i>d</i>	Diameter of the focusing lens
<i>DI</i>	Deionised water
<i>DLP</i>	Digital light processing
<i>DOF</i>	Depth of focus
<i>DPL</i>	Dip-pen lithography
<i>EBL</i>	Electron beam lithography
<i>f</i>	Focal length
<i>FIBL</i>	Focused ion beam lithography
<i>g</i>	Gap between lens and screen
<i>GIF</i>	Graphics interchange format
<i>H</i>	Intrinsic viscosity
<i>HF</i>	Hydrogen fluoride
<i>I</i>	Iodine
<i>I_{x,t}</i>	Intensity of exposing radiation
<i>IL</i>	Interference lithography
<i>JPEG</i>	Joint photographic experts group
<i>K</i>	Calibration constant
<i>KI</i>	Potassium iodide
<i>M_{x,t}</i>	Normalised concentration of the inhibitor in photoresist
<i>MAEBL</i>	Multi axis electron beam lithography
<i>MED</i>	Maskless exposure device
<i>MEMS</i>	Micro electromechanical systems
<i>MIT</i>	Institute of measurement and information technology
<i>MOPL</i>	Maskless optical projection lithography
<i>n</i>	Refractive index of the medium
<i>NA</i>	Numerical aperture of the focusing
<i>PNG</i>	Portable network graphics
<i>PR</i>	Photoresist
<i>R & D</i>	Research and development
<i>RIE</i>	Reactive ion etching
<i>Rpm</i>	Rotations per minute

<i>SEBL</i>	Scanning electron beam lithography
<i>SU-8</i>	Name of a commonly used negative photoresist
<i>T</i>	Thickness of photoresist
<i>TIF</i>	Tagged image file format
<i>TM</i>	Trinocular microscope
<i>UV</i>	Ultraviolet light
<i>VLSI</i>	Very large scale integration
<i>VTT</i>	Technical research centre of Finland
<i>W</i>	Size of features on developed image
<i>W_{min}</i>	Minimum feature size
<i>x,y,z</i>	Cartesian coordinates
<i>XeF₂</i>	Xenon fluoride
<i>XGA</i>	Extended graphics array
<i>ZPAL</i>	Zone plate array lithography
<i>α</i>	Optical absorption
<i>α_a</i>	Angle between the edge and optical axis of the system
<i>θ</i>	Angle
<i>λ</i>	Wavelength of light
<i>μ</i>	Symbol for micron measurement
<i>ω</i>	Number of rotations per minute (rpm)

1. INTRODUCTION

Photolithography is an important process in microfabrication and, literally the word ‘photolithography’ means ‘light-stone-writing’ in Greek [1]. It is an optical means by which the patterns on a semiconductor can be defined by using light. Photolithography is the basic tool for creating small scale features of integrated circuits and generally it is a binary pattern transfer technique, as it neither transfers colour or gray scale information nor depth to the image [2].

Photolithographic procedure involves multiple stages with accurately defined processing conditions. The procedure starts with the coating of a photosensitive emulsion on a substrate surface, followed by patterning of the same by ultraviolet light exposure through a photomask [3]. The photomask contains patterns to be printed onto the substrate surface and is an expensive component. Photomasks are produced by industrial companies by using high precision devices. In many practical photolithographic applications, to fabricate certain microstructures, more than one photomask is usually required. The cost of a photomask depends on the nature of the features required on it and the resolution needed. Moreover as the size of features decreases, the requirements for minimum resolution becomes tighter and tighter [4].

Because of complexities and dramatically escalating cost involved in photomask manufacturing, alternative maskless photolithographic techniques become more attractive since those could lead to cost-effective small-scale manufacturing with various flexibilities [5]. The world wide efforts and researches for maskless lithographic techniques are basically in two directions, as one for charged particle maskless (CP-ML2) methods and another for optical maskless (O-ML2) methods [6].

Many successful methods like Zone Plate Array Lithography (ZPAL), Dip-Pen Lithography (DPL), Multiaxis Electron Beam Lithography (MAEBL), Scanning Electron Beam Lithography (SEBL), Focused Ion Beam Lithography (FIBL), Interference Lithography (IL), Maskless Optical Projection Lithography (MOPL) etc. can be seen in the scientific world of maskless lithography, but most of them require expensive instrumentation and highly controlled experimental environments [7].

Some other techniques utilising comparatively less expensive instrumentation are also seen in the direction of maskless lithography. Most of the optical maskless concepts are based on the idea that the illuminating light beam with image information is reflected

from a Spatial Light Modulator (SLM) like a Liquid Crystal Display (LCD) or a Digital Micromirror Device (DMD). Some existing examples are mentioned below [8].

A system named Optofluidic Maskless Lithography (OFML) operates in order to replace the photomasks by a MEMS spatial light modulator and therefore, the mask images are dynamically configured by a two-dimensional array of micromirrors. In this technique, various microstructures can be fabricated in microfluidic channels by photo patterning of liquid-phase photo curable polymer materials by making use of ultra violet light reflected from the micromirrors [9].

A Projection Micro-Stereolithography (P μ SL) system also works on software mask which can be dynamically drawn using CAD software. The P μ SL makes use of focused ultra violet light spot scanning over the photo curable resin surface and then, a light-induced photo-polymerisation for constructing solid microstructures [10].

The SF-100-Intelligent Micro Patterning LLC maskless printing technology utilises reflective microoptoelectromechanical (MOEM) elements instead of photomasks and spatially modulates parallel planar light to write patterns directly on a surface [11]. The MOEM and mixing and imaging lenses in the system function together to project direct custom circuit patterns designed in any windows based program onto a substrate surface [12].

One important dynamic mask machine system in this context is the Alpha Micro-Rapid Prototyping system. The image projected by a DMD chip in this system is directed to a Pins Array Mask (PAM) via a relay lens and a telecentric lens. The length and width of each exit pupil in the PAM is half the size of the original pixel in the DMD chip. By matching each magnified pixel with each micro exit pupil in PAM, the pixels can be scattered by it, and the image projected by PAM can be finally projected onto a resin surface through zoom lens [13].

Certain experimental results have illustrated the great potentials of femtosecond lasers for future applications in maskless nonlinear super-resolution lithography. In lithography using laser beams, there are two possibilities. First, exposure of the desired pattern in a layer of photoresist and afterwards, develop it. Second, skip the developing procedure and use femtosecond laser pulses for direct photoresist ablation (or disintegration). Even if some good results are available on the basis of the said two possibilities more studies are required in these directions for practical implementations [14].

Liquid Crystal Display Projectors (LCDP) have also been utilised in the experiments for maskless photolithography. A maskless system with a modified LCD projector and exchangeable objective lenses is in use at the Institute of Advanced Biomedical

Engineering and Science, Tokyo. Even though, patterns produced by a personal computer can be projected to a surface via reduction lenses, the exposure in this system is limited to images of 800x600 pixels only with a fixed resolution [15].

In certain cases, very simple and cost effective maskless systems are made possible by making use of commercially available low cost devices. For instance, the projected image from a DMD chip of a commercial projector can be modified by a stereomicroscope in such a way that the diminished image could be used for exposures on a photoresist [16]. This idea has given motivation for designing a maskless lithographic system out of low cost devices and that is the basis of this thesis.

Consequently a very simple and cost effective optical photolithographic device named 'Maskless Exposure device' (MED) using visible light is presented in my thesis. The device transfers images and layouts created on a computer, easily and effortlessly to different substrate surfaces. A Digital Light Processing (DLP) projector is the main component device of the MED. A projector, a laptop computer, a stereomicroscope and a substrate carrying screen function together to act as the MED.

The device can be mainly used in research and developmental applications in MEMS production, microfluidic systems, semiconductor and biosensor designs, patterning of cell culture substrates, electrode structures etc. Research on design of microsensors and microactuators could be confronted extremely cost effectively with maximum time saving considerations. In many academic and industrial research activities, different types of microstructures and microelectrode configurations like microchannels, microelectrode array's (MEA's) etc. may be required and those can be either purchased from companies or fabricated in special cleanroom attached laboratories. Direct purchasing of one or two samples for experimental research may be highly expensive and also the samples may not be readily available with the immediate research specifications and requirements. This situation forces the researcher to fabricate the desired microstructure in cleanrooms using the conventional photolithographic instruments. This is not a complicated task in usual experimental situations, but each fabrication may require a specially designed expensive photomask. A photomask used for a certain microstructure is usually not suitable for another one and this changes the simplicity and cost effective priorities of the context. Therefore in a basic research where microstructures are widely required, it is not an easy task to buy different photomasks for the fabrication of different structures. The solution to these problems is a readily available cost effective device that can be repeatedly used for the fast prototyping of microstructures. The Maskless Exposure Device is an effective tool in this circumstance as it transfers patterns from a computer screen onto microscopic areas. Interestingly, MED doesn't require any mask but the drawing software, together with the computer screen plays the role of a mechanical mask. This brings about unbelievable flexibility in layout drawing and surprising speed in prototyping of

microstructures. In short, the MED is surely a good tool in microscale research since, any such research requires a large number of microstructures and many of them would be materialised by the MED.

The Finnish Academy project named Stemfunc under the Department of Biomedical Engineering plans a number of experiments on stemcell research and hence, different types of microelectrode array's are required. Our 'Sensor Technology' research group is therefore collaborating with them and participating in the Stemfunc project in designing and fabricating MEA's and, the Maskless Exposure Device has a wide range of applications in this context.

Analysis of the final working conditions of the device primarily considers the patterns imprinted on silicon and gold plated glass surfaces, scientific evaluation of the properties of the created patterns and the optimisation conditions of the various parameters of the device.

2. FUNDAMENTALS OF PHOTOLITHOGRAPHY

Photolithography is a kind of imprinting by which circuit drawings, geometrical figures, layouts etc. are transferred on to a wafer surface and is normally carried out in a specially designed and dust controlled room named cleanroom. This is a multistage process and each stage requires keen attention for fabricating a defect free microstructure.

2.1. Wafer and Surface Preparation

The entire process starts with the proper selection of a substrate material and preparation of its surface. Different types of contaminants like solvent residues, water residues (moisture), vacuum grease, oil, old photoresist or developer solution residues from previous photolithography, bacteria, common dusts, dandruff, micro fibres etc. might be residing on the surface. Depending on the situation, a variety of surface preparation techniques like ultrasonic agitation with acetone or methanol or deionised water, acetone-isopropanol cleaning, nitrogen gun, oxygen plasma-organic residue removal etc. can be used. The surface cleaning is followed by coating of a visible or UV light sensitive thin layer of an organic polymer (photoresist). Even though several methods like spray coating, lamination and spin coating are available, the spin coating method is widely used. In the spin coating method, the positive or negative photoresist is dispensed onto the surface of the wafer placed on a Resist Spinner machine by means of neat ink filler. The wafer is fixed in place on the resist spinner by a vacuum chuck and then is spun at a high angular velocity. The spin coating settings can be seen in the figure 1.

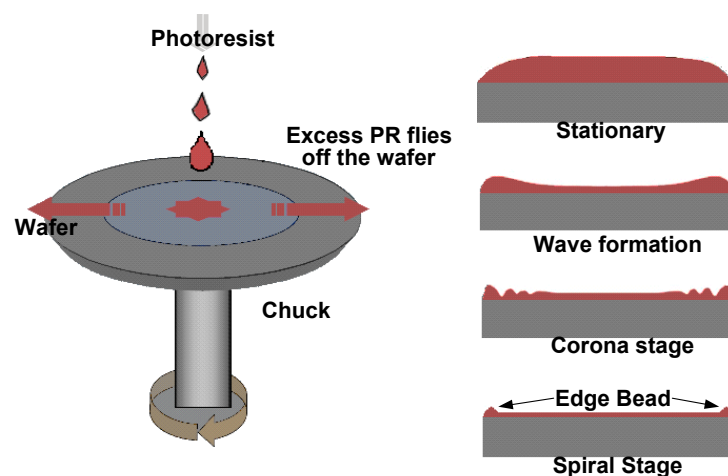


Figure 1. Spin coating arrangement and different stages of thin film formations during spinning.

The spinning velocity depends on the required thickness and the viscosity of the photoresist. The rotation causes centrifugal forces and brings the solution to the edges where it starts to build up until expelled out of the wafer when the surface tension is exceeded. The thickness of the photoresist is thus a function of spin velocity, molecular weight (measured by intrinsic viscosity) and concentration. The empirical relation for the thickness T of the photoresist is given by [17]

$$T = \frac{KC_l^\beta \eta^\gamma}{\omega^\alpha} \quad (1)$$

where K is the calibration constant, C_l the polymer concentration in grams per 100 ml solution, η the intrinsic viscosity, and ω the number of rotations per minute (rpm). When the exponential factors α , β and γ are determined, the equation can be exclusively applied in practical situations. In practice the value of ω ranges from 3000 – 6000 rpm for 15 - 60 seconds and T falls in the 1-2 μm range. It is obvious from the above equation that the thickness of the photoresist decreases with the increase of angular velocity of the spinning machine.

The thickness of edge bead is 20 – 30 times the thickness of the photoresist. In practice large wafers increases and sharp edges decreases the edge bead thickness.

The spin coated polymer is fixed completely to the surface by a prebaking process. A hot plate (90 – 120 °C, 1-2 minutes) or convection oven (90 – 120 °C , 20 minutes) is used with specific predetermined temperature and time according to the nature and solute-solvent proportion of the photoresist polymer. Generally hot plates are widely used as those are more controllable, faster than the convectional oven and do not trap any solvent. The prebaking improves etch resistance, uniformity, adhesion and line width control. The quality of photoresist adhesion depends on resist chemistry, wetting characteristics of resist, moisture, surface contamination, surface smoothness, stress from spin coating and delay in exposure and prebake. However, certain chemicals named photoresist primers like HMDS vapour prime can be used to improve the resist adhesion. A proper prebaking helps to optimise the light absorption characteristics of the photoresist.

2.2. Photomask and Exposure

The stencil intended to generate patterns over photoresist coated wafer is called a photomask. The photomasks can be classified as a light field mask or a dark field mask and are generally produced either by Projection printing or Electron Beam Lithography. However, simple research and development (R & D) masks for less complicated features can be created on a transparency by a good quality paper printer. Some general features of important commercial masks are tabulated in the table 1.

Table 1. General features of common commercial masks.

Model	Features
Cr on Quartz glass	Expensive and for Deep UV
Cr on Soda Lime glass	Most common
Photographic emulsion on soda lime glass	Less expensive
Fe ₂ O ₃ on soda lime glass	Semi transparent to visible light
High resolution laser printing on transparency	Less expensive

After the photomask is aligned properly in the x, y and θ parameters with the wafer, the wafer is exposed to UV through the mask. The near (350 – 500 nm) and deep UV (150-300 nm) areas from the electromagnetic spectrum are used normally in exposure.

2.3. The break-down of the costs of photomask manufacturing

The entire photolithographic procedure may last for many hours until the required structure and features are obtained on the substrate surfaces. Out of all the required materials for a lithographic procedure, the photomask is the most important one. A photomask is a transparent film or plate usually made of quartz, onto which opaque regions are created by geometrical features usually drawn by chrome metal [18]. The masks are fabricated by commercial mask producers by means of a process called Electron Beam Lithography (EBL) which does not require a mask. The photomasks are extremely expensive since, as the accuracy and fineness of masks increases the cost also increases. The break-down of the costs of photomask manufacturing can be understood from the figure 2 [19].

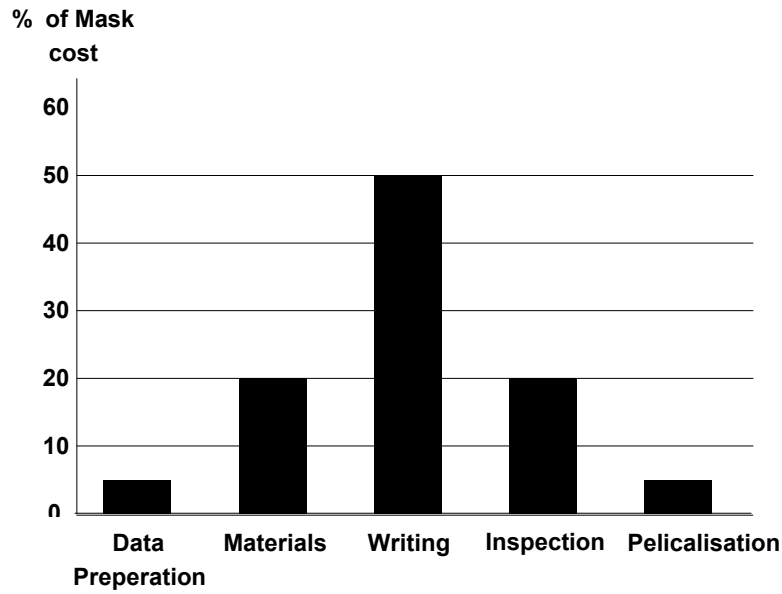


Figure 2. The break-down of costs of photomask manufacturing.

The market for defect free flat quartz and fine chrome, which are the main materials for mask manufacturing are highly demanding and they contribute to 20% of the total mask cost. The mask pattern generator contributes to nearly 50% of the total cost and this is the largest contribution. This depends on the type of the mask pattern generator, the beam used (e- beam or laser), delivery mechanism and the type of the scan (raster scan or vector scan). Nearly 20% comes from the inspection and repair steps in the manufacturing. Even if high speed inspection tools have emerged they have not yet been properly utilised and incorporated in mask production. The repair cost depends on the tools (focused ion beam, micro-mechanical, laser) used in repairing techniques, in manufacturing and the duration of usage of the tools. The remaining 10 % of the cost is contributed by the data preparation stage and the nature and quality and cost of pellicle [20].

2.4. A mathematical expression of mask cost and comparison of mask costs for various lithographic methods

The mask cost (CM) can be roughly calculated by the formula, [21]

$$CM = \frac{\text{Material Cost} + \text{Mask Production Cost}}{\text{Mask Yield}} \quad (2)$$

The raw material and pelicle costs are included in the material cost. The cost increases in proportion to the time of exposure of electron beam and thus, the cost per hour during one generation is in proportion to the cost of equipment. Mask yield is evaluated by making use of the technical values of the masking material. A comparison of general mask costs as per the mentioned formula is given in the figure 3 [22].

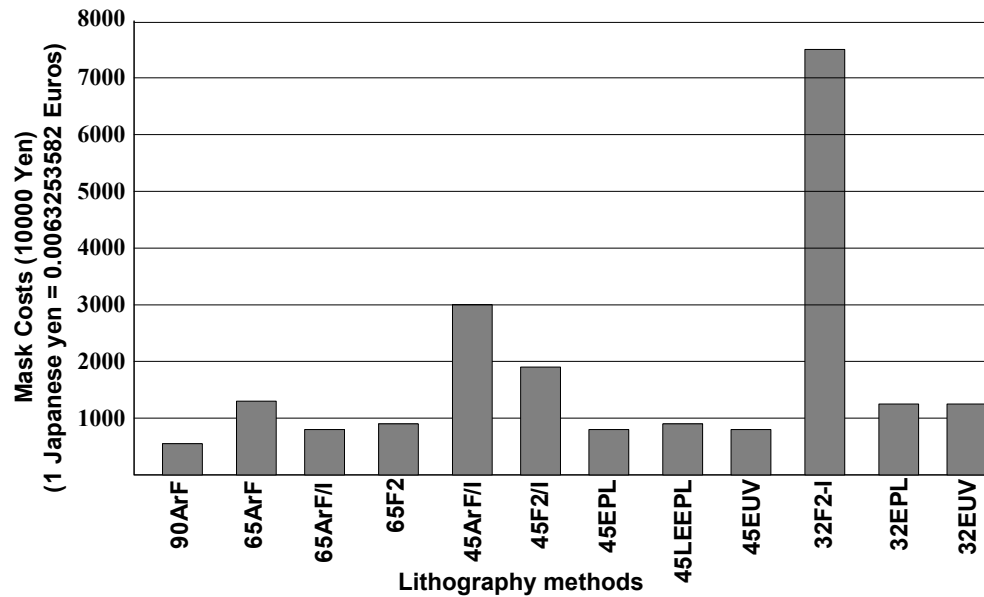


Figure 3. Comparison of general mask costs of important commercial masks.

However the costs of masks are being supposed to be decreased 15 % every year by the improvements in the processes and tool developments.

2.5. Contact, proximity and projection exposure methods and their comparison

In practice, there are contact, proximity and projection exposure methods for photolithographic exposure. Those are presented in the figure 4.

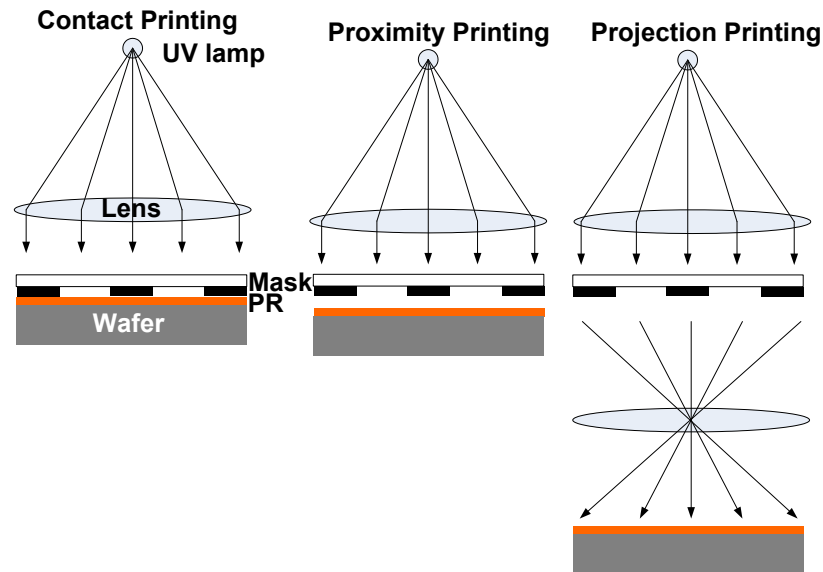


Figure 4. Contact, proximity and projection printing arrangements in photolithography.

A comparative study of nature and general characteristics of contact, proximity and projection printing method are given in the table 2.

Table 2. Comparison of nature and characteristics of contact, proximity and projection exposure methods.

Contact Method	Proximity Method (Shadow printing) (10 μm to 20 μm gap between mask and wafer)	Projection Method
Good resolution (0.1 - 1 μm)	Diffraction and corresponding poor image and resolution (2-4 μm)	Good resolution (0.1 - 1 μm)
Chances for contamination	Reduced contamination	Extremely limited contamination
Mask degradation and short mask life time	No degradation and long mask life time	Image reduction possibility by lens system
Standard Mask aligners	Standard Mask aligners	Mask production is less challenging
Unsuitable for VLSI manufacturing		Expensive
(but widely used in research and development purposes and sensor prototyping)		Slow
		Pattern generators.

2.6. Involvement of Photoresists in Photolithography

The interaction of photons with chemical bondings in photoresists results in bond breaking in positive photoresists (positive tone) or induces cross linking (photopolymerisation) in negative photoresists (negative tone). A photoresist consists of three main chemical components namely a polymer (base resin), a casting solvent and a sensitizer. When a photoresist is exposed to light, the polymer changes its structure and the reactions are controlled by the sensitizer. The casting solvent helps the spreading by spinning properties and formation of thin layers over substrates. During the exposure a photochemical reaction in positive photoresists weakens the polymer by rupture or scission of the main and side polymer chains and thus the exposed areas becomes more soluble (nearly ten times more soluble than that of the unexposed areas). But in a negative photoresist the photochemical reaction strengthens the polymer by inducing random cross linkage of the main chain or pendant side chains and thus the exposed areas becomes less soluble. The reason of the increased insolubility of negative resists is the increase in molecular weight by means of free radical cross linking or acid-catalysed cross linking polymer reactions. The optical absorption α in the photoresist is mathematically expressed by [23]

$$\alpha = A * M_{x,t} + B, \quad (3)$$

where $M_{x,t}$ is the fraction (used in normalised concentration) of the inhibitor after the exposure at a particular position at a particular time. A is exposure dependent and B is exposure independent absorptions and collectively known as Dill parameters [23]

The decrease in inhibitor concentration depends on intensity of exposing radiation and sensitivity of the resist to the radiation as follows [24]

$$\frac{\partial M}{\partial t} = -I_{x,t} * M_{x,t} * C \quad (4)$$

where $I_{x,t}$ is the intensity and C is the sensitivity and also called Dill C . The dill parameters A , B and C are wavelength dependent quantities. To reduce mathematical difficulties simulation method is extensively preferred to analytical solutions for resist exposures.

A comparison of some important properties of positive and negative resists can be seen in the table 3.

Table 3. Important properties of positive and negative photoresists [25].

Characteristic	Positive Resist	Negative Resist
Adhesion to Si	Fair	Excellent
Available compositions	Many	Vast
Cost	More expensive	Less expensive
Developer	Aqueous based (ecologically sound)	Organic solvent (less ecological)
Photospeed	Slower	Faster
Image width to thickness	1 : 1	3 : 1
Plasma etch resistance	Very good	Not very good
Sensitiser quantum yield Φ	0.2 – 0.3	0.5 – 1
Swelling in developer	No	Yes
Minimum feature size	0.5 μm	$\pm 2 \mu\text{m}$
Thermal stability	Good	Fair
Wet chemical resistance	Fair	Excellent

Commercially, negative photoresists have widespread market compared to positive resists due to its low cost and high sensitivity.

2.7. Developing and Etching

After the exposure of the photoresist to the radiation, the photoresist structure is modified at the exposed and unexposed areas differently. A chemical dual classification is formed and a selective removal of exposed or unexposed photoresist is possible by

making use of certain solutions named photoresist developers. Each photoresist has its own developer solution. The developing process in negative and positive resists is illustrated in the figure 5.

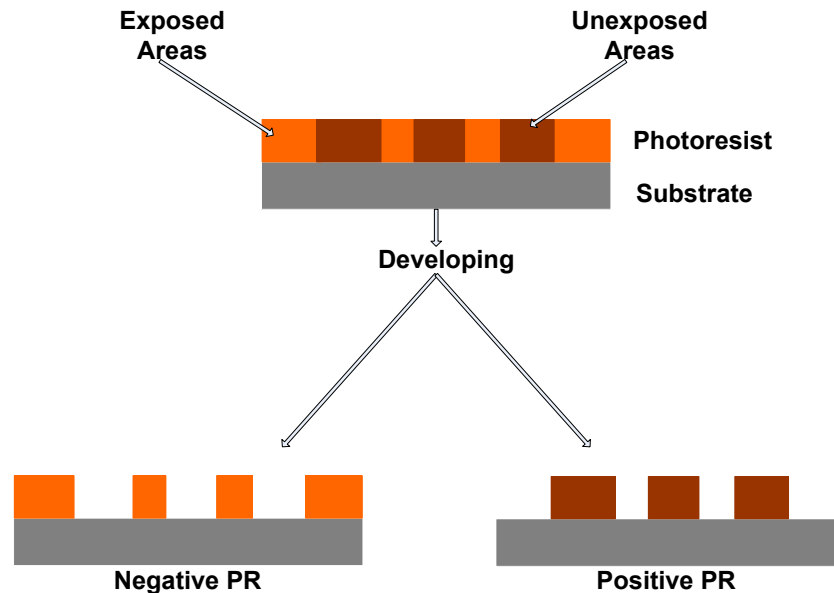


Figure 5. The action of developing solution in negative and positive photoresists.

During development, the exposed areas in a negative resist become polymerised and insoluble in the developer and remain on the substrate, while the unexposed areas will be selectively removed then. The opposite of this happens in a positive resist i.e. the exposure weakens the polymer chains in the positive resists and thereby the exposed areas are dissolved in the developer. The development thus transfers the patterns on a photomask to the substrate indeed! There are wet and dry development processes and the wet developing process have wide acceptance in circuit and micro machine manufacture. The wet developing may be an immersion process (cassette loaded wafers are batch immersed in a bath of developer solution) or a spraying process (directing fresh developing solution to the wafer surface by means of fan type sprayers). The temperature and development times are extremely important in all developing process for obtaining a highly accurate structure on the wafer surface as per expectations.

2.8. Post Bake and Processing

After the photoresist development, the desired pattern or layout is formed on the substrate surface. This is a two dimensional figure indeed and a three dimensional structure is required to convert the substrate into a functional micromechanical or microelectromechanical system. The process of removal of different areas of a substrate after the photoresist developing is termed as etching. The etching can be advanced either isotropically or anisotropically. If the etch rates are constant in all crystal directions, the mechanism is referred to as isotropic etching while if the rates are different in different crystal directions the mechanism is referred to as anisotropic etching. Figure 6 shows the etching patterns in anisotropic and isotropic etching [26].

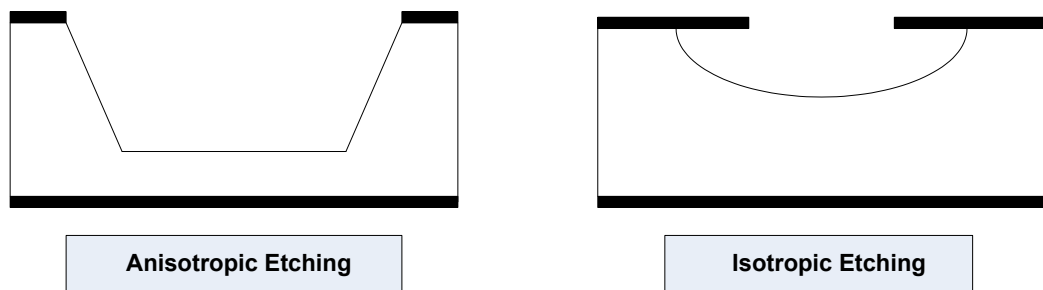


Figure 6. Formation of structures in anisotropic and isotropic etching.

Generally, etching can be performed by using chemically active liquids (wet etching), chemically active gases (dry etching) and certain ion beams (ion etching).

In wet etching the substrate material is dissolved when it is immersed in a chemical solution and a suitable mask is required for selective etching. The masking material either should not dissolve or should show slow etching in contrast to the substrate to be etched in the etching solution. The process is illustrated in the figure 7 [27].

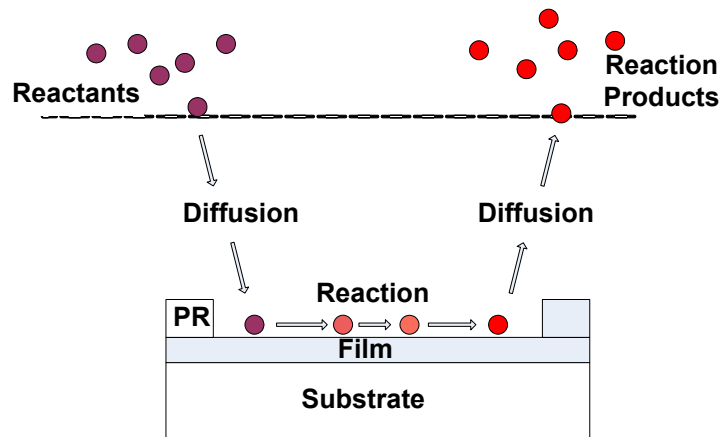


Figure 7. Selective etching of substrate material from unwanted areas.

The reactants from etching liquid diffuses to the substrate surface, initiate reactions, produce products and finally the products diffuse from the substrate surface to the etching liquid. The etching rate and needed etched feature depends on the type of substrate, specific masking material, chemistry of etchant, temperature and proper stirring throughout etching.

Even if the wet etching is less expensive, it provides straight vertical cuts only at certain wafer cuts in anisotropic etching and creates undercuts in isotropic etching. In order to get almost straight vertical cuts, a dry etching mechanism can be applied.

Dry etching can be usually classified as vapour phase etching, plasma assisted etching, Reactive Ion Etching (RIE), and sputter etching. In vapour phase etching the substrate to be etched is placed in a closed chamber containing the etchant molecules in gaseous form. The etchant molecules interact with the substrate surface and gaseous products are formed. Silicon dioxide etching using hydrogen fluoride (HF) and silicon etching using xenon fluoride (XeF_2) are the two most widely used etching techniques. In plasma assisted etching, RIE and sputter etching, special chambers containing specific gaseous molecules and plasma or ion producing techniques are used. The produced ions are then used to etch the substrate in different ways. Compared to wet etching, dry etching mechanisms are complex and the equipment's are expensive.

The mentioned etching techniques are generally acceptable classifications, however, different etching processes are emerging due to various technological advancements.

2.9. List of important subtractive processes

A practically useful list of important subtractive processes is presented in the table 4.

Table 4. List of important subtractive processes [28].

Subtractive Technique	Used for (Applications)	Remarks
Wet chemical etching	Si spheres, domes, grooves, Si angled mesas, nozzles, diaphragms, cantilevers, bridges	Iso: Little control, simple Anis: With etch- stop more control, simple
Electrochemical etching	Etches p-Si and stops at n-Si (in n-p junction), etches n-Si of highest doping (in n/n ⁺)	Complex, requires electrodes
Wet photo etching	Etches p-type layers in p-n junctions	No electrodes required
Photo electrochemical etching	Etches n-Si in p-n junctions, production of porous Si	Complex, requires electrodes and light
Dry chemical etching	Resist stripping, isotropic features	Resolution better than 0.1 μm , loading effects
Physical /chemical etching	Very precise pattern transfer	Most important of the dry etching techniques
Physical dry etching, Sputter etching, and ion milling	Si surface cleaning, unselective thin film removal	Unselective and slow, plasma damage
Focused ion- beam (FIB) milling	Microholes, circuit repairs, microstructures in arbitrary materials	Long fabrication time: >2h including set-up
Laser machining (with and without reactive gases)	Circuit repair, resistor trimming, hole drilling, labeling of Si wafers	Laser beams can focus to a 1 μm spot.
Ultrasonic drilling	Holes in quartz, silicon nitride bearing race rings	Especially useful for hard, brittle materials
Electrostatic discharge machining (EDM)	Drilling holes and channels in hard brittle metals.	Pore resolution (> 15 μm), only conductors, simple, wire discharge machining resolution much better.
Mechanical turning, drilling and milling, grinding, honing, lapping, polishing and sawing	Almost all machined objects surrounding us	Prevalent machining technique

2.10. Objective of the thesis work

Photolithography plays an important role in transferring patterns from a mask to a substrate and thereby becomes the basic tool in semiconductor, IC, many microstructures and MEMS production. The technology, energy source manipulation and processing speed have developed rapidly and day by day the photolithography

becomes better and better at resolving extremely small features. However the general procedural photolithographic steps,

1. Wafer cleaning
2. Photoresist deposition on substrate containing an oxide layer
by spin coating
3. Prebaking
4. Exposure to radiation through a photomask
5. Developing the resist
6. Postbaking
7. Removal of the resist
8. Etching the substrate through resist openings etc

remain the same and this thesis work specifically concentrates on the fourth step – ‘Exposure to radiation’ and trying to replace the expensive mask involved UV exposure method by a simple DLP projector involved maskless pattern transfer technique. Therefore all other steps excluding step four are used in the entire lithographic procedures and experiments which are going to be described in the following sections.

3. MASKLESS PHOTOLITHOGRAPHY

We have already seen that one of the important steps in photolithography is the use of specially constructed photomasks which are highly expensive. The expensive photomasks can be replaced by the Maskless Exposure Device (MED) and the details of the MED are discussed below.

3.1. A general outline of Maskless Exposure Device for photolithographic pattern transfer

The Maskless Exposure Device consists of a laptop computer, DLP projector, trinocular microscope, and a specially aligned screen. The schematic of the device is presented in the figure 8.

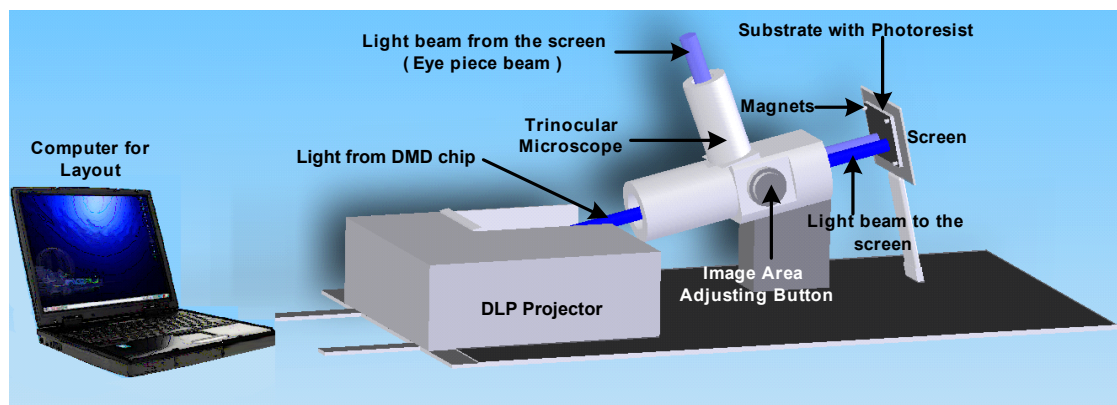


Figure 8. Maskless Exposure Device and its component devices.

The laptop used in this set up is of Dell Latitude C 800 with a selectively fixed screen resolution of 1024 x 768 pixels. The laptop is connected to the Viewsonic PJ458D DLP projector. The resolution of the projector is also 1024 x 768 (XGA display standard of IBM). Inside the projector the light from the 200 W user replaceable lamp is focused to a 1.4 cm (diagonally) DLP chip of Texas Instruments. The chip has physical dimensions of 1.1 cm x 0.8 cm. In normal use of the projector, the image of the same size from the chip is magnified by the optics and big images are obtained on distant screens. But in

our device, because extremely small images are required to be produced at small distances from the DLP chip, the Viewsonic optics was totally removed. This space was then occupied by the camera port of the trinocular microscope. The microscope used was the Stemi 2000 C with 0.63x objective and 16x eyepiece lens combinations.

The rays after entering through the camera port come through one of the objective lenses of the microscope to the specially aligned screen where the substrate with photoresist film is fixed. The light coming out of the microscope thus consists of features of images or figures drawn on the laptop screen and, when this substrate is exposed to this light, the same features will be imprinted to the photoresist chemically. However, the light rays should fall on substrate without any blurring or edge modifications and this can be ensured by the eye piece of the trinocular microscope. The second objective of the microscope brings the formed image from the substrate surface to the eye piece lens and therefore by looking through the eye piece and adjusting the image screen distance from the DLP chip, maximum focused image with minimum aberrations can be ensured. During exposure, the formed image can be clearly seen on the substrate surface.

The circuit diagrams, microelectrode structures, micromechanical structures etc. can be thus drawn on the laptop screen using different programmes like Microsoft paint, Paint.NET, Microsoft Visio etc. and those can be easily transferred to the substrate surface without using any expensive photomasks. Thus the device entirely replaces the photomasks at least in academic situations and therefore a teacher or student can easily transfer micro images to a substrate and test it for research and development purposes. Moreover the device is expected to be one that can be utilised in fabricating microsensors in academic research.

3.2. Maskless Exposure Device experimental set up

All the experiments were carried out in the cleanroom of the Department of Automation Science and Engineering located in the room Se209A. This 22 m² clean room with ESD floor was constructed by Luwa-Zellweger with UV-protected windows and yellow working lights. However throughout the experiments no temperature or humidity control options were possible.

The thin film coating apparatus Laurell WS-400A-6NPP/LITE spinner used is a programmable spinner operating in between 100 – 6000 rpm. A manual dispensing of photoresist was carried out in entire lithographic procedures.

VWR 815-HPS stirrer/hotplate (Max 400°C) was used for photoresist baking and mixing chemical solutions (magnetic stirring). The developed photoresist was always

washed by deionised water produced by Millipore Direct-Q 3 water purification system. The apparatus was able to provide 0.6 l/min with resistivity of 182 kΩm.

The images on the substrate after development of the photoresist were examined through the stereo inspection Zeiss Axio Imager A1m microscope. The microscope has maximum 500x magnification with dark or bright field characterisation properties. The DIC (Nomarsk) prism for “3D” imaging and camera adapter port for fixing external camera etc. in the microscope were extremely helpful in analysing the results.

The Optical Profilometer Wyko NT1100 located in Optoelectronic Research Centre of TUT was also used in some contexts for 3D surface measurements of the etched photoresist and characterisation of results.

The substrate used was <100> n-type silicon and both of the sides of the wafer could be used in experiments as those are commercially available with silicon dioxide coating on both sides. Acetone followed by isopropanol chemical cleaning was performed before all photoresist coating. An adhesion promoter (primer) hexamethyldisilazane (HMDS) for resists was always applied in small quantities to the substrate for getting extreme resist adhesions to the oxide layers.

3.3. Component devices of the Maskless Exposure Device

3.3.1. Laptop and layout drawing software.

Laptop is the vital part in the Maskless Exposure Device (MED). In a mask-oriented photolithography, the pattern to be imprinted onto a substrate is drawn first on a photomask and that mask is used in further lithographic procedures. The purpose of a laptop in the MED is to function as a temporary, repeatable and user friendly software mask. Different diagrams and layouts can be drawn on the laptop screen using a variety of softwares. After drawing a feature in a particular programme say for e.g. in MS Paint, there are two options to send the drawn image to the projector. First, one is showing the direct image from MS Paint programme to the MED screen and second one is setting the drawn image as a background image of the laptop and displaying the same fixed background on the ES screen. From various experiments the latter one seemed to be the best method for obtaining nice results with extremely limited drawbacks. However, before setting a drawn image as a desktop background the user is always requested to save the image first in a particular image saving format. Even if different saving formats like JPEG, PNG, BMP, GIF, TIF etc. are available, a suitable one without minimum image compression or processing can be selected. Moreover in order to avoid unnecessary complications, the screen resolution of the laptop in the tab of the computer

display settings should be set to 1024 x 768 pixels as to match that with the DLP projector display resolution.

3.3.2. Projector

The projector optics is totally modified by removing the complete lens system and therefore the DLP mirror chip becomes visible from the outside front area of the projector. The projector is accurately fixed and locked on the MED platform and no projector adjustments are expected in x and y directions after locking. See figure 9 for projector platform and its locking position.

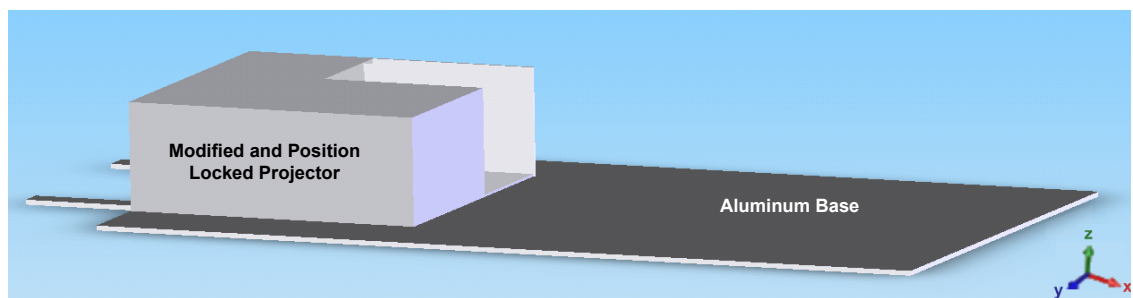


Figure 9. Locked projector and aluminium MED platform.

However 0 to less than 4 cm height adjustments (z variations) at the front and back sides of the projector are possible and this helps the user to adjust the image properties manually to obtain a comparatively accurate image on the MED screen. A metal cover is used at the opened area of the projector to block out the unnecessary light and heat rays coming out of the projector to the operator's body.

The viewsonic projector in our device is a Digital Light Processing (DLP) projector. The DLP technology developed by Dr. Larry Hornbeck of Texas Instruments is based on an optical semiconductor technology named Digital Micromirror Device (DMD). The DMD chip has got the name digital micromirror device due to the fact that all of its pixels are formed by microscopically small semiconductor based mirrors. The image of such a micromirror is given in the figure 10.

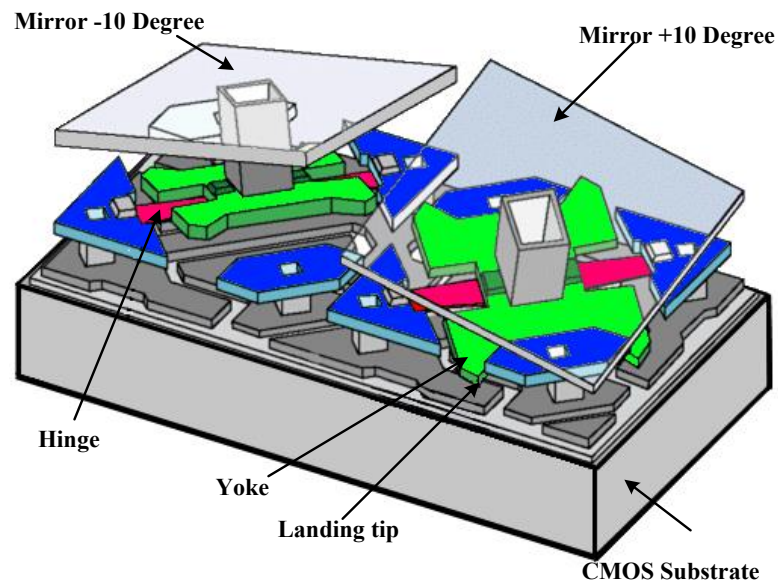


Figure 10. The micromirror used in a DMD chip and its important parts. The mirror tilting is in between -10^0 and $+10^0$ and is fully controlled by the activation of electrodes beneath the mirror [29].

The surface of the chip in our projector thus has a rectangular array of a total of 786432 micromirrors and all these micromirrors can be individually addressed and tilted. Each micromirror acts like a light switch and can be controlled by a digital signal.

In combination with a light source and a projection lens, these micromirrors can produce high quality graphics and videos in proportion to the input signal. Thus this set up processes light pulses digitally and hence the name digital light processing.

The tiny electrode beneath each micromirror is activated by a digital or graphical input signal and this activation causes the micromirror to tilt either towards or away from the light source. The tilting towards the light source reflects a single white pixel towards the projection lens and then onto the screen (digitally ON condition). But the tilting away from the light source doesn't reflect any light (digitally OFF condition) and that corresponds to a dark pixel space.[30]

The DMD mirrors are extremely small and it can be switched on and off thousands of times per second. Depending on the 'on' and 'off' reflection timings, different shades of gray are produced. If one mirror is switched on more than off, it reflects a light gray

pixel but when it is switched off more than on, it reflects a dark gray pixel. This mechanism allows the DMD mirrors to reflect up to 1024 shades of gray and this can impart a highly detailed gray scale image.

The last step in digital light processing is the addition of colour to monochrome images. In most DLP systems this is obtained by the placement of a spinning colour wheel in between the light source and the DMD mirror panel. The set up is given in the figure 11. When the colour wheel spins, it causes the primary colours red, green and blue to fall on the DMD mirror. For instance to produce the colour ‘purple’, the micromirror is allowed to tilt towards the light source only when the blue and red colours are falling on it. Human eye combines these colours and provides the feeling of the colour purple. Thus when the flashes of the coloured lights are coordinated properly with on and off timings of each mirror, the entire DLP system can produce more than 16 million different colours.

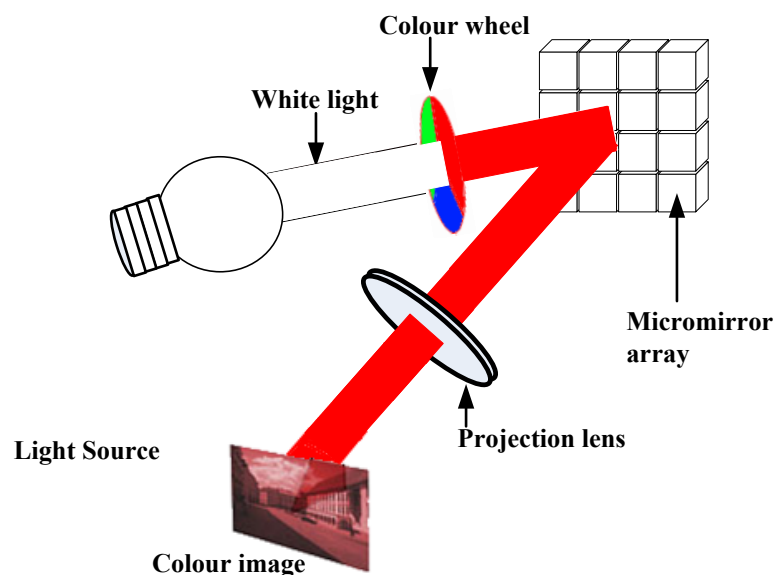


Figure 11. Digital Light Processing set up. The monochrome is changed to colour image by a spinning colour wheel introduced in between the light source and micromirror array [31].

Different techniques like adding more colours to colour wheels, placing more colour wheels in between the DMD chip and light source, installation of more DMD chips etc are being widely utilised in high quality projection strategies and very big projection

situations like a movie theatre. However normal DLP projectors and DLP televisions use a single DMD system with a light source, colour wheel and a projection lens as discussed above.

3.3.3. Trinocular Microscope (TM) - the heart of the device – and its functioning

The schematic of the Trinocular Microscope is presented in the figure 12.

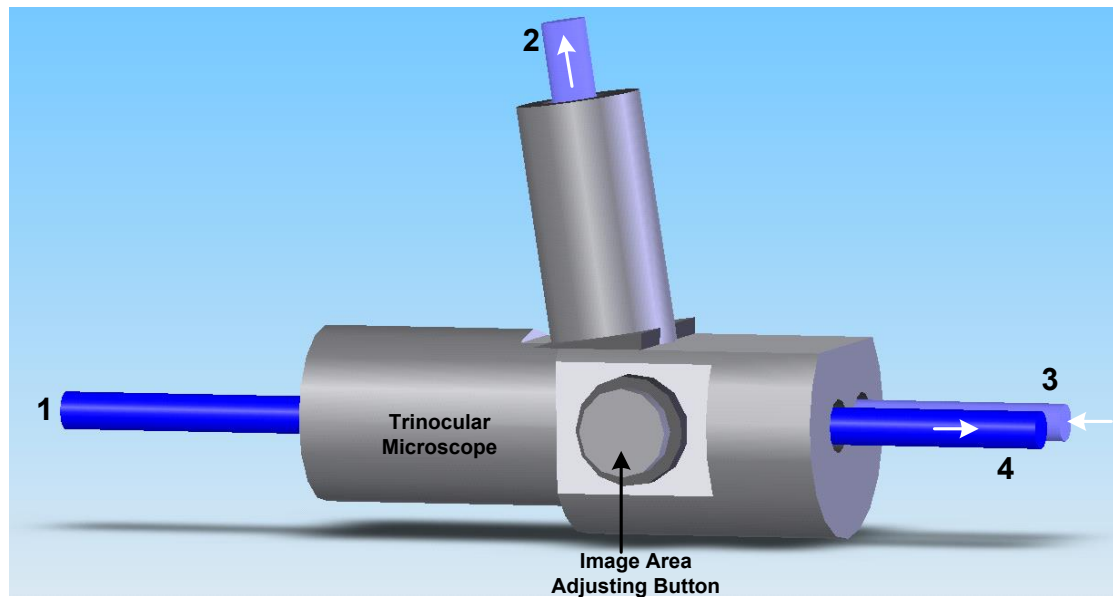


Figure 12. Trinocular Microscope and light channels through it.

In the figure 12, the ports 3 and 4 are objective lens areas, the port 2 is the eye piece area and the port 1 the camera port. However, in the MED, the port 1 is facing the micromirror of the projector, hence the light from the projector enters the microscope through that. After this, the rays travelling through the optics of the TM come out to the objective lens port 4 and fall to the photoresist on the substrate. A portion of the rays from the image formed at the substrate surface i.e. the reflected rays, are fed to the eye piece port 2, via the objective port 3. The image size adjusting button of TM acts like a stepper button by providing six fixed image sizes.

The TM is fixed on the base of the MED using a special metal stand and clamp arrangement so that it can be slightly rotated in x-y and x-z planes mainly. This rotation brings fine alignment of the microscope to the rays coming from the micromirror and this alignment is one of the very tedious and important tasks of designing the MED.

Any misalignments or mismanagements in this regard will create a lot of image clarity problems.

The stereomicroscope of the MED is Motic (SMZ-168-BL) and basically designed to study three-dimensional objects or dissect biological specimens. Technically the stereomicroscope has two stages:

- 1) Frosted glass stage – for the observation of samples that are thin or transparent, such as leaves, insect wings etc
- 2) The black and white stage- for non-transparent objects or for dissection.

The important parts and parameters of the microscope are shown in the figure 13 [32] and table 5 [33] respectively.

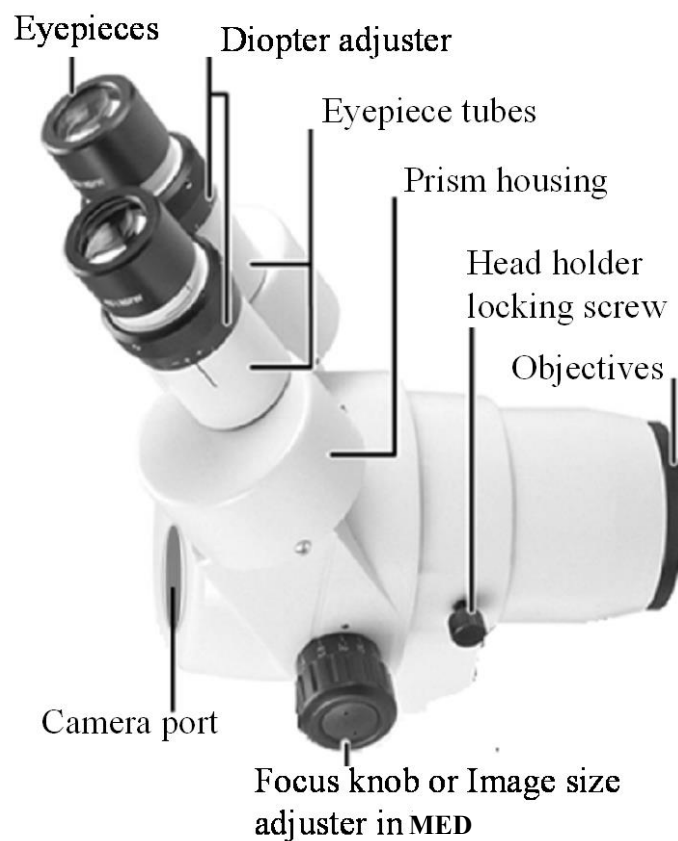
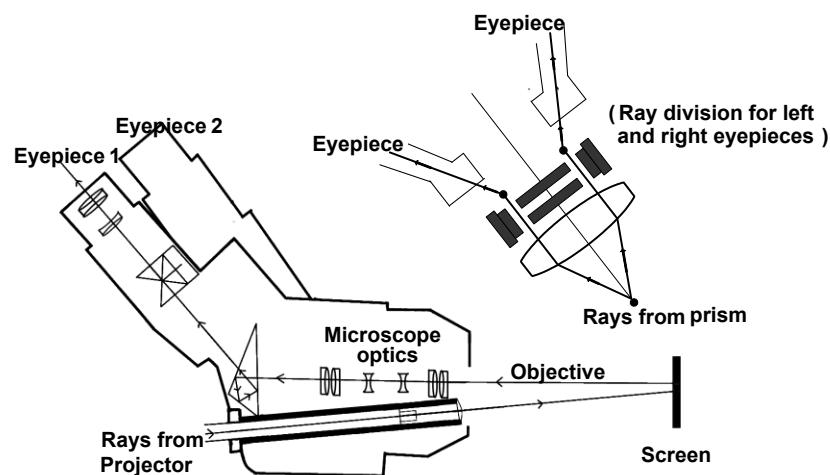


Figure 13. Trinocular microscope and its parts [32].

Table 5. Important working parameters of Trinocular Microscope [33].

Stereomicroscope parameters	
Max. field of view	102 mm
Total magnification	2.25x - 320x (Max)
Zoom body magnification	0.75x - 5x
Zoom ratio	6.7 : 1
Working distance & Max. working distance	113 mm 324 mm
Observation angle	35°
Interpupillary distance adjustment	52 mm to 79 mm
Diopter Adjustment	±5
Eyepiece	2-WF 10X/23 High Eyepoint permanent ones
Objective	0.3X W.D.=324 mm

In the MED, the microscope is placed in between the projector and the screen. The rays coming out of the projector go through the camera port and come out through the objective side and then fall on the screen. A portion of the rays from the image formed on the screen enters the objective again and goes to the eyepiece via a prism. The rays from the prism are divided for left and right eyepieces by a beam splitting arrangement. The details are shown in the ray diagram presented in the figure 14.

**Figure 14.** Ray diagram of the stereomicroscope optics. [34][35]

The stereomicroscope is rigidly fixed in the MED by making use of a suitable holder and screws. The original focus knob of the microscope is used as the image selector. This knob has five steps in turning and each step can fix a certain constant area of image on the screen. Therefore initially the MED is designed for five constant areas and thereby image sizes. However stepper optics (lens or lens system) can be placed in front of the real objective lens of the microscope and images having a variety of area can be produced by altering the relative position of the stepper optics with respect to the objective.

3.3.4. Leaning Screen

The screen is simply a metallic screen indeed but the placing of the screen in the MED is an extremely complicated one. The rays coming out of the projector via Trinocular Microscope are neither horizontal nor vertical to the base of MED. Hence, the alignment of the screen, so that the rays are parallel to the long side of the MED becomes difficult. The illustration in the figure 15 shows the position and direction of the light beam coming out of the projector.

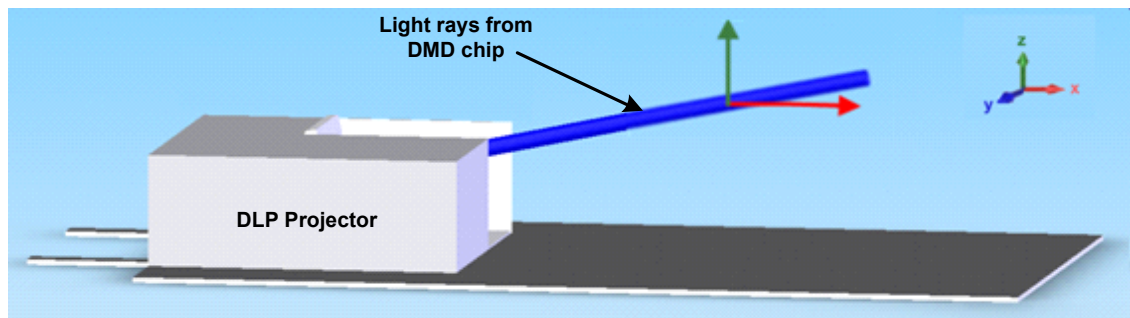


Figure 15. Representation of the rays coming out of the projector.

Therefore a rough calculation of the angles between the ray direction and the x and y directions were required for arranging the screen correctly. The final and suitable arrangement of the screen in front of the projector is presented in the figure 16.

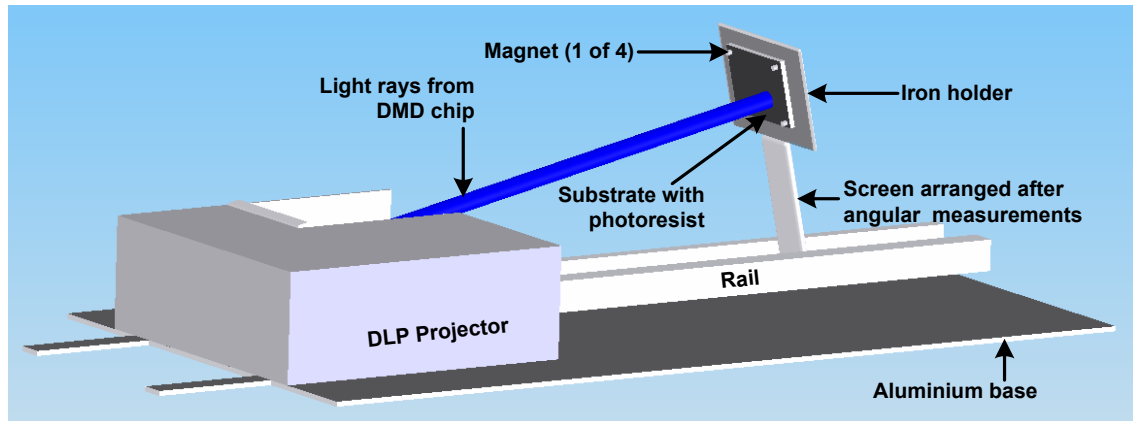


Figure 16. Placing of the MED screen for the formation of images.

From the figure 16, it is seen that the substrate with photoresist can be held firmly in between the iron holder and four magnets. Small magnets having diameters less than 6 mm are suitable for this purpose. The iron holder is fixed in place by an aluminium stand and this stand can be moved back and forth on a rail. This entire set up forms the movable screen of the MED.

3.4. Operation and focusing of the Maskless Exposure Device

The operation and focusing of the MED can be roughly interpreted from the following real images of the device in the figures 17 and 18.

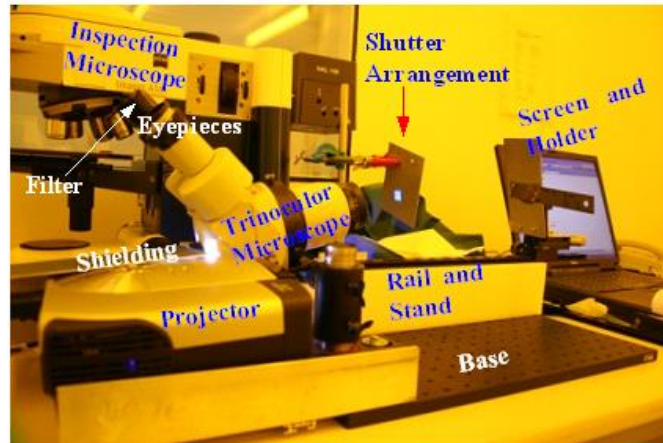


Figure 17. Maskless Exposure Device (MED) in cleanroom's yellow light environment. All the important components related to the MED like projector, projector shielding, eyepieces, filter, inspection microscope, trinocular microscope, shutter arrangement, screen holder, drawing computer, base, rail and stand are marked in the image.

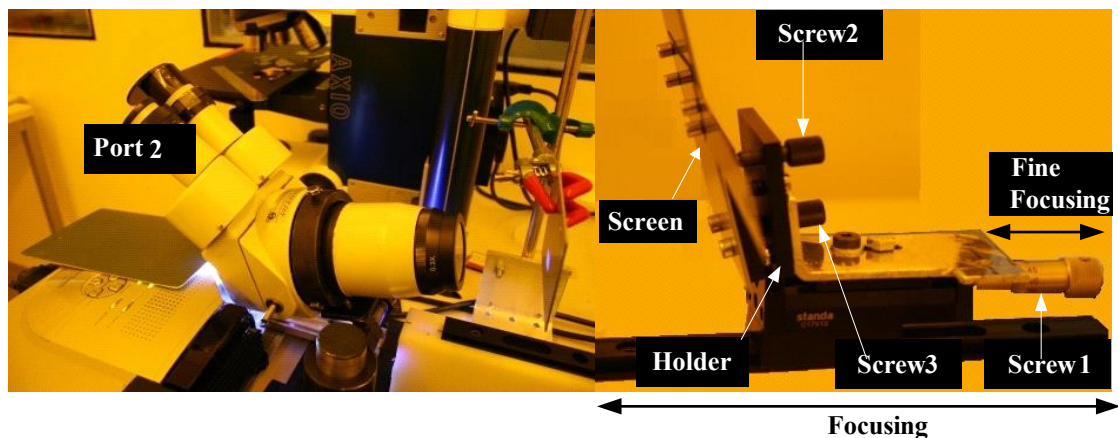


Figure 18. Left image: Installation of Trinocular Microscope (TM) in front of the projector and the temporary shutter for controlling the light from the TM. Right image: Substrate holder and screen. Substrate attaching magnets and position tilting screws are also visible.

The stages of operation of the device including the fine focusing are listed below.

1. Open the drawn image using the suitable software and fix the line colour (blue or black) and background (blue or black) in the software.
2. Activate the computer to projector projection mechanism and check the image formed on the screen
3. Select the size of the image using image selector screw.
4. Fix the proper photoresist coated substrate on the screen using the magnets. Initially select a not so important area of the substrate for the entire focusing procedures.
5. Adjust the screen roughly by looking directly at the image formed and get an image as sharp as possible.
6. Tight the screen on the rail at that state.
7. Look through the microscope eyepiece (port 2) and check the sharpness of the image.
8. Turn the fine focusing screw (screw 1) at the backside of the screen until an extremely focused stage is obtained. (the depth of focusing creates some strain in this stage, therefore a little patience and experience is required here)
9. When the final focusing condition is obtained, fix the fine focusing screw at that state and then again look through the microscope and check the edge width variations (parallax variations) on the image.
10. The image parallax problems can be minimised up to a limit by the screw 2 and screw 3 at the backside of the screen. Screw 3 controls the horizontal tilting and screw 2 controls the vertical tilting. Fix the screws in a good position finally.
11. Now the ES components are ready for exposure. Place the exposure on-off screen in between the microscope and the screen.
12. Exposure conditions are obtained now but the area (which is not so important) which was used for focusing is fully exposed now and therefore change the position of the substrate and bring the area where the real exposure is required to the proper position of light.
13. Use an experimental timer for counting the time of exposure.
14. Expose the photoresist to the light and control the time of exposure using the screen placed for that purpose.
15. After the exposure the substrate is freed from magnets and removed carefully from the screen.
16. Develop the exposed area and check the features through inspection microscope and accordingly proceed with the next exposure.

The focusing and aberration corrections are thus manually obtained and the microscope of the MED is thus a vital part of the entire procedure. Because of this reason, there are

chances to have minute depth of focus and parallax condition variations from person to person as each person's vision characteristics of the eye are different from that of the other person's. However one or two test exposures will clearly give a general idea to the operator by which the real focusing and exposure conditions are to be established as per his vision characteristics. A clean substrate surface with proper photoresist coating and an accurate exposure experiment will impart extremely reliable and comfortable results definitely.

4. PRELIMINARY TESTS USING THE MASKLESS EXPOSURE DEVICE

After coordinating the different operational steps of the Maskless Exposure Device a number of tests were performed. The purpose of the tests was to analyse the working status of the device and to configure it to better standards.

4.1. Processing conditions

Initially a negative photoresist SU-8 was exclusively used for experiments. Basically SU-8 is highly sensitive to near UV radiation; therefore wavelengths that are very close to near UV in the visible spectrum were selected for testing. Compared to other wavelengths in this connection blue ($\lambda \approx 475 \text{ nm}$) seemed to be the optimum one for drawing lines and figures on laptop screen and giving good results. Possibilities of dark field (blue lines on black background) and bright field (black lines on blue background) were experimented. Requirements for SU-8 thin film formations are given in the table 6.

Table 6. Requirements for the formation of SU-8 thin films suitable for Maskless Exposure Device [36].

Resist	Spin coating [rpm] [s]	Prebake Hotplate [°C], [s]	Development [s]
SU-8	3000 rpm 20 sec	Oven: 90 °C 60 sec	55 sec

4.2. Two initial general tests and their details

In all MED experiments, the proper intensity of blue is expressed in the range of 0-255. This is because, almost all graphics software's are setting the brightness value of a particular colour in this range. Therefore the blue with a brightness value 255 is an extremely light blue while that with a brightness value 0 is an extremely dark blue.

Since the MED exclusively depends on graphic softwares, the intensity of blue is hereafter expressed in 0-255 range throughout this manuscript.

The following two diagrams were tested for the very first time and results are presented in the figures 19 and 20.

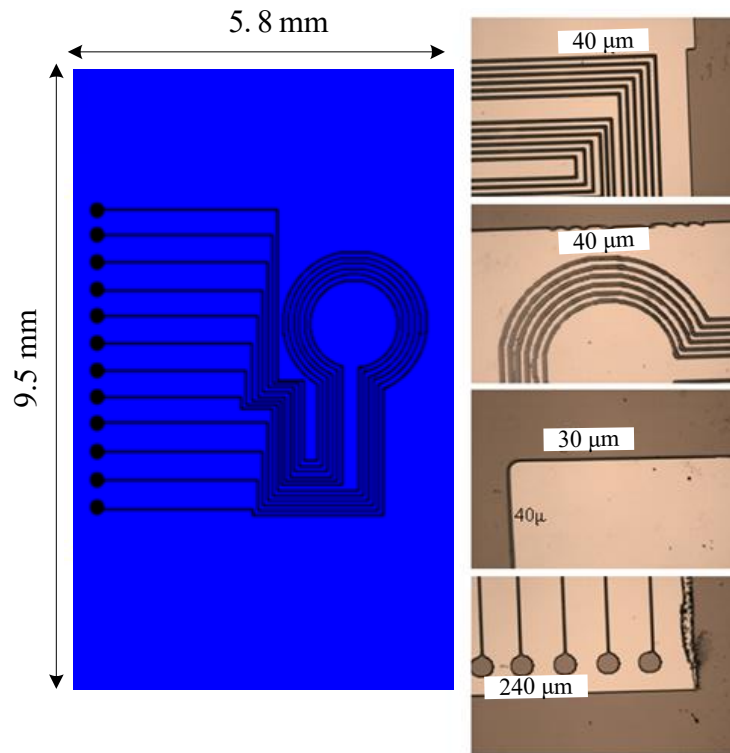


Figure 19. First Test: The Left figure is the layout drawn in black colour on blue background. The photographs of the resultant development are given at the right side. Closed parallel wiring lines, concentric wiring circles and circular electrodes were tested and those are visible as grooves in the photoresist. The minimum line width obtained was about 30 μm .

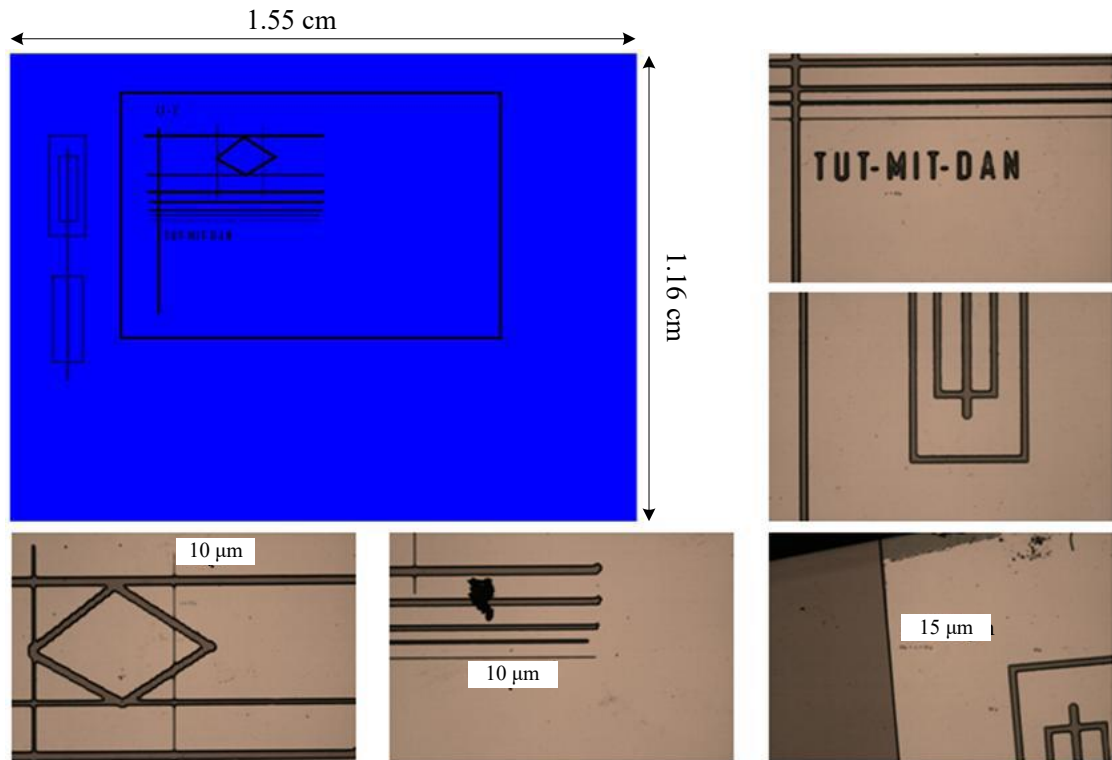


Figure 20. Second Test: The black drawing on blue background is the image used in exposure. Results are shown on the right side and the bottom images. Horizontal, vertical and diagonal circuit wiring lines were tested and those are visible as grooves in the photoresist. The minimum line width obtained was about 10 μm .

4.3. Bright Field and Dark Field tests

In order to understand the variations in image formation according to the variations in area of exposure, a number of experiments were done, by keeping the same image on the computer screen and selecting different areas of exposures using the movements of Trinocular Microscope optics. In the first set of experiments a bright field image (black script on blue background) was used. This was followed by the second test using a dark field image (blue scripts on black background).

First Test: Bright field test.

The image used for the bright field test is given in the figure 21. The photographs of the results are tabulated in the table 7.

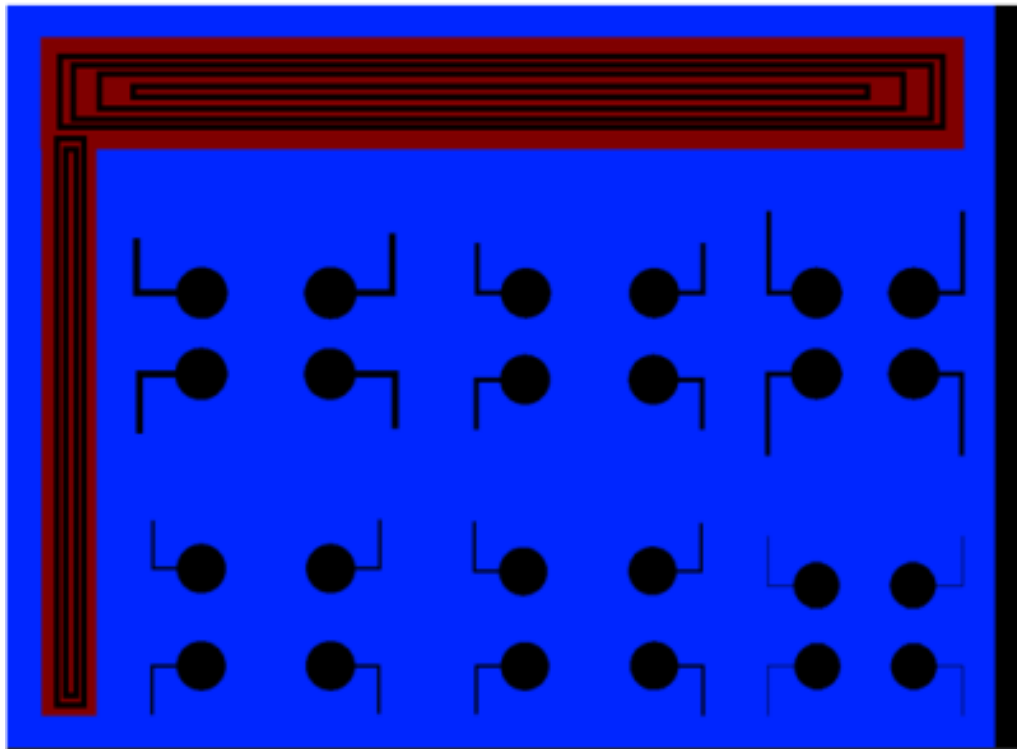
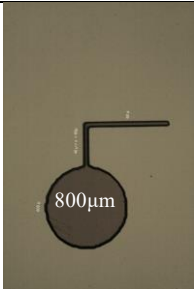
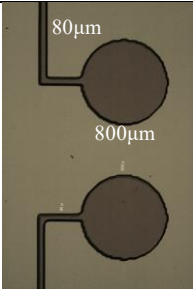
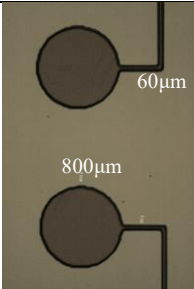
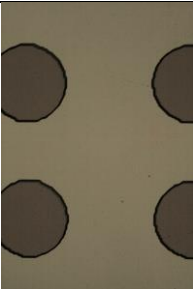
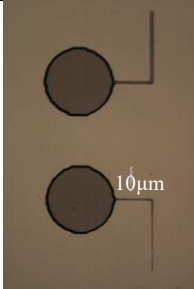

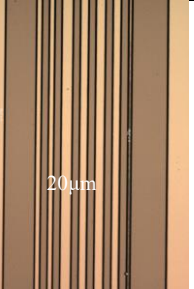
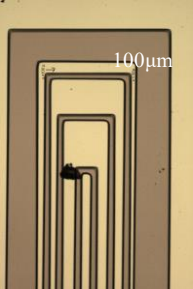
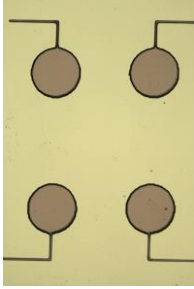
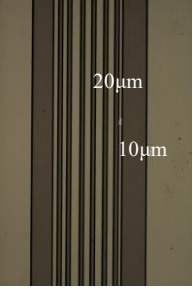
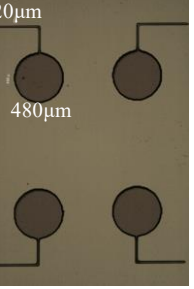
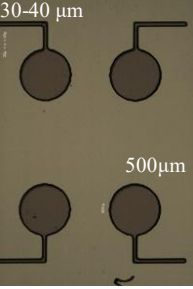
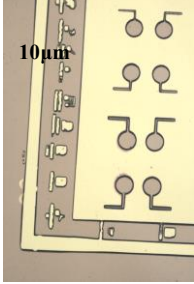
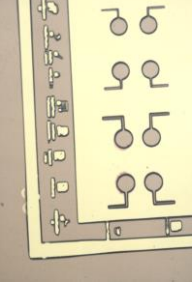
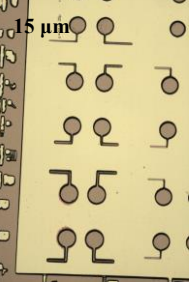
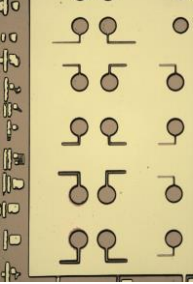


Figure 21. The layout for bright field test consists of electrode circles of different diameter and wiring lines of different widths. The features in the image were intended to be utilised for optimising the minimum possible diameters and line widths in layout drawings.

Table 7. Photographs of results from bright field tests. The layout was exposed to four different areas of substrates (silicon) and electrode wiring width upto 10 μm was obtained. The obtained features are shown here as grooves on developed photoresist.

Electrode circles of different diameters and wiring lines of different widths were drawn and used those for 1.92 cm^2 to 9.1 mm^2 sized exposures.				
Area of exposure 1.6 cm x 1.2 cm Exposure time- 40 s				
Area of exposure 1.3 cm x 1 cm Exposure time- 40 s				
Area of exposure 1 cm x 0.8 cm Exposure time- 40 s				
Area of exposure 3.5 mm x 2.6 mm Exposure time- 15 s				

The experiments were done randomly and results from this helped to organise the experiments for optimisation of various parameters of MED in the very last step.

The image photographs were taken at different conditions and minute focusing variations. Therefore the colour variations appeared in the processed photographs even though the substrate surface of all the above 16 results had the same colour and unique flatness.

Second Test: Dark field test.

The image used for dark field test is given in the figure 22. The photographs of the results are tabulated in the table 8.

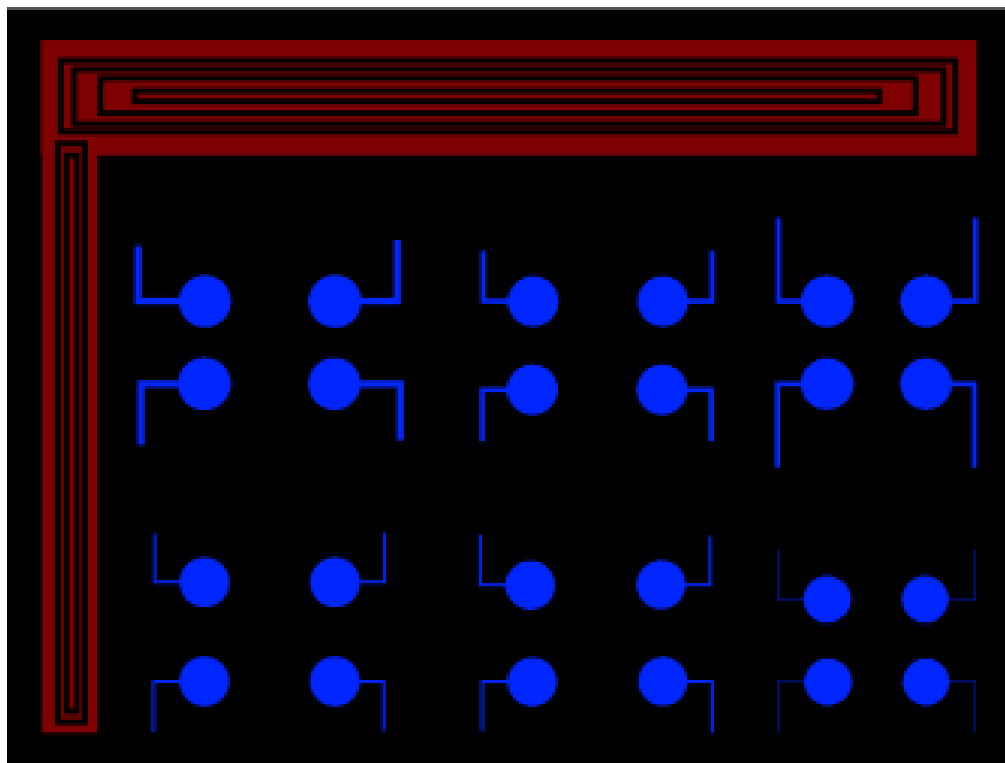
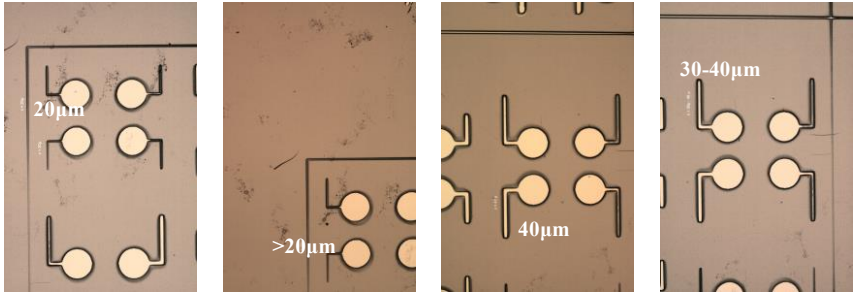


Figure 22. The layout for dark field test consists of circles of different diameters and lines of different widths. The image was also intended to be utilised for optimising the minimum possible diameters and line widths in layout drawings.

Table 8. Photographs of dark field test results show, wiring lines and electrode circles formed on developed photoresist.. Some reasonable good line widths in between 15 μm and 10 μm were obtained.

Exposure time- 30 s.	Areas from 60.8 mm ² to 22.6 mm ² were tested and the images from the latter one only are tabulated.
	 <p style="text-align: center;">5.5 mm x 4.1 mm</p>

The bright field and dark field experiments showed that both possibilities can be utilised in exposure. By simply inverting a bright field layout to a dark field layout on computer, the development after exposure gets inverted from a positive to a negative photoresist nature. The examination of the developed samples using inspection microscope showed that the line widths were less than 20 μm . This can be seen in the images in the tables 7 and 8.

4.4. Verification of some test results using profilometer

The surface parameters of the substrate were studied with the help of an optical profilometer. Profilometer is an instrument used to measure the depth and length of different features usually in micro and nanometers, so that the surface profile (topography) is obtained graphically and numerically. The important objectives were to understand the thickness of photoresist coating and to measure different line widths drawn on the photoresist using the MED. Three samples were tested on the WYKO measurement system profilometer placed at the ORC laboratory and the obtained data was analysed by the software named WYKO Vision. The software provides surface statistics such as maximum profile peak height, maximum profile valley depth, peak to valley difference and the average and root mean square roughness. The device has a scan length range from 50 μm to 30 mm with a vertical resolution of 0.5 nm.

The important results from the profilometer analysis of four important samples are presented here in the figures 23 to 38.

Sample 1

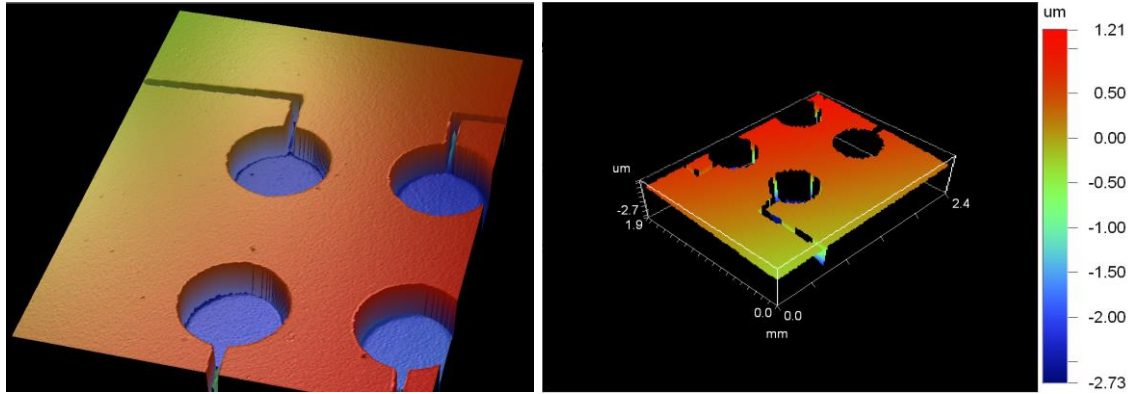


Figure 23. 3-D view and 3-D plot of sample 1 through Profilometer. The colour bar indicates the photoresist thickness variations on the surface.

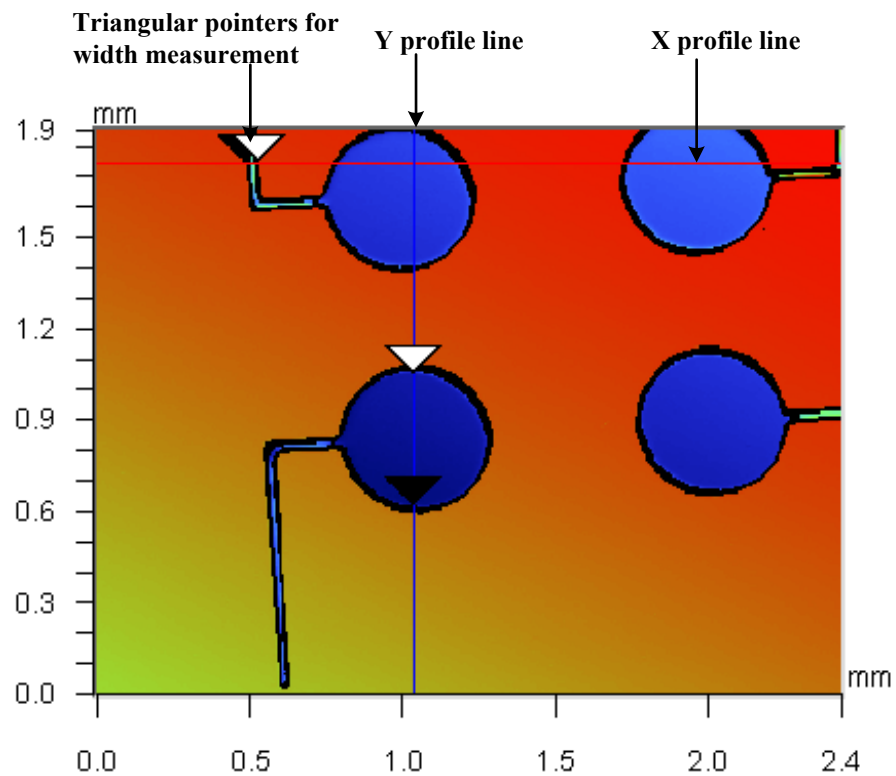


Figure 24. Topographic surface profile measurements of sample 1. The feature area is 2.4 mm x 1.9 mm.

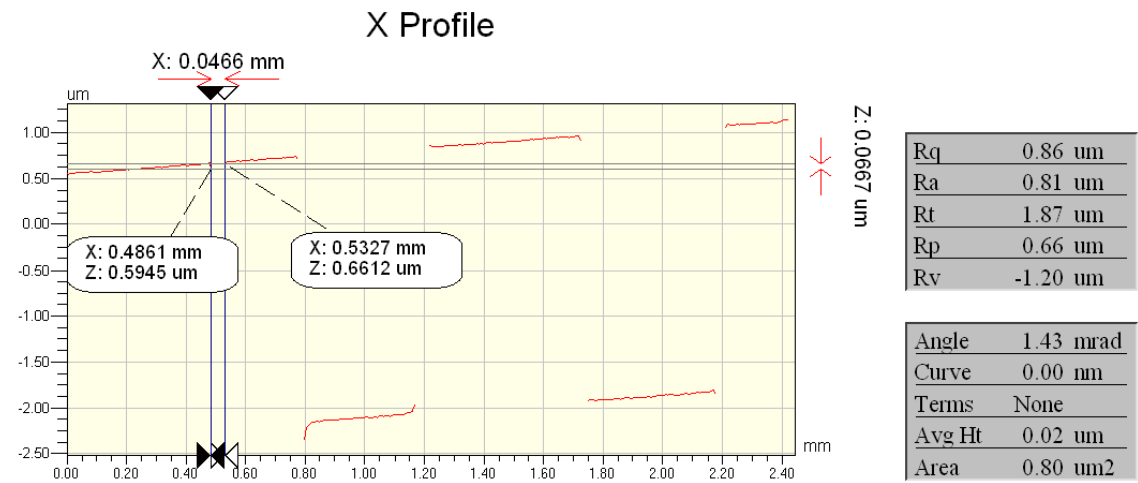


Figure 25. X profile analysis of sample 1. The width of the line is about 47 μm.

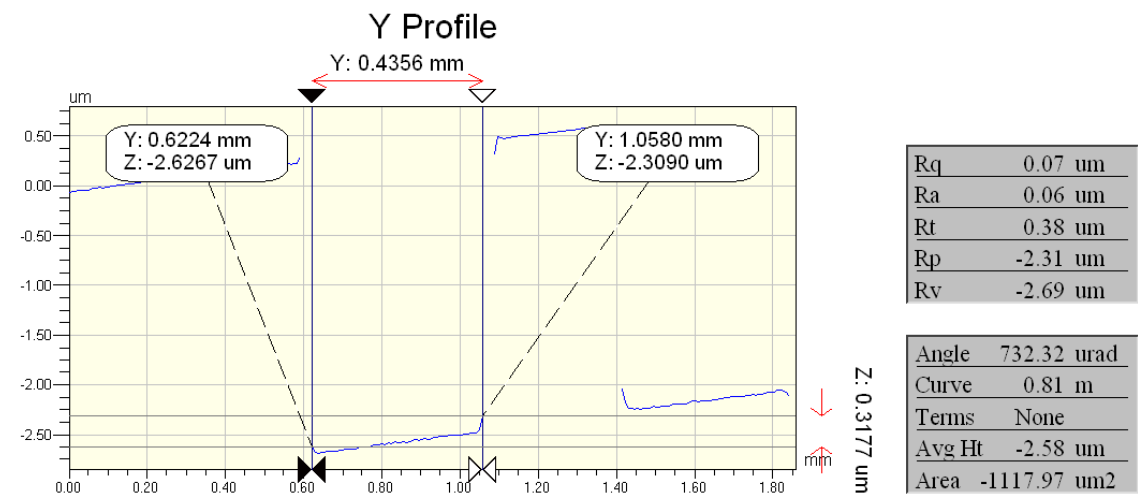


Figure 26. Y profile analysis of sample 1. The diameter of the circle is about 436 μm .

Here Rp is the maximum profile peak height, Rv is maximum profile valley depth, Rt is the peak to valley difference, Ra is the average and Rq is the root mean square roughness.

Sample 2

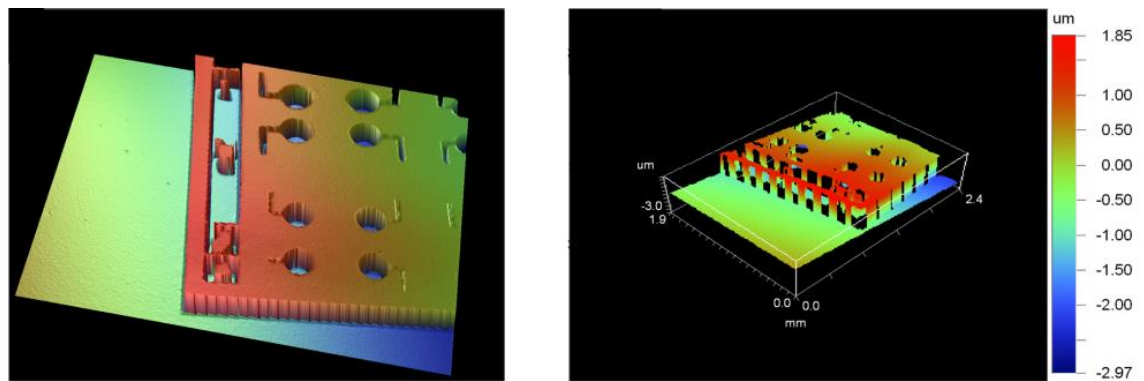


Figure 27. 3-D view and 3-D plot of sample 2 through Profilometer. The colour bar indicates the photoresist thickness variations (in micrometers) on the surface.

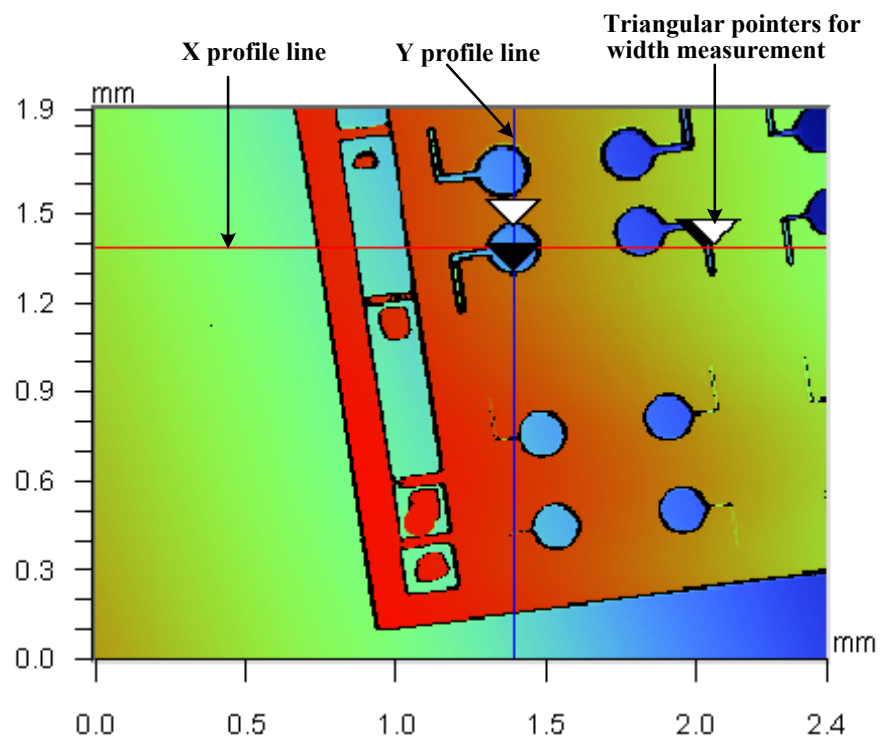


Figure 28. Topographic surface profile measurements of sample 2. The feature area is 2.4 mm x 1.9 mm.

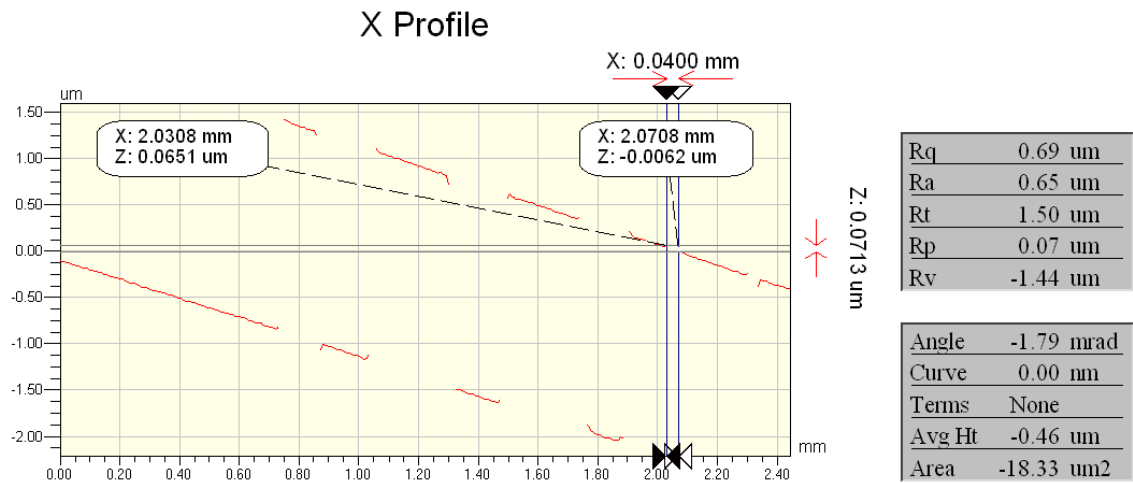


Figure 29. X profile analysis of sample 2. The width of the line is about 40 μm .

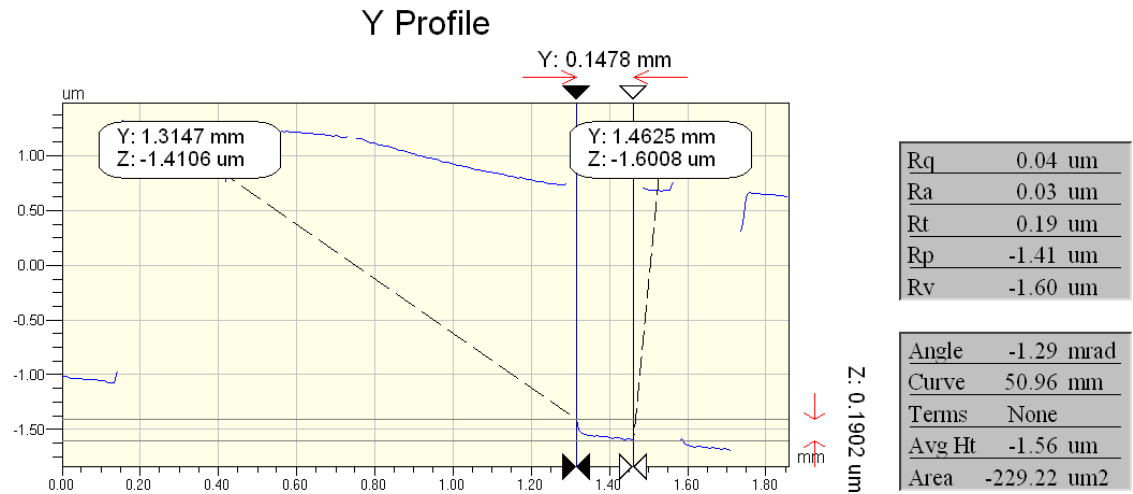


Figure 30. Y profile analysis of sample 2. The diameter of the circle is about 148 μm .

Sample 3

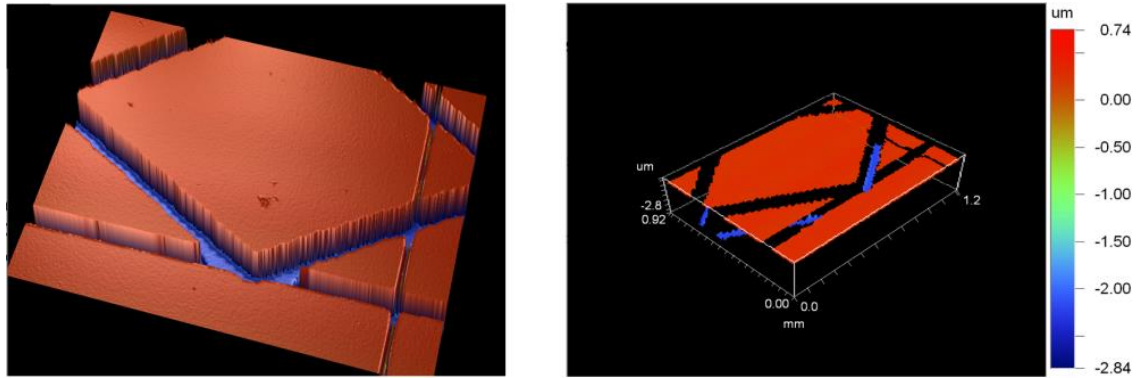


Figure 31. 3-D view and 3-D plot of sample 3 through Profilometer. The colour bar indicates the photoresist thickness variations on the surface.

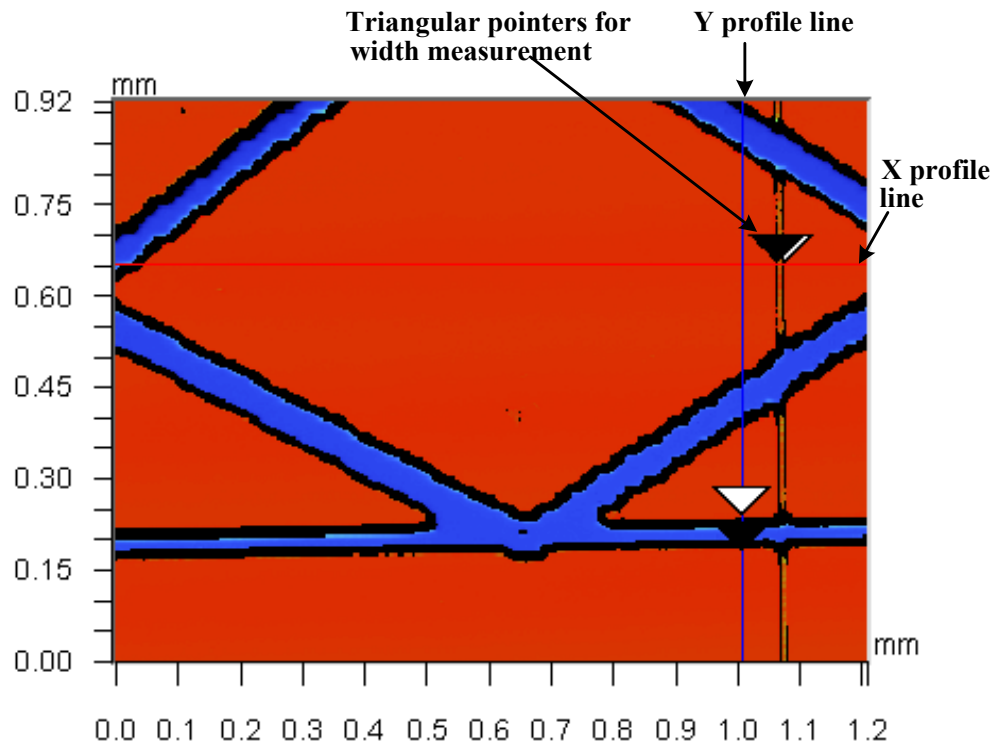


Figure 32. Topographic surface profile measurements of sample 3. The feature area is 1.2 mm x 0.92 mm, containing vertical, horizontal and diagonal lines.

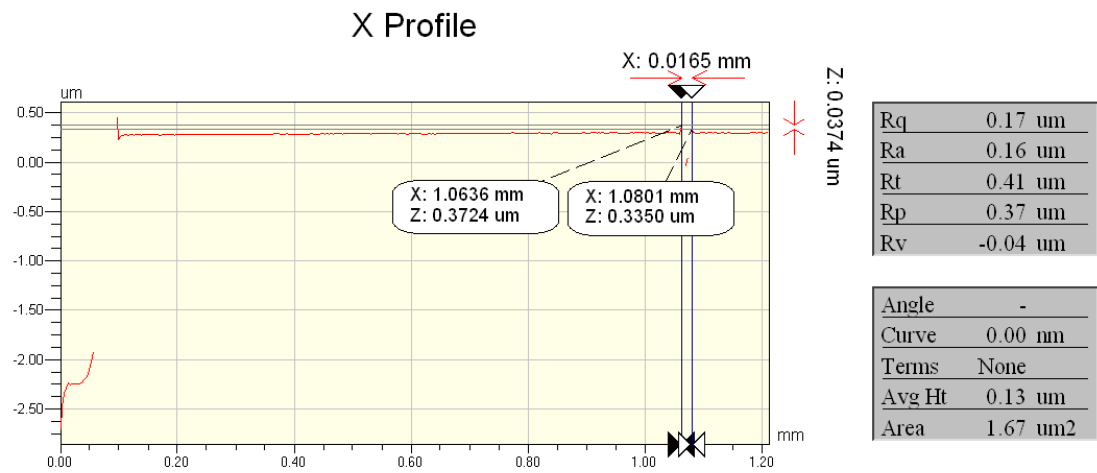


Figure 33. X profile analysis of sample 3. The width of the vertical line is about 17 μm

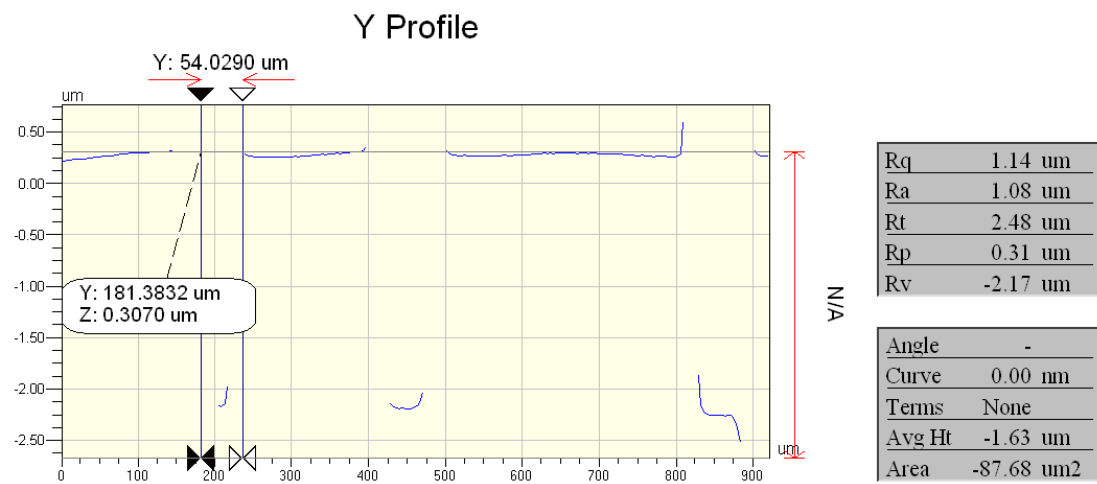


Figure 34. Y profile analysis of sample 3. The width of the horizontal line is about 54 μm .

Sample 4

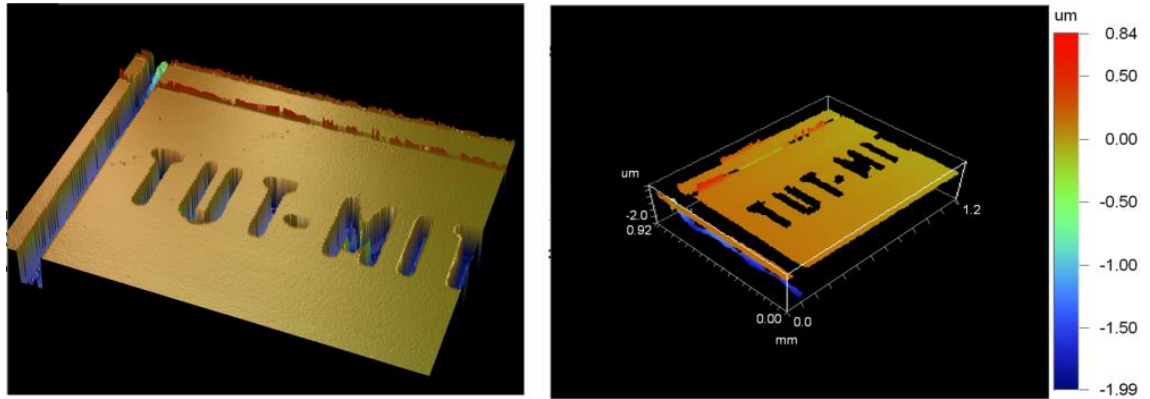


Figure 35. 3-D view and 3-D plot of sample 4 through Profilometer. The colour bar indicates the photoresist thickness variations on the surface.

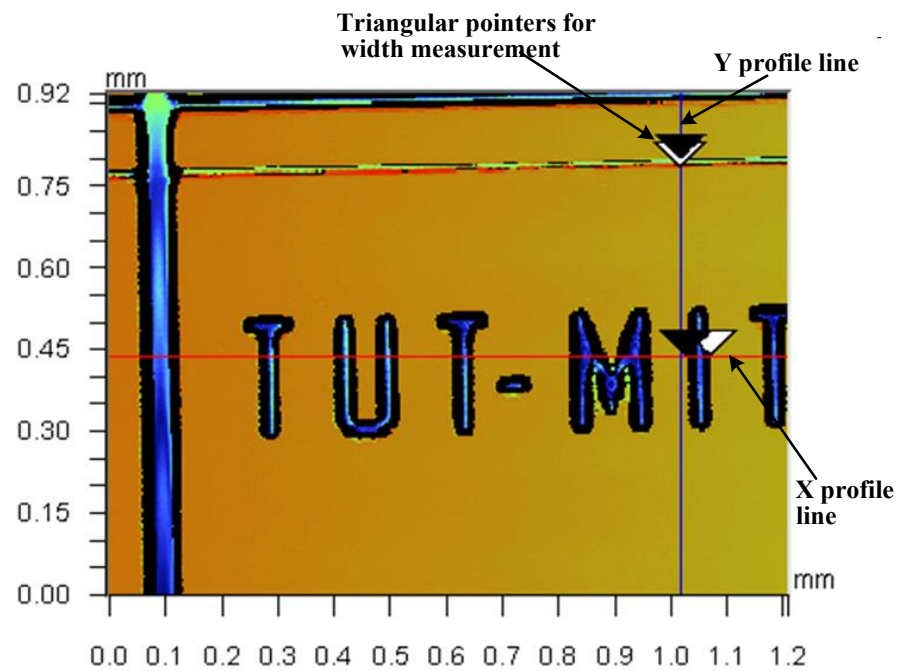


Figure 36. Topographic surface profile measurements of sample 4. The feature area is 1.2 mm x 0.92 mm, containing vertical and horizontal lines.

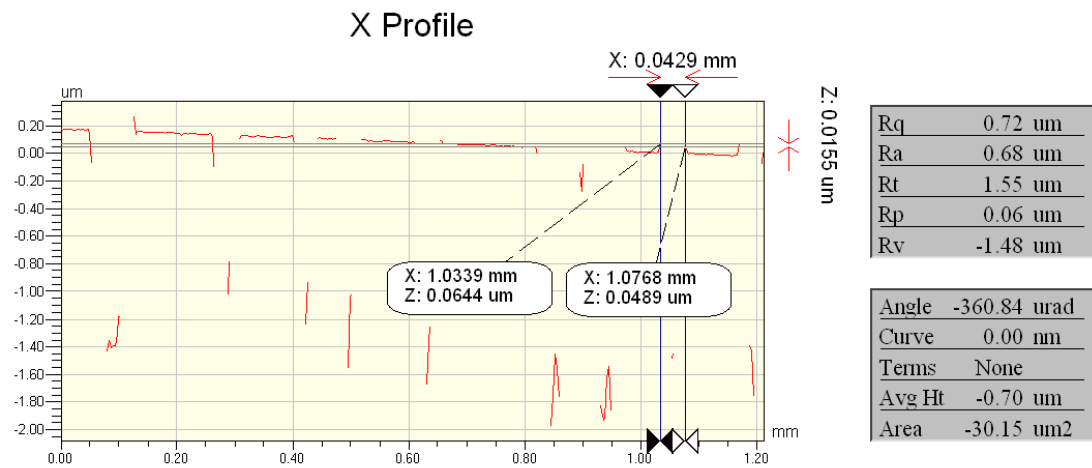


Figure 37. X profile analysis of sample 4. The width of the English letter ‘I’ is about 43 μm.

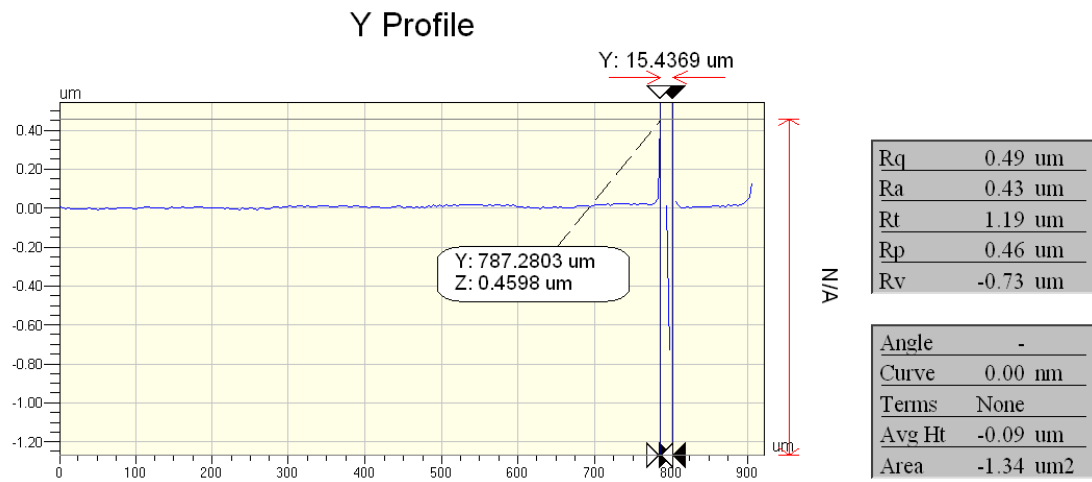


Figure 38. Y profile analysis of sample 4. The width of the line above the English script is about 15 μm.

4.5. Pixel size calculations

Computer Image

Native resolution from the PJ458D, DLP Projector = 786432 pixels (1024 w x 768 h)

Calculation 1

Size of the image on the substrate = 1.6 cm x 1.1 cm (Using inspection microscope)

Thus the 1.6 cm width includes 1024 pixels and 1.1 cm height includes 768 pixels

Therefore the width of 1 pixel = $1.6 \text{ cm} / 1024 \text{ pixels} = 15.6 \mu\text{m}$

And the height of 1 pixel = $1.1 \text{ cm} / 768 \text{ pixels} = 14.3 \mu\text{m}$

So 1 pixel size is $15.6 \mu\text{m} \times 14.3 \mu\text{m}$

Calculation 2

Size of the image on the substrate = 6 mm x 4.3 mm (Using inspection microscope)

Thus the 6 mm width includes 1024 pixels and 4.3 mm height includes 768 pixels

Therefore the width of 1 pixel = $6 \text{ mm} / 1024 \text{ pixels} = 5.9 \mu\text{m}$

And the height of 1 pixel = $4.3 \text{ mm} / 768 \text{ pixels} = 5.6 \mu\text{m}$

So 1 pixel size is approximately $5.9 \mu\text{m} \times 5.6 \mu\text{m}$

It is possible to imprint horizontal and vertical lines of 1 pixel size on the substrate. But non- horizontal and non vertical features require more pixels to produce good results. A gap of 1 pixel size in between two lines or circles is also possible with good focusing.

4.6. Image intensity compensation

A number of continuous exposures and further developments, including the previously tabulated ones (table 7 and 8) showed that whatever be the care taken in the alignment of the microscope towards the rays coming out of the micromirror, a perfect aligning situation was not obtained. These minute misalignments could be recognized after the development of the substrate, by small variation in line width on the left side of the image compared to the right side and on the top side of the image compared to the bottom portion, even if the layout drawn on the computer was having lines of equal widths. These features are explained in the figures 39 to 42. The real image drawn on the computer is given in the figure 39. The photograph of the result is given in the figure 40.

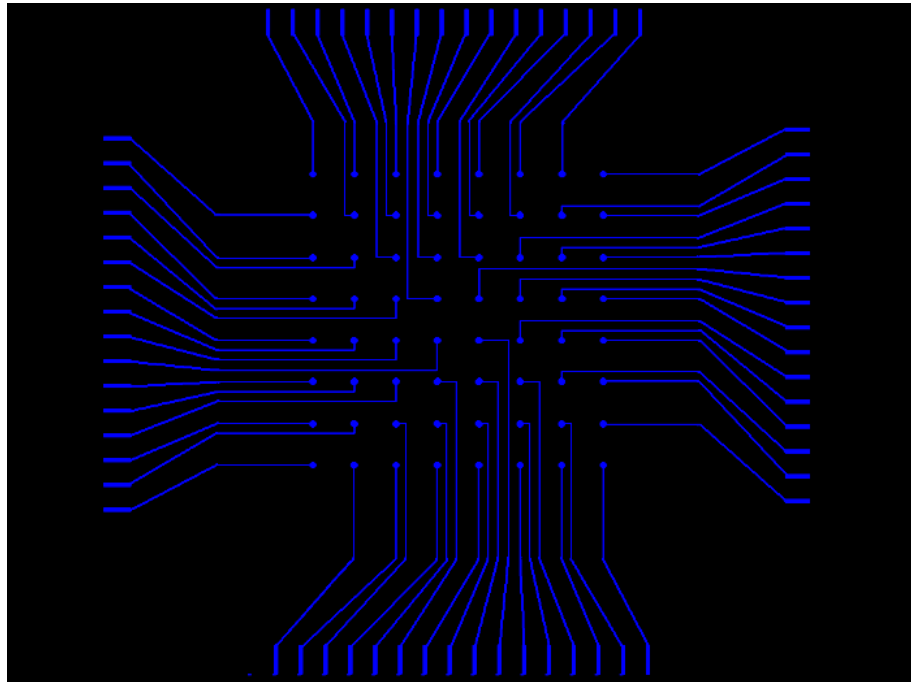


Figure 39. Layout of a matrix electrode system drawn on computer, uniform blue lines and circles on black background

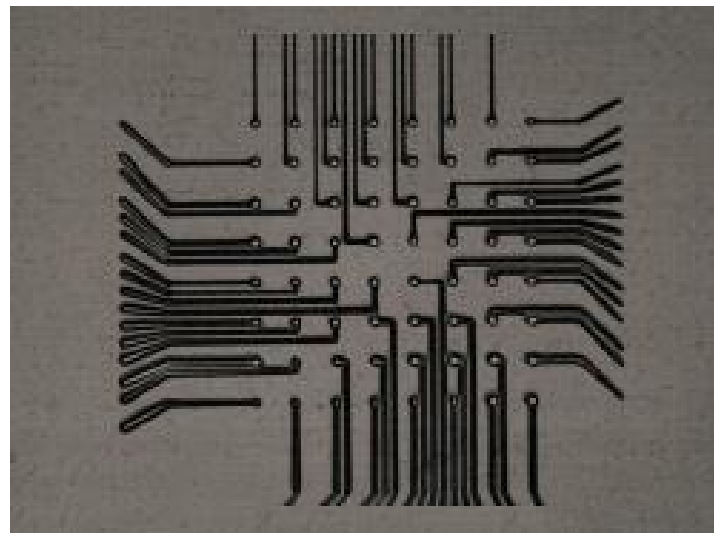


Figure 40. Image of developed photoresist. Widths of electrode lines are not uniform on photoresist.

The reason of unequal line widths was the unequal distribution of intensity on the surface and a modeled image illustrating this unequal intensity distribution is given in the figure 41. It shows that certain areas should be provided with low intensity values compared to certain other areas. This leads to a kind of intensity compensation

technique. Such an intensity compensation was performed by making use of matlab commands. The image lay out created for perfect exposure is given in the figure 42.



Figure 41. Modeled image for non-uniform intensity distribution.

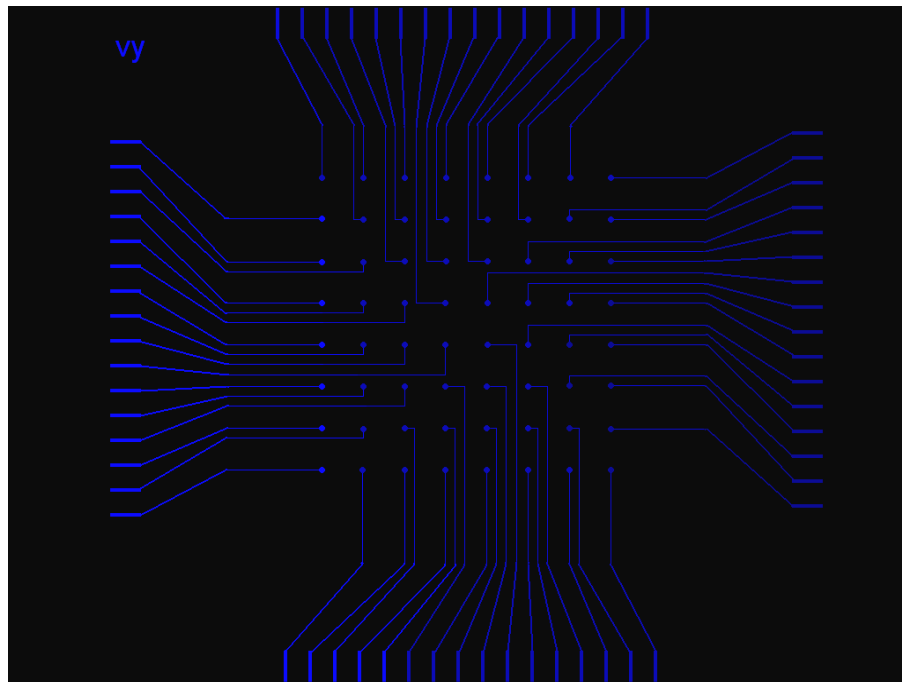


Figure 42. Modified layout by matlab for compensating the unequal distribution of intensity. Unlike the layout in figure 39, this image is provided with higher blue values at left and bottom regions and lower blue values at top and right regions.

The unequal line widths on the developed image were due to the unequal distribution of intensity during exposure. This was caused by the minute misalignments in the installation of Trinocular Microscope in front of the projector. Ideally the camera port of the microscope should be exactly parallel to the light beam coming out of the projector. Even an extremely slight variation of the microscope from the beam direction may produce intensity variations on the surface of substrate. A hardware alignment for bringing intensity errors as close to zero was performed first and the still remaining minute errors were brought to zero by software compensation. The software intensity compensation was performed by means of Matlab image processing commands. So when an image is drawn, a greater blue intensity value was given to the lines on the left side while a less blue intensity was incorporated with the same on the right side of the image. Therefore, to get good results either a hardware treatment - a keen alignment of the projector, Trinocular Microscope and the screen to avoid any sort of parallax errors - or a software treatment - fix the components with possible perfection and compensate the intensity logically- is required in the present situations.

4.7. Etching of the substrate patterned by the Maskless Exposure Device

The initial experiments of the MED were followed by the experiments for fabricating 3D structures using the images transferred by the MED on the substrate surface. A suitable gold coated glass plate made by VTT was used and the thickness of the gold layer on the glass plate was 46 nanometers. An intensity compensated image was projected to the photoresist coated gold plate.

After the normal exposure and development, the gold etching was performed using potassium iodide. The standard etching solution of I, KI and DI water in the ratio 1:4:40 was prepared and the gold plate was soaked in it. The normal etching rate of KI is 0.5 to 1 $\mu\text{m}/\text{min}$ at room temperature. The layout used after intensity compensation is presented in the figure 43 and important results are presented in the figures 44 and 45.

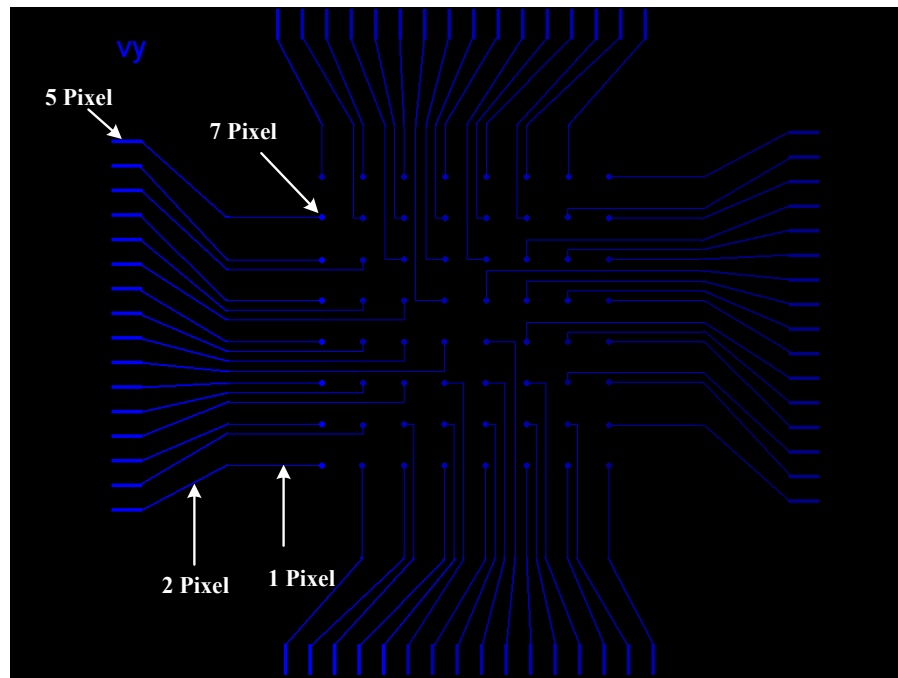


Figure 43. Intensity compensated layout. Used for exposure on to a gold plated glass plate followed by gold etching.

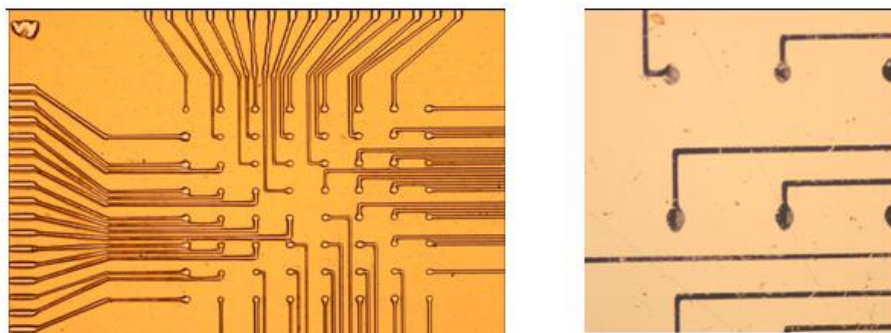


Figure 44. Photograph of the gold coated glass plate after 5 seconds of etching. The layout was patterned by a positive photoresist on gold. During etching, the gold beneath the layout was removed. The width of wiring lines are 8-10 μm and electrode circles are of size 30-40 μm .

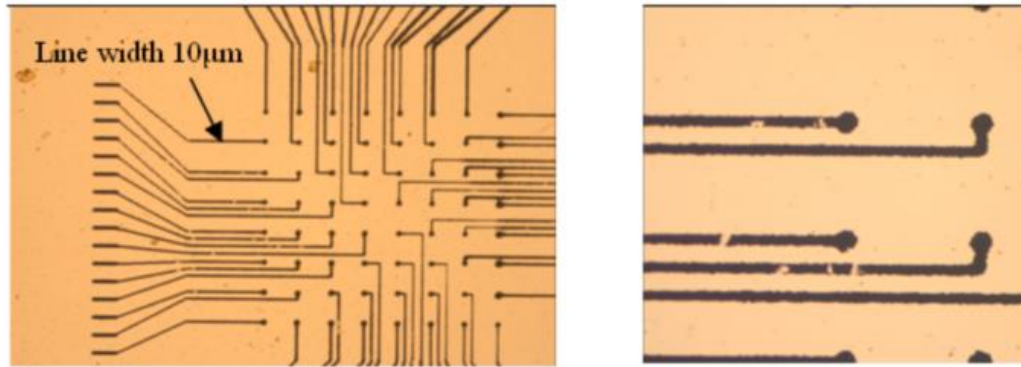


Figure 45. Photograph of the gold coated glass plate after 40 seconds of etching. The layout was patterned by a positive photoresist on gold. During etching, the gold beneath the layout was removed. The width of wiring lines is about 10 μm .

The gold was not totally etched here, but the purpose of the experiments was to ensure the possibilities of creating 3D structures by methods like etching, and test results proved that the images transferred by MED can be definitely utilised for real and practical applications.

5. THE THEORY BEHIND THE MASKLESS EXPOSURE DEVICE

In the normal ‘projection printing lithography’, the mask image is projected at a distance in a reduction ratio in between 4:1 and 10:1. Even though many advantages are there for this technique over the contact and proximity printing, the diffraction effects limit the accuracy of pattern transfer. Let us consider the detailed theory behind the pattern transfer in conventional and maskless photolithography.

5.1. Physics of Optical Lithography

Being an electromagnetic wave, light exhibits wave nature too along with particle nature. When a wave interacts with obstacles during its propagation, bending of the wave takes place around the obstacles and this refers to as diffraction. Diffraction effects are most common for waves whose wavelengths are in the order of diffracting objects. The beautiful colour exhibitions on the writing surface of a CD and on the spider web etc. are some everyday examples of diffraction. In a CD the closely packed tracks act as diffraction grating and the same is true in a spider web too. Therefore in principle diffraction arises in situations similar to grating lines. The fundamental reason of diffraction is interference and when two light waves combine after certain obstacles, depending on the phase difference between the two waves its displacements are added up generating a greater or lesser total displacement and intensity. In photolithographic projection printing contexts, the light is always interacting with grating like mask features or other components. Hence the basic diffraction may arise here too and as a result of this, a composite light may split up or a monochromatic light may create unnecessary imaging formalities though out the wafer surfaces.

When the wafer is placed far away from the mask as in the figure 46(In maskless lithography immediately after the final lens), the fine features are limited by Fraunhofer diffraction limit [37].

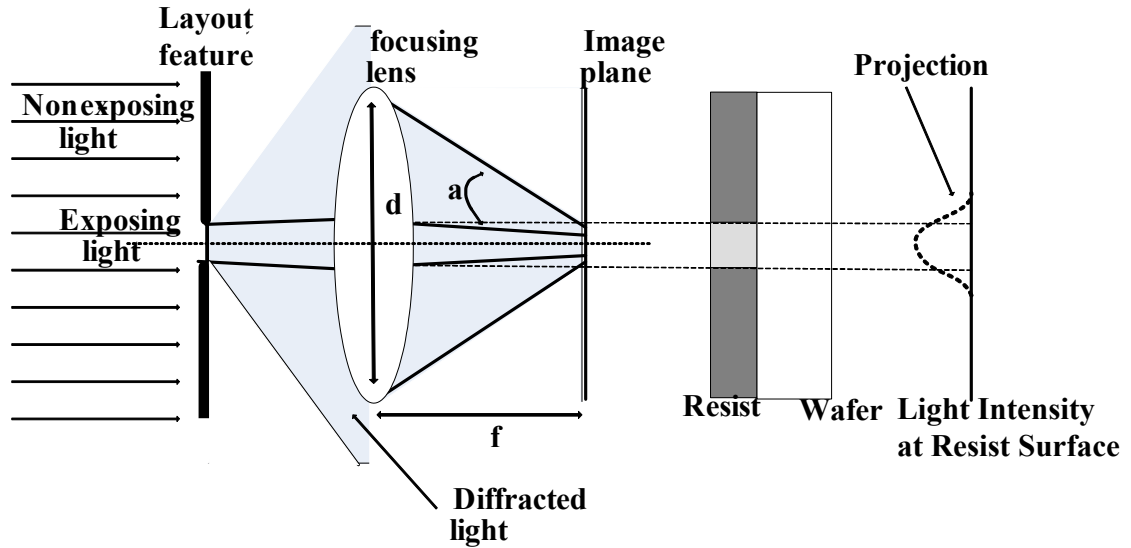


Figure 46. Diffraction in photolithographic arrangement. Fraunhofer diffraction limits the minimum feature size that can be achieved in experiments.

The Fraunhofer diffraction limit can be mathematically expressed as [37].

$$W^2 \ll \lambda \sqrt{g^2 + r^2} \quad (5)$$

Here W is the feature size, λ the wavelength, g the gap, d the diameter of the focusing optics and f the focal length. If n is the refractive index of the medium and α_a is the angle between the edge of the focusing optics and optical axis of the system, d can be written as,

$$d = 2[n(f \sin(\alpha_a))], \text{ and } n = 1 \text{ for air.} \quad (6)$$

A typical far field image can be scientifically understood from the following normalised intensity curve as shown in the figure 47. The resolution - how small a feature can be made - of a projection system is thus finally determined by the diffraction and that too is marked on the intensity curve [37].

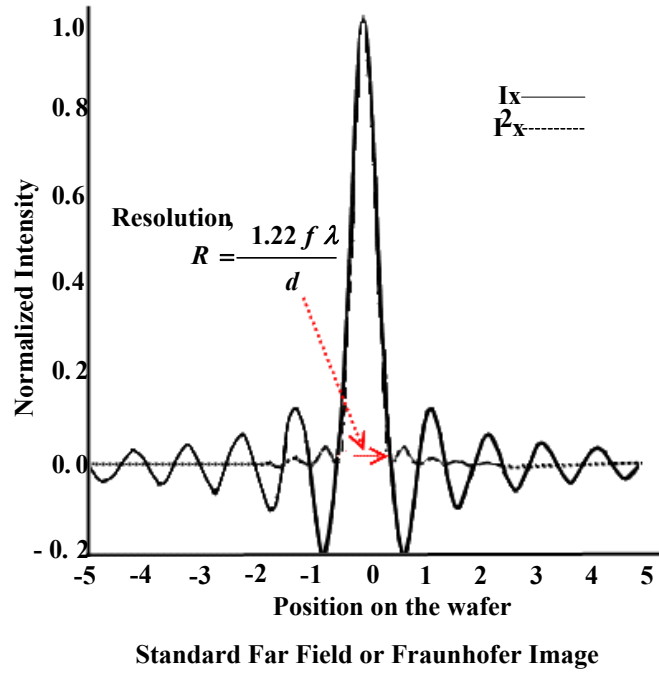


Figure 47. Normalised intensity curve [37]

According to Rayleigh's law the resolution is

$$R = \frac{1.22 f \lambda}{d} = \frac{1.22 f \lambda}{n(2f \sin(\alpha))} = \frac{0.61 \lambda}{n \sin(\alpha)} = \frac{0.61 \lambda}{NA} \quad , \quad (7)$$

where NA is the numerical aperture of the focusing system, which determines the focusing strength of the projection system. The above derivations are being done by considering a point source approximation, however in practical situations that is not the case. This can be solved by considering a general constant k and attaching that to the point source approximation. Thus the equation for minimum feature size (or the resolution) can be finally written as

$$W_{\min} \approx k \frac{\lambda}{NA} \quad , \quad (8)$$

where k will be a process related constant with a numerical value ≥ 0.5

Thus it is clear that the minimum feature size can be greatly controlled by NA, but the increase of NA beyond a limit alters (actually decreases) the Depth of Focus. This can be understood from the following explanations and drawings in the figure 48 [37].

Depth of focus is expressed as

$$DOF = \sigma = \frac{\lambda}{NA^2} \quad (9)$$

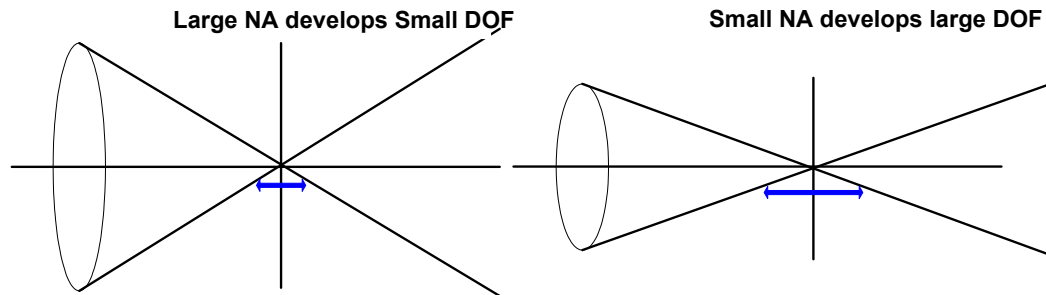


Figure 48. Numerical aperture (NA) and Depth of Focus (DOF) relation. Large NA results in small DOF and small NA results in large DOF when the medium is unchanged.

Thus, the resolution can be increased by increasing the NA, but that creates subsequent focusing complications. So logically it can be stated that ‘extremely superb resolution is obtained only at the cost of extremely complicated focusing methodologies’.

5.2. Problems faced with the design of the device and their possible solutions.

The main problems confronted with the design of the MED were unnecessary heating, vibration and parallax error.

5.2.1. Heat and Vibration problems

The heat is mainly coming from the projector bulb. There are heat reducing rotating fans and the rays are coming out after passing through the optical system of the projector. But the normal optics of the projector is completely removed. Therefore the rays are coming out of the projector to an externally placed Trinocular Microscope and

a portion may scatter to the surroundings. These rays also contain intense IR and increase the temperature in the surroundings. So in order to limit the heat coming out of the device, a heat absorbing mechanism could be installed but, at the moment, instead of using an absorber a metal shielding is used just to stop the rays. So even if the temperature increase in the working environment is not going to drop much, the scattering rays and especially the rays towards the operator can be prevented.

The vibration of the device was also very dominant initially. When the projector is running, two heat reducing fans are working and making mechanical vibrating movements. The entire device is arranged on an aluminium platform and therefore the vibrations of the projector produce vibrations on trinocular microscope, screen and the substrate attached to the screen. During lithographic exposure, the layouts from the computer are transferred to micron and submicron dimensions and the vibrations, even if those are very minute, create line width variations. So even if a particular line say of 10 μm width is supposed to be obtained on photoresist, it may become 13 or 14 μm due to vibrations. So to increase the accuracy and line width quality characteristics, the vibrations should be limited and so the total MED was modified accordingly after the initial experiments. Initially a number of aluminium mechanical parts were employed and all the unnecessary parts were removed in the second stage. The screen of MED was specially redesigned with minimum mechanical stuff and by increasing the weight of the screen. As the weight of the screen increases the magnitude of vibration decreases tremendously and at the moment the MED works smoothly and the vibration and related effects are controlled upto a limit. But a complete vibration removal is not possible indeed as the projector brings minute mechanical vibrations continuously. Normally the projector is recommended to be used only in an open area as it may produce harmful ozone in some situations. But the chances of formation of ozone could be neglected in our case, as the cleanroom is equipped with additional ventilations than that in a normal room.

6. USE OF POSITIVE PHOTORESIST MA-P 1225 AND OPTIMISATION EXPERIMENTS

Even though the negative SU-8 photoresist was used in the initial experiments, it was then replaced by the positive ma-P 1225 photoresist due to commercial and availability reasons. The processing conditions of ma-P 1225 and some test results are discussed in the following sections.

6.1. Positive Tone Photoresist ma-P 1225

This photoresist has a good thermal stability of the resist patterns and supports aqueous alkaline development. Its high stability in acid and alkaline plating baths give rise to extremely high electroplating characteristics. The physical properties and standard processing data sheet of ma-P 1225 are as listed in the table 9 [38].

Table 9. List of important physical properties and standard processing data of ma-P 1225.

Suitable for	Broadband UV exposure
Film thickness [μm]	1.0 ± 0.1
Dynamic Viscosity [mPa s]	12 ± 1
Density [g cm^{-3}]	1.026 ± 0.003
Spin coating [rpm] [s]	3000 30
Adhesion promoter	HMDS for Si and SiO ₂ substrates
Prebake Hotplate [$^{\circ}\text{C}$] [s]	100 60
Exposure dose [mJ/cm^2] (Broadband exposure)	35 ± 5
Development (ma-D 331) [s] (Immersion development)	30 ± 10
Best patterning conditions	At temperatures of 20 – 25 $^{\circ}\text{C}$ and a relative humidity of 40 – 46 %.
Processing environment	Processing under yellow light.

The general spin curve of the ma-P 1210 is shown in the figure 49 and the refractive index versus wavelength relation using Cauchy equation is shown in the figure 50.

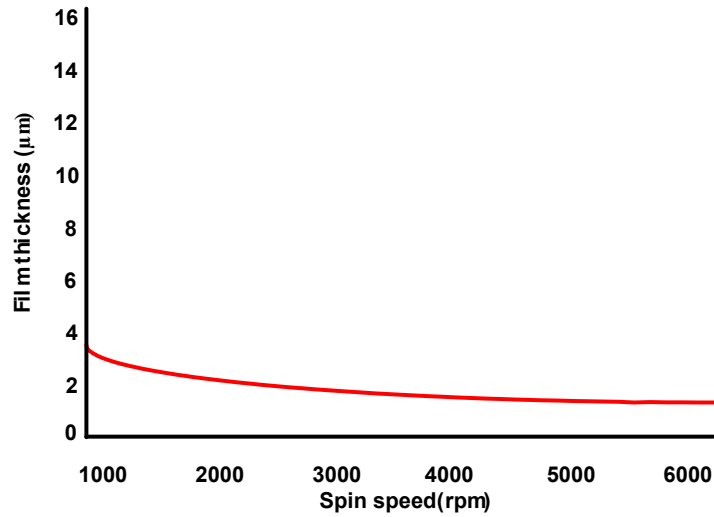


Figure 49. Spin Curve of ma-P 1210 for 30 s spin time [38] .

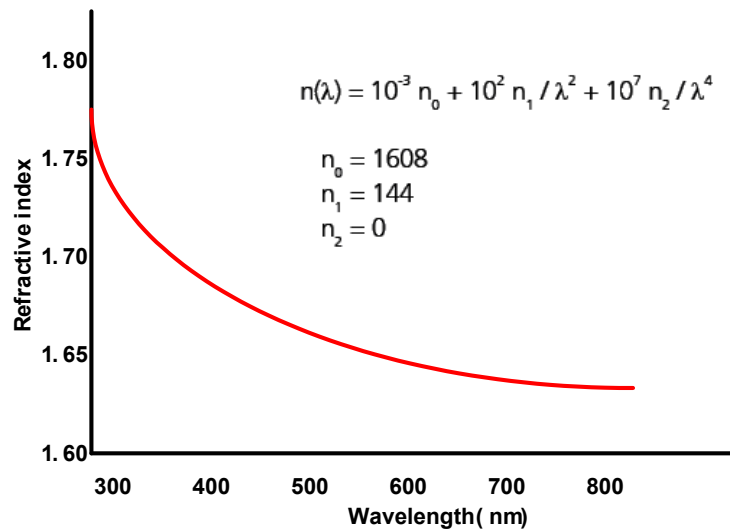


Figure 50. Refractive index as a function of wavelength for ma-P 1210 [38].

This data was used as the base of the optimisation experiments of the MED. The different exposure and development parameters of ma-P 1225 were defined for UV absorption conditions and those were to be redefined fully in accordance with the visible light (especially blue) conditions in the MED.

6.2. Optimisation experiments

The different parameters of the MED device for the proper functioning of the device were tested and finalised using a number of continuous optimisation experiments. The various factors affecting the size and quality of the images formed on the substrate are listed below.

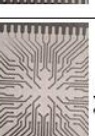



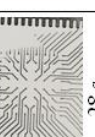

1. Brightness or proper intensity of blue
2. Exposure time and development time
3. Image size
4. Software program that is used for drawing a layout
5. Resolution of the device

6.2.1. Brightness or proper intensity of blue

Blue is the working color of the MED and the particular intensity of blue that gives nice results was tested. The value of red and green were set to be 0 and different values of brightness for blue can be selected from major image viewing softwares. However the MED gives good results when the blue value is in between 110 and 140 and therefore the values from 90 to 150 were given to blue and the red and green values were kept as 0, and step by step exposures were made on the substrate.

The basic objective of the brightness test is, keeping the exposure time constant and testing a particular brightness and finding out the needed development time. This was repeated for 7 different brightness cases and the results can be seen in the table 10.

Table 10. Optimisation of proper intensity of blue. The exposure time was kept constant to be 34 seconds. 7 different intensities of blue (one row for one intensity) were tested. The sample after a particular blue intensity exposure was developed from a minimum development time to a time until which clear features were visible. (columns in a row show the successive developments)

Exposure Time : 34 Seconds,		Developing Times are at the bottom of each image..							
1	B=90 G=0 R=0	 19 s	 34 s	 49 s	 64 s	 79 s	 94 s	 109 s	 124 s
2	B=100 G=0 R=0	 19 s	 34 s	 49 s	 64 s	 79 s	 94 s	 109 s	 124 s
3	B=110 G=0 R=0	 34 s	 43 s	 52 s	 61 s	 70 s	 79 s	 88 s	 97 s
4	B=120 G=0 R=0	 16 s	 19 s	 22 s	 25 s	 28 s	 31 s	 34 s	 37 s
5	B=130 G=0 R=0	 16 s	 19 s	 22 s	 25 s	 28 s	 31 s	 34 s	 37 s
6	B=140 G=0 R=0	 16 s	 19 s	 22 s	 25 s	 28 s	 31 s	 34 s	 37 s
7	B=150 G=0 R=0	 16 s	 19 s	 22 s	 25 s	 28 s	 31 s	 34 s	 37 s

Conclusion:

The experiments with different intensities of blue, keeping the exposure time constant, gave a result that a blue intensity value in between 120 or 140 can give smooth results. As a general conclusion the following data in the table 11 from the above experiments can be utilised for the practical processing procedures of the MED.

Table 11. Optimum development times for different blue values ranging from 90 to 150. The exposure time is kept constant to be 34 seconds.

Blue Value	Exposure Time (s)	Developing Time (s)	Average Developing Time
90	34	> 200	200
100	34	> 150	150
110	34	> 100	100
120	34	31 – 34	32.5
130	34	34 – 37	35.5
140	34	28 – 31	29.5
150	34	19 – 22	20.5

Thus it is clear that as the brightness value of blue increases the time required for development decreases and this can be graphically plotted as in the figure 51.

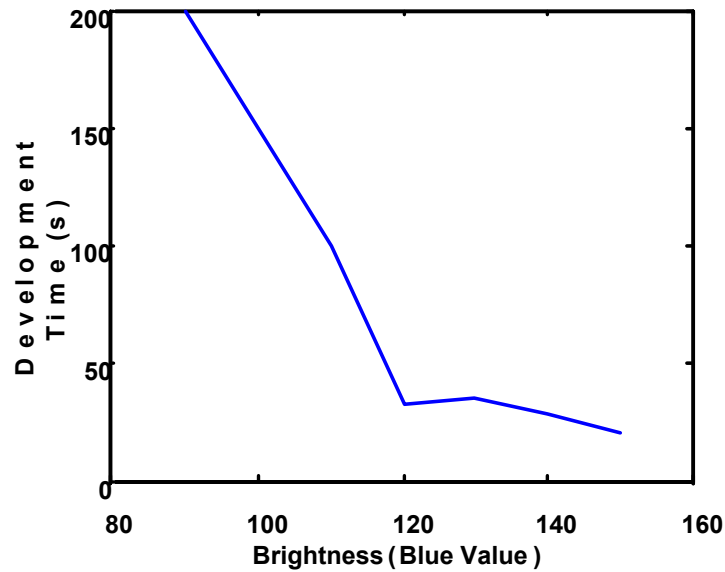


Figure 51. Development time as a function of brightness.
Thus intensity values in between 120 and 140 can be used for practical applications.

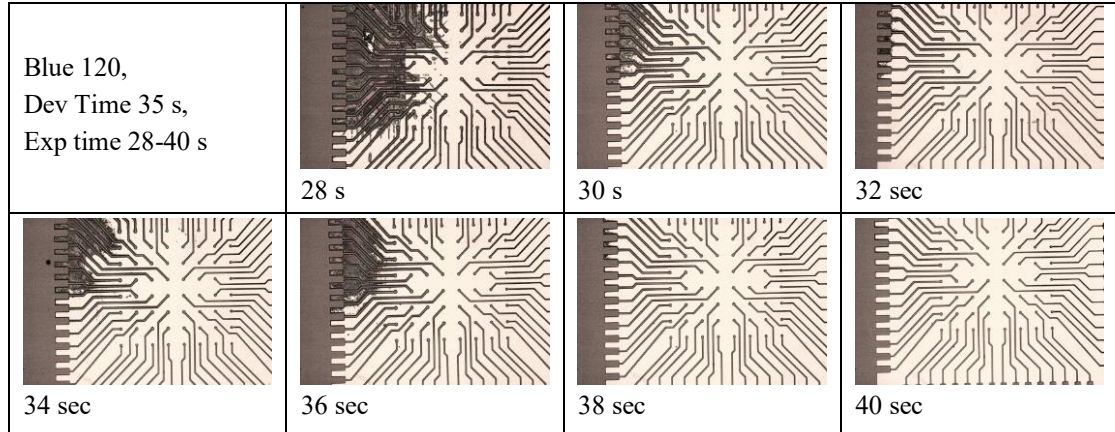
6.2.2. Exposure time and development time

The normal dose and exposure time of a photoresist is defined by considering the energy condition of UV and in the MED the blue part of visible spectrum is used. So, proper exposure time for a particular image was to be verified. The tests for exposure time for a particular image size are nothing but the determination of the suitable dose of exposure. From the optimum brightness experiments, it has evolved that intensity values 120 to 140 work well in providing smooth results. The basic objective of the exposure time optimisation test is, keeping the brightness and developing times constant, and applying different exposure times. The results are tabulated in the tables 12 and 13.

1st Test

In the first set of experiments the value of blue was set to be 120 and development time was set to be 35 seconds. Different exposure times ranging from 28 to 40 seconds were used. The results are tabulated in the table 12.

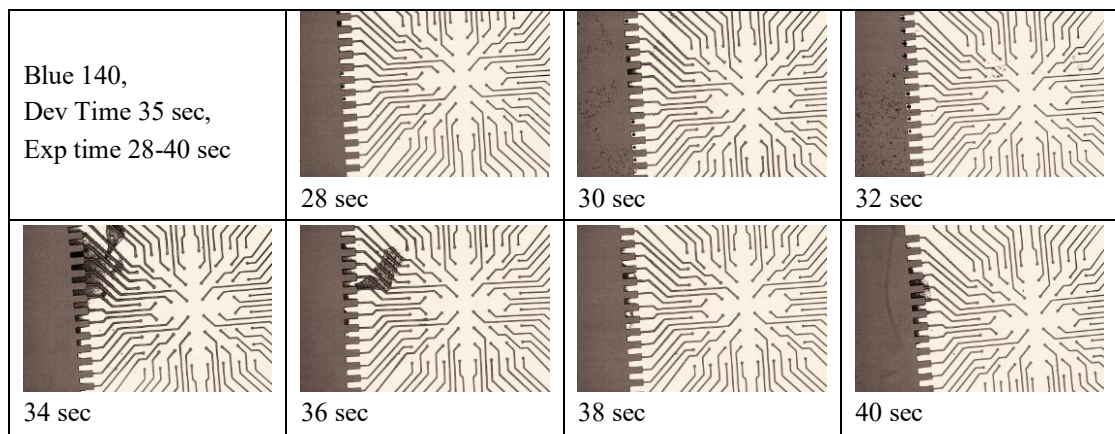
Table 12. First set of developed photoresist images from exposure time optimisation experiments. The development time (35 s) and blue value (120) were kept as constants. The value under each image shows the time of exposure for that sample. Seven exposure times from 28 to 40 seconds were used.



2nd Test.

In the second set of experiments the development time remained unchanged but the value of blue was changed to 140. Different exposure times ranging from 28 to 40 seconds were given. The results are tabulated in the table 13.

Table 13. Second set of developed photoresist images from exposure time optimisation experiments. The development time (35 s) and blue value (140) were kept as constants. The value under each image shows the time of exposure for that sample. Seven exposure times from 28 to 40 seconds were used.



Conclusion:

The above two testes showed that the time of exposure is an important factor in providing accurate results. The conclusive results from the above experiments are tabulated in the table 14.

Table 14. Optimised developing times for two intensities of blue.

Brightness	Exposure Time	Developing Time
120	38 to 40 sec	35 sec
140	28 to 30 sec	35 sec

The above data can be used in practical application of the MED. The test results of the proper intensity of blue and exposure time experiments can be utilised for interpreting proper development times for the MED.

6.2.3. Image size

The size of the image can be manually set to six different values using the image selector button in the Trinocular Microscope (TM). The last lens from the objective optics of the TM can be removed and then 6 other image areas are possible. Thus a total of 12 area combinations are possible and the details of these combinations are given in the table 15.



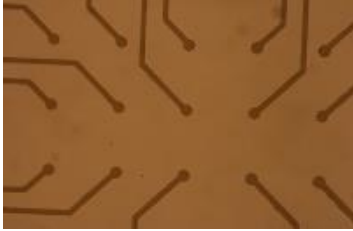


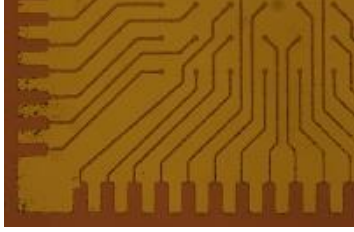

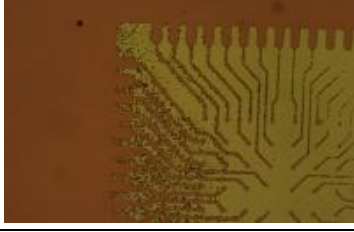
Table 15. List of all possible image areas that can be set by using the Trinocular Microscope.

	Area		Distance between objective and screen
	Mode (Image area selection, in the descending order)	Length, breadth & cm ²	
Without the last lens (0.3x lens) from the objective optics	1	1.5 cm x 1.1 cm, 1.65 cm ²	10.4 cm
	2	1.1 cm x 8.5 mm, 0.94 cm ²	10.9 cm
	3	5.99 mm x 4.5 mm, 0.2699 cm ²	11.15 cm
	4	4 mm x 3 mm, 0.12 cm ²	11.2 cm
	5	3.3 mm x 2.5 mm, 0.0825 cm ²	11.25 cm
	6	2.7 mm x 2 mm, 0.054 cm ²	11.3 cm
With full objective optics.	7	4.3 cm x 3.2 cm, 13.76 cm ²	between 20 & 50 cm
	8	3.5 cm x 2.6 cm, 9.1 cm ²	between 20 & 50 cm
	9	1.9 cm x 1.4 cm, 2.66 cm ²	between 20 & 50 cm
	10	1.3 cm x 1 cm, 1.33 cm ²	between 20 & 50 cm
	11	9.3 mm x 7 mm, 0.651 cm ²	between 20 & 50 cm
	12	8 mm x 6 mm, 0.48 cm ²	between 20 & 50 cm

All the above 12 image areas can be chosen by using the 0.3 x objective lens and adjusting the position of the screen with respect to the TM. The table 15 shows that the maximum area available is 4.3 cm x 3.2 cm. Areas beyond this can be obtained only by placing some additional optics immediately after the objective of the TM. Attempts were tried in this direction too and discovered that any good quality concave lens with an aperture greater than 3 to 3.5 cm can be used for obtaining bigger images on the screen.

To understand the quality of images developed at different image area configurations some tests were performed and the resultant images are given in the table 16.

Table 16. Photographs of results from experiments using different image areas. By keeping constant exposure time, development time and blue value, four different areas were tested. The photographs were taken after photoresist development.

	Experiments without using 3x objective lens Blue value = 120	
Image area 15 mm x 11 mm Exp = 300 sec Dev = 478 sec Line width = 57 μm		
Image area 11 mm x 8.5 mm Exp = 300 sec Dev = 254 sec Line width = 44 μm		
Image area 4 mm x 3 mm Exp = 300 sec Dev = 40 sec Line width = 16 μm		
Image area 3.3 mm x 2.5 mm Exp = 120 sec. Dev = more than one minute Line width = 13 μm		

On the basis of a number of experiments and developed images the suitable way of drawing a layout can be discussed by considering the diagram in the figure 52.

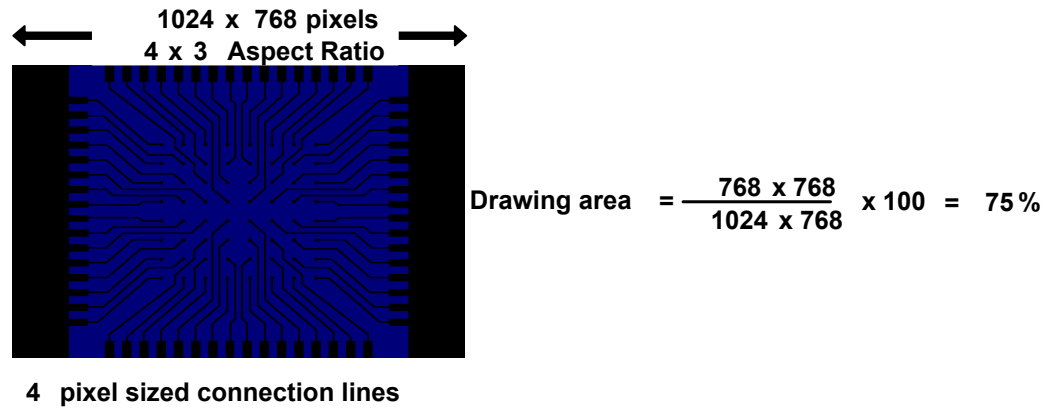


Figure 52. The drawing occupies 75 % of the total available drawing area. This drawing style can be used in MED layout drawings.

Thus, practical layouts on substrate surface can be created by choosing a comparatively big area of projection and drawing features accordingly on the software. Consideration of 75 % area of 1024 x 768 pixel area, and drawing of 4 pixel sized connecting lines will give good results in the first three areas presented in the table 15. The line width will be then in between 60 and 30 μm . On the basis of this example, by keeping the same area and intensity of exposure and adjusting the pixel line width, different features can be transformed onto the substrate surface as per the requirement. Therefore the desired line width can be prefixed roughly before the exposure itself.

6.2.4. Software program and image file saving formats

Simple commonly available programs like MS Paint, MS Visio, and Paint.Net etc. were tested for knowing which of them could be utilised for practical layout drawing applications effectively. The image saving formats like JPEG, GIF, BMP, PNG, TIFF, ICER, ILBM, PCX, PGF, TGA etc. are freely available in many graphical software packages and can be utilised and applied in tests. In some file saving formats like JPEG an image processing or an image compression is carried out and thereby a portion of the visual quality of the actual drawing is lost and cannot be restored. Hence a JPEG compression format is a 'lossy compression' and file formatting like PNG, TIF etc. are recommended over JPEG in the MED as they can store the image data in 'lossless' formats. In the MED the normal practice of projecting an image can be followed by the following 5 steps.

- a) Draw the layout in a suitable software like MS Visio and save the same in a suitable 'lossless' format.

- b) Set the computer monitor resolution to 1024 x 768 pixels which is comparable to the resolution of the DLP projector used in the MED. This can be done via Start → Control panel → Appearance and themes → Display → Settings → Screen Resolution.
- c) Open the image with 'Windows Picture and Fax Viewer' and press 'Set as Desktop Background' icon from the right mouse click on the image. Now the image will be displayed on the screen perfectly without any edge or side modifications.

Experiments using differently formatted and saved layouts showed clearly that the exposures using JPEG images were not very suitable in producing good results with sharp edge features but those with PNG and BMP formats were really suitable in producing fine results with sharp edges feature characteristics.

6.2.5. Resolution of the device

According to Rayleigh's law the resolution R or the minimum possible line width W_{\min} is

$$R = W_{\min} \approx k \frac{\lambda}{NA} \quad (10)$$

where k will be a process related constant with a numerical value ≥ 0.5 , $NA = n \sin \alpha$ is the numerical aperture of the optics. In the MED, $\alpha \approx 50^\circ$, $n = 1$, $\lambda = 450-495$ nm (blue) and $k \approx 10 - 11$, hence the resolution according to Rayleigh's law is approximately 10 μm .

Many experiments were performed to obtain the line widths as thin as possible. Two results, one using a gold substrate and another using a Si substrate are given here.

1st Test: Gold substrate.

The images from a developed gold substrate are shown in the figures 53 and 54 and its profile analysis is shown in the figures 55 and 56.

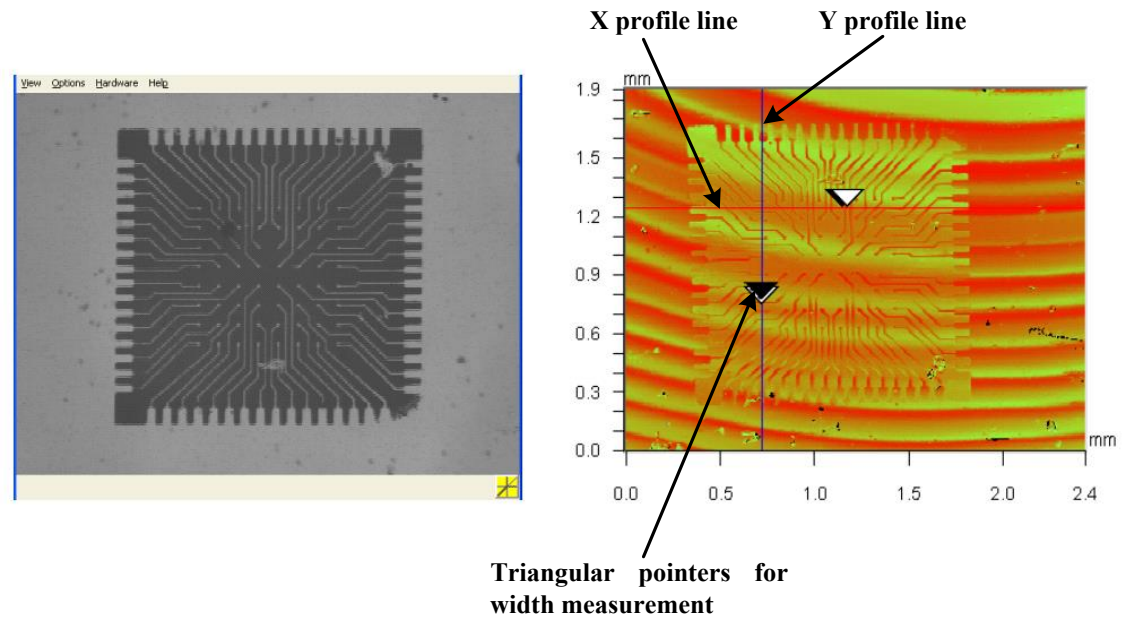


Figure 53. Left image: Photograph of an etched gold microelectrode array. Right image: Profile analysis of the microelectrode array.

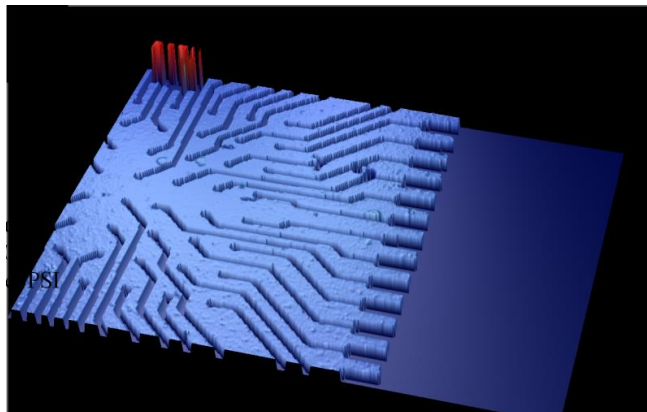


Figure 54. 3D view of a portion of the layout on gold substrate.

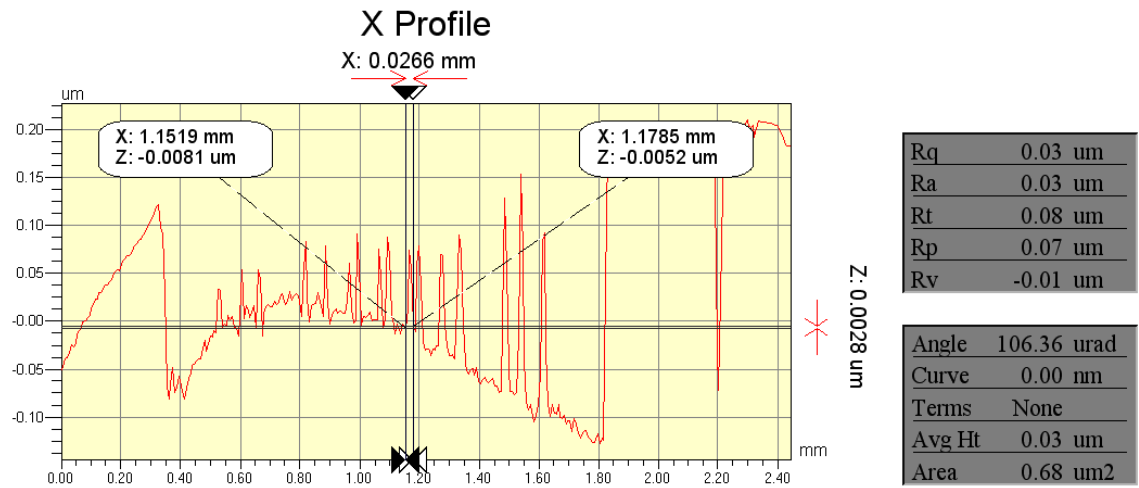


Figure 55. X profile analysis on gold substrate. The width of the line is about 27 μm .

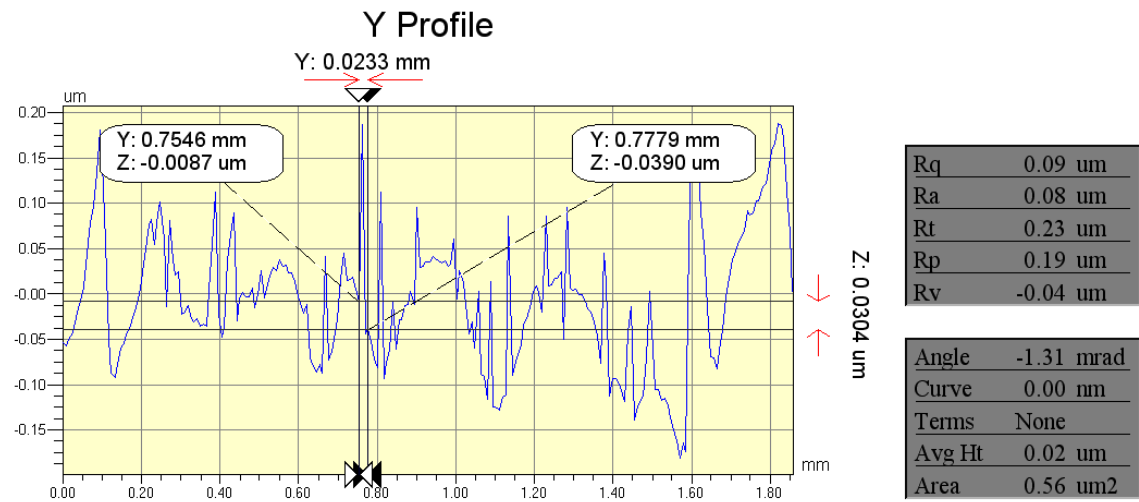


Figure 56. Y profile analysis on gold substrate. The width of the line is about 23 μm .

2nd Test: Silicon substrate.

The images of the microelectrode array formed as grooves in developed photoresist on silicon substrate are shown in the figures 57 and 58. The surface profile measurements 1) for line widths are shown in the figures 59 and 60 and 2) for diameter of circles are shown in the figures 61 and 62.

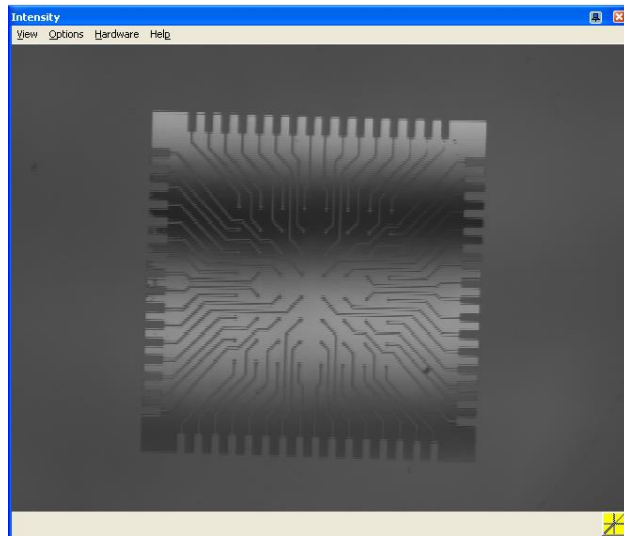


Figure 57. Photograph of the microelectrode array formed as grooves in developed photoresist on silicon.

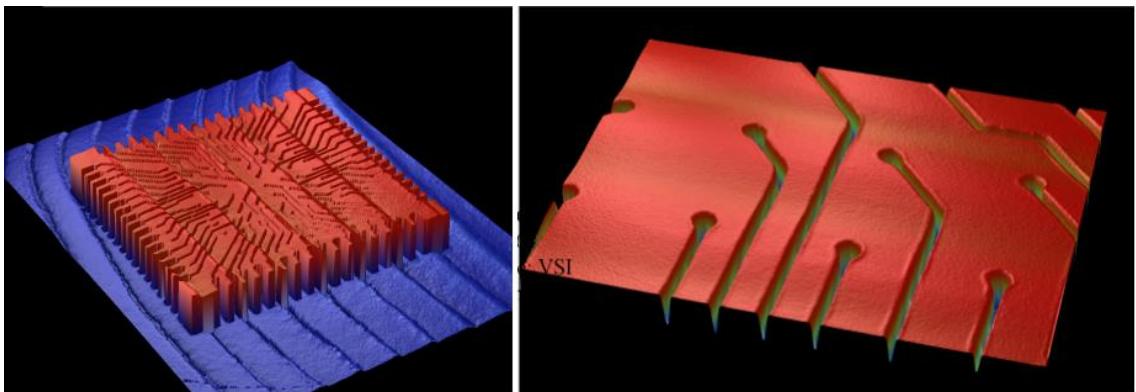


Figure 58. 3D views of the microelectrode array grooves on silicon and a magnified portion of the wiring grooves.

The surface profile measurements of microelectrode configuration formed by the patterning of photoresist development were carried out, first for measuring the width of wiring lines and then, for the diameter of circular electrodes. The results are presented in the figures 59 to 62.

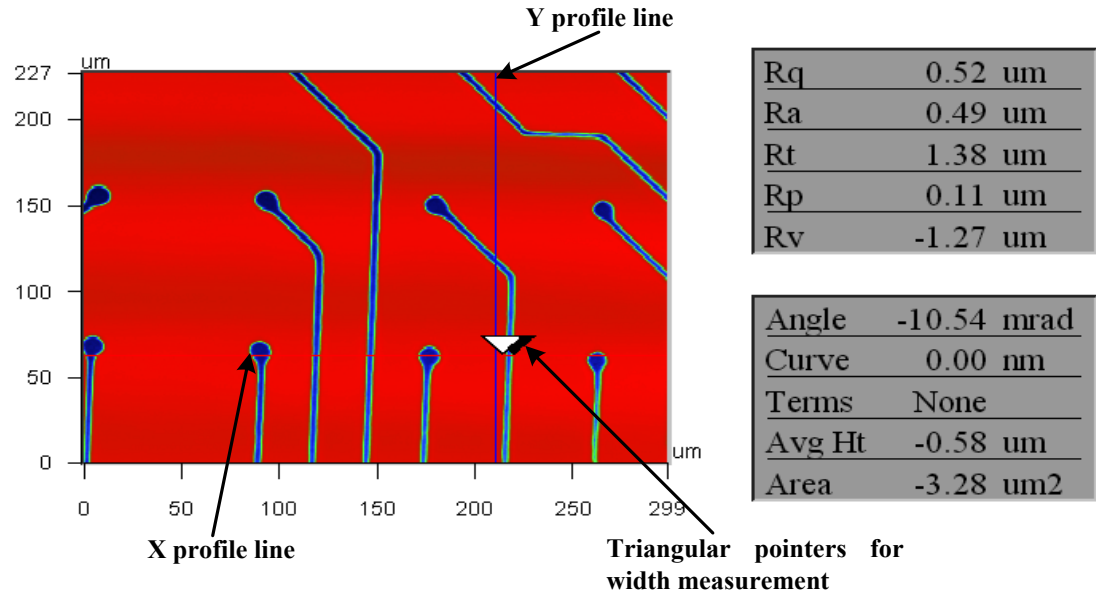


Figure 59. First topographic x profile analysis for measuring the width of microelectrode wirings (grooves in the developed photoresist). The measurement graph is given in the figure 60.

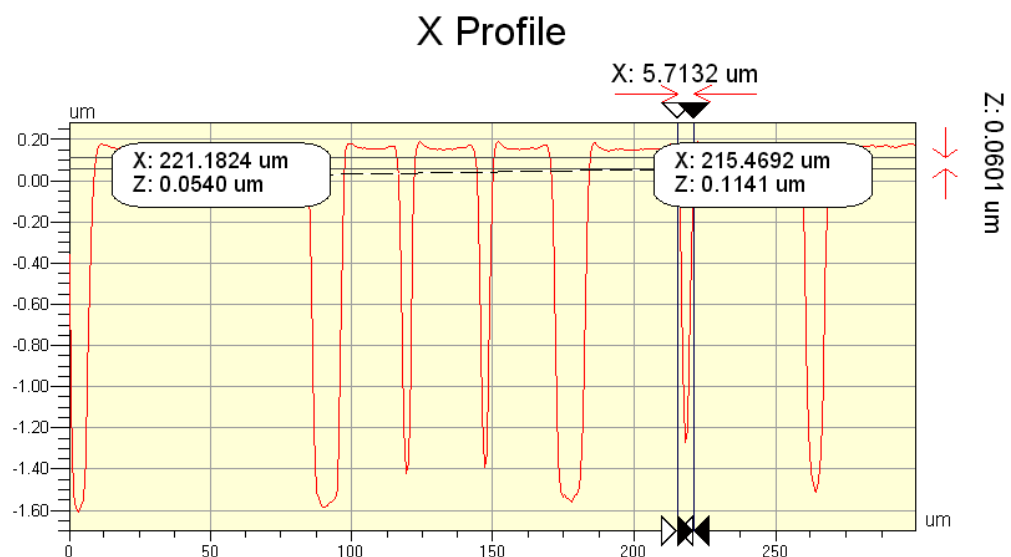


Figure 60. X profile analysis shows that the width of the wiring line (groove in the developed photoresist) is about 6 μm .

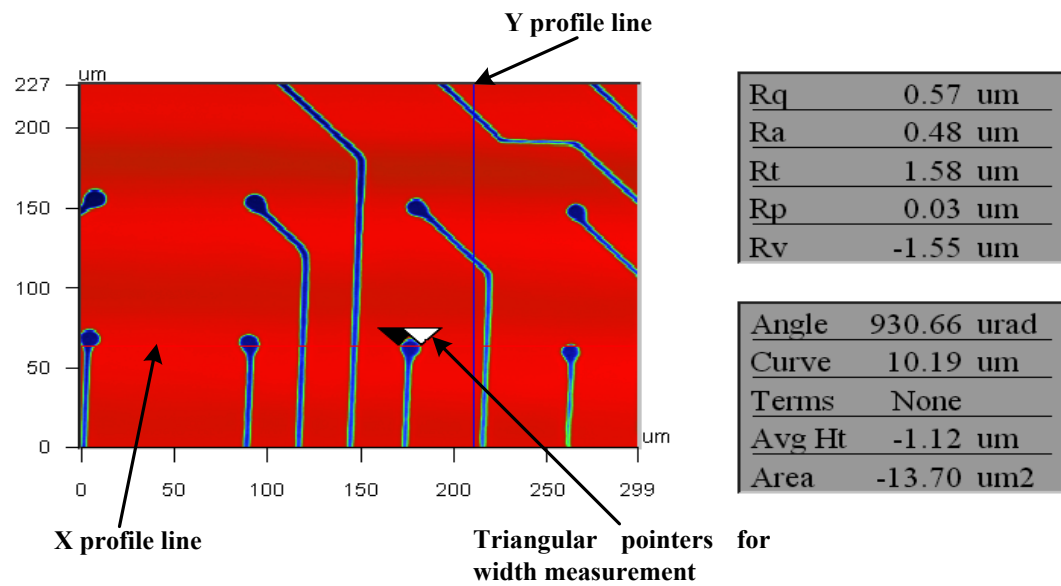


Figure 61. Second topographic x profile analysis for measuring the diameter of microelectrode circles (grooves in the developed photoresist). The measurement graph is given in the figure 62.

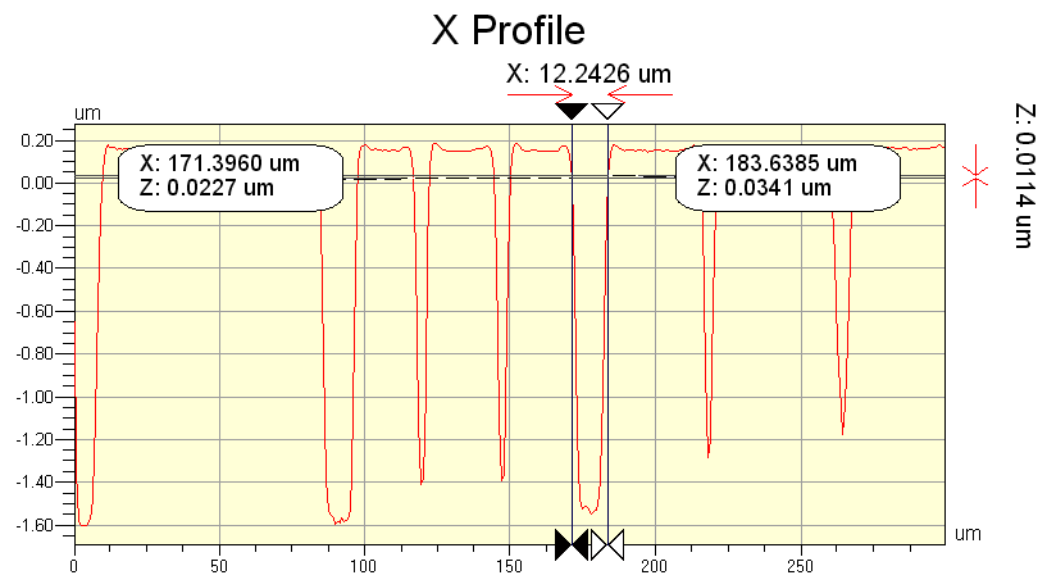


Figure 62. X profile analysis shows that the diameter of the microelectrode circles (grooves in the developed photoresist) is about 12 μm .

The resolution is approximately 6 μm and this was the smallest one ever obtained by the MED and the value is not far from the approximated 10 μm resolution. The samples after photoresist development were observed first through the inspection microscope and then good samples were verified again by profile analysis. It would have been possible to have etched all the good samples, but the etching was done only for a few samples.

7. EXPERIMENTS FOR FABRICATION OF A MATRIX ARRAY OF ELECTRODES ON GOLD COATED GLASS PLATE

In certain times, the MED has to confront with extreme line width varying layouts. The areas in a layout with thicker lines and features can be transformed to the substrate even at high intensity exposures but the same intensity may not be good enough for extremely thin lines and features. So a layout containing lines or features with varying thicknesses should be transferred in multiple exposures.

7.1. Multiple intensity exposure

A heterogeneous layout should be handled properly during the experiments. So by successive exposures using different areas of the image at different intensities, this can be solved. An example of such an exposure is explained below. The feature to be transformed is shown in the figure 63.

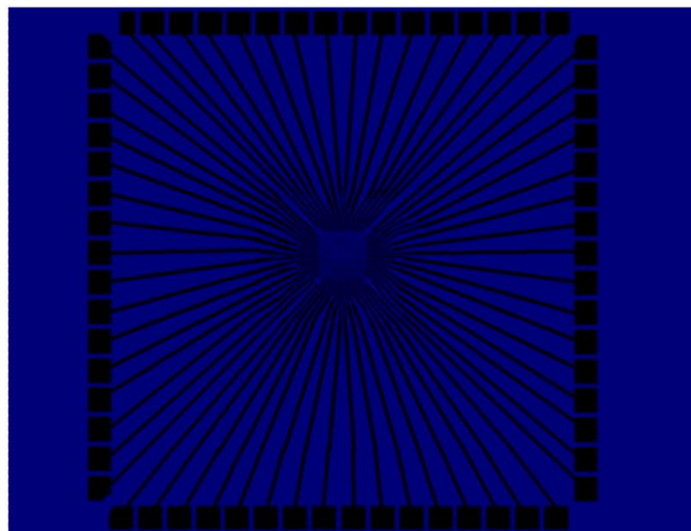
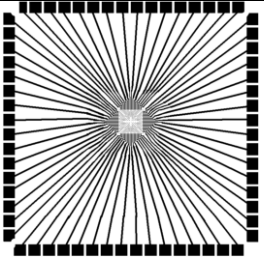
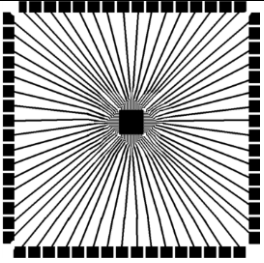
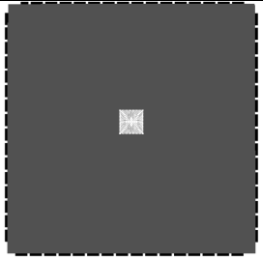
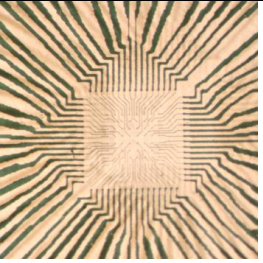


Figure 63. The layout used for multiple intensity exposure and fabrication of a matrix array of electrodes. More explanation is given in the figure 64.

The layout consists of electrode wiring lines of different widths. The width of electrode lines in the inner region is less than that at the outer region. Therefore if equal intensity is given to the entire layout, that may give good results for thicker lines but a worse result for thinner lines. The intensity optimised for the thicker lines may be a destroying one for the thinner lines. Therefore the value of the intensity has to be reduced at the central region, and this can be carried out in 3 steps as follows. The image parts have to be separated in the computer as shown in the table 17 for the simplicity of the procedure. This means that two to three successive images are saved with continuous numbers eg. 1Matrix.bmp, 2Matrix.bmp, 3Matrix.bmp etc.

Table 17. Successive image saving and exposure in multiple intensity exposure. Drawing1: Actual layout to be imprinted. 1Matrix.bmp: Image saved from the previous one by darkening the central region. 2Matrix.bmp: Image saved from the actual image by darkening all regions except the central region. Result: Photograph of the result from gold plated glass plate. The explanation of the result can be seen in the figure 65.

			
<p>Drawing 1</p> <p>The layout consists of The layout consists of electrode wiring lines of different widths.</p>	<p>1Matrix.bmp</p> <p>The central area is blackened totally. This image is set as the desktop background and the exposure is performed. The exposure creates only the outer thicker lines.</p>	<p>2Matrix.bmp</p> <p>Here the outer region which is already exposed is blackened. Now select and set this image as desktop background. The inner area only is exposed in this stage at an intensity around half of that applied for the outer lines.</p>	<p>Result</p> <p>Photograph of the produced microelectrode configuration. More explanation of the result is given in the figure 65.</p>

These types of configurations require some effort in producing good results. Generally what is recommended is performing a trial exposure experiment and then recording the relevant data. Then depending on the quality of the developed image adjust the intensity and exposure time a little bit backward or forward and perform the same experiment to

get maximum satisfactory results. A general assumption that can be considered here is that, a relatively non uniform feature can be transformed to a substrate surface in less than an hour duration whatever be the complexities appearing on the drawing.

7.2. Matrix array of electrodes

Matrix type electrode configurations have an important functional role in many types of biological and industrial sensors and transducers. For instance, a matrix type electrode array is being used for sensing eukaryotic tissue and cell characteristics and the sensed data can be used in many biological, medical and physiological applications. The normal techniques of producing those types of matrix arrays are quite expensive unless a mass production is possible. In industrial applications, normally a large number of matrix configurations are produced using a single expensive photomask. However in the research and development (R&D) applications in laboratories of educational institutions, buying a highly expensive mask for a single test may be really problematic due to technical and financial aspects. Moreover, in R&D different test experiments are carried out with different microelectrode configurations and many of those may be worthless and finally only a single configuration may be successful and selected. Therefore buying different types of photomasks for different test experiments makes the situation more complicated as those are expensive and also there is a considerable time lag between the ordering of a mask and collecting it after its production from a company. This situation, at least in many cases, can be handled by the MED as it does not require any photomask. Any electrode structure can be drawn on a computer screen and that can be cost effectively transferred to the wafer and test experiments can be carried out. The procedure can be repeated again and again with different layouts and finally a most suitable successful configuration can be selected. Therefore the MED directly reduces the photomask production time and money required for that in many test situations at least.

In order to understand the use of MED in creating a microelectrode configuration, some tests were performed in that direction. A microelectrode configuration as in the figure 64 was drawn on the computer using Microsoft Visio software and used in two test exposures.

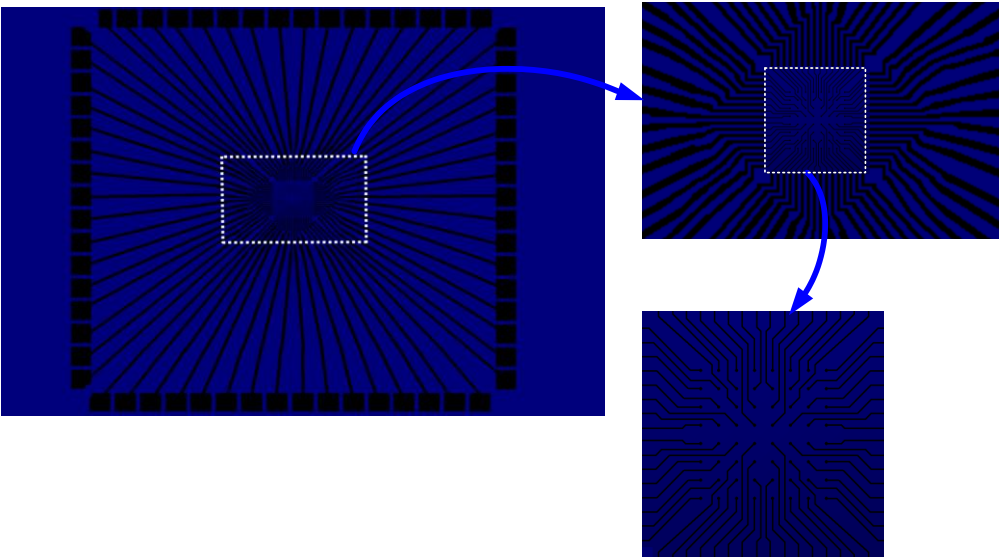


Figure 64. The layout used for the fabrication of matrix array consisting of 256 (16 x16) electrodes. The left image shows the entire layout, the right top image shows the magnified portion of the central region, and the right bottom image shows the microelectrode configuration at the centre of the entire layout.

Two different areas of exposures were chosen and the processing parameters used in the multiple intensity exposures are listed in the table 18.

Table 18. Maskless Exposure Device and photolithographic processing parameters for the multiple intensity exposure in fabrication of microelectrode array.

Parameters (Dark field image, 16 x 16 matrix)	Smaller Image (Inner region)	Bigger image (Outer region)
Exposure intensity	100	255
Area used on substrate	14 mm ²	2.8 cm ² – 14 mm ² = 2.66 cm ²
Substrate type	Gold coated glass.	
Photoresist	ma-p 1225	
Exposure time	50 s	35 min
Etching agents	Standard Gold Etching chemicals	
Thickness of the inner lines obtained	8.9 μm.	

The images in the figure 65 show the produced microelectrode array after photoresist development and gold etching. Two images were photographed directly and one was photographed through inspection microscope.

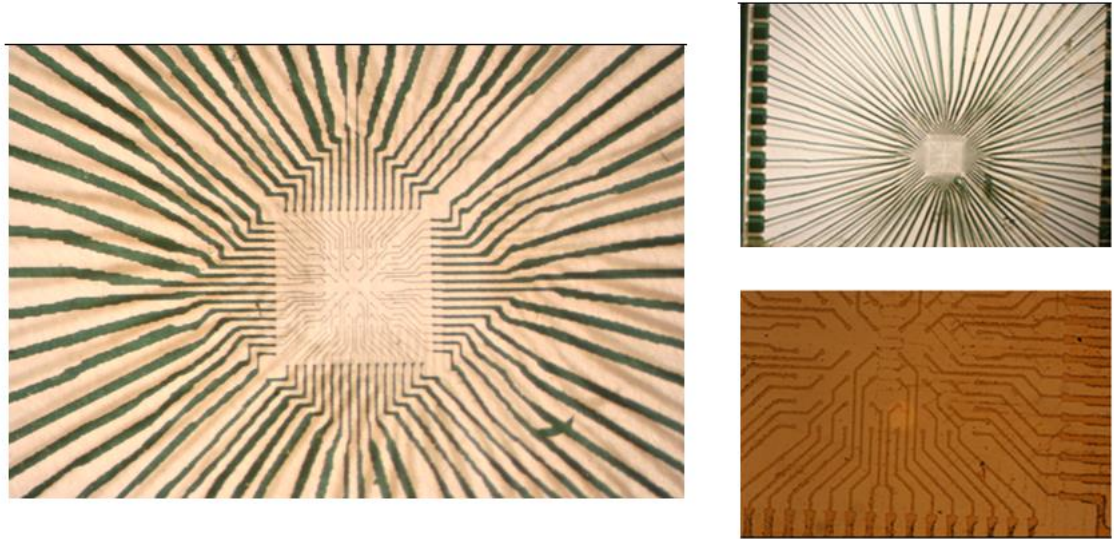


Figure 65. Images of an electrode array fabricated on a gold plated (46 nm) glass substrate after gold etching. After photoresist patterning the gold layer on glass plate was fully etched. Left image: Magnified direct photograph of the 256 (16x16) electrodes array. Right top: Normal photograph of the same sample. Right bottom: Inspection microscope photograph of the contact points between the inner electrode configuration and outer wiring lines.

The above microelectrode configuration was more scientifically verified by using the Profilometer and the profile study details are given in the figures 66 to 68.

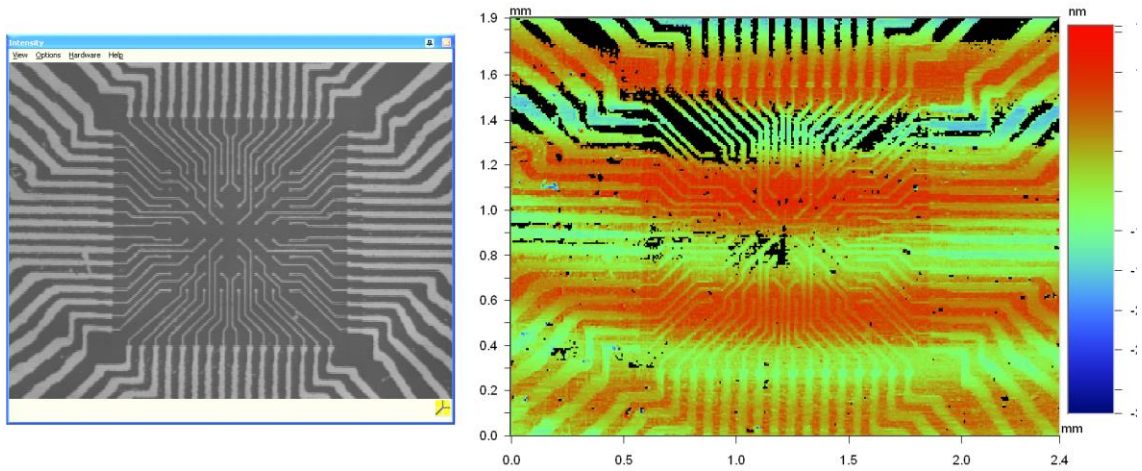


Figure 66. Profilometer photographs of the gold microelectrode array on glass substrate. Left image: The 256 (16x16) electrode array image from profilometer. Right image: Photograph of the surface profile of the same sample from the profilometer.

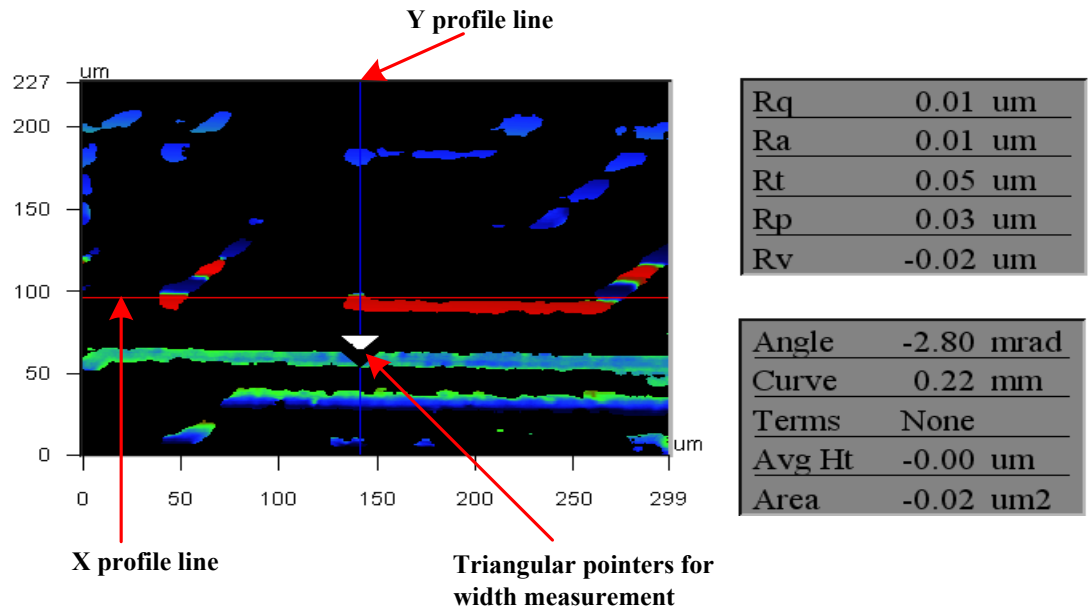


Figure 67. Topographic surface profile measurements on microelectrode array. The feature area considered was 299 μm x 227 μm. The profile measurement photograph is given in the figure 68.

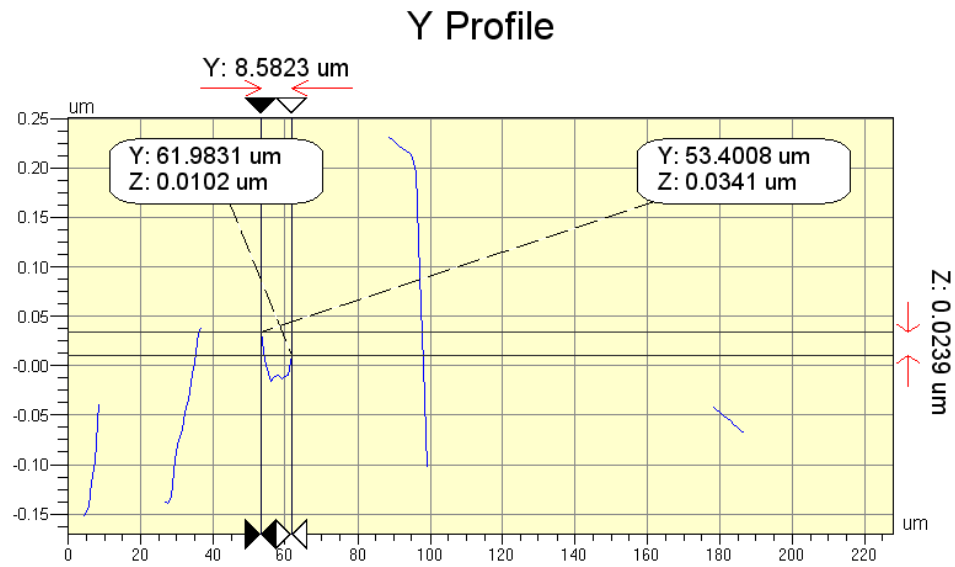


Figure 68. Y profile analysis on the microelectrode array. The width of the electrode at the centre of the configuration is measured to be about 9 μm .

The profilometer measured the width of the inner lines as less than 9 μm . Thus all the experiments clearly proved that the MED can give features with line widths upto 7 μm and hence the device can be used in many practical laboratory applications effectively. Even though the device's final resolution features are not meant for industrial competitiveness, highly user controlled photolithographic tests shall be performed very cost-effectively within a short span of time. Therefore the MED is a good tool in micro fabrication and some problematic boundaries of microtechnology can be met or altered in many engineering situations.

8. CONCLUSION AND DISCUSSION

Microscaled devices and their applications are increasing day by day. Uses of microstructures are also prominent in different research fields all over the world. Most of the microscaled products are fabricated in cleanrooms by making use of techniques of photolithography. It's an expensive, time consuming step by step procedure. The pattern which is planned to be imprinted onto a substrate must be first obtained on a photomask and this photomask is then used in the photolithographic procedure. The photomasks are normally prepared by different companies within a few weeks after the submission of suitable layouts. Together with the expense and time required in photomask production, the photomask designed for one microstructure might not be suitable for another one. This increases the complexity of the situation and reduces the speed of research and other activities which have been planned by the use of those microstructures. The objective of this thesis was to develop a cost effective, fast prototyping machine that could work without using photomasks, and the result is this 'Maskless Exposure Device' (MED). The MED consists of a laptop computer, a DLP projector, a stereomicroscope, a special screen and mechanical supports [39][40][41].

The laptop of MED works as a software mask where different features and layouts can be drawn. Availability of good drawing softwares' brings extreme flexibility in the preparation of software masks. A mask drawn and saved on a proper format is displayed as an image using a projector. When the activities using one software mask are over, it can be either modified or replaced by another drawing, and thus it becomes the new software mask. Hence the MED's software masks, replaces the hardware photomasks. The DLP projector in the MED is used after the removal of the optics installed by the company. The projection lens system and filters of the DLP projector are totally removed and the developed free space is occupied by the camera port of the stereomicroscope. The resolution of the projector is an important factor, as high resolution projectors convey more information usually. The digital micromirror device (DMD) chip reflects light with image information, and these rays are directed to the stereomicroscope. Possibility of adjusting different projection parameters of the projector brings quality and more flexibility in image projection. The stereomicroscope has two roles in the MED; to work as the optics for the projector to produce diminished images on the screen and to allow the operator to ensure the sharpness of the image formed on the screen. The microscope has been installed in a way to coordinate these two functions equally well. The light coming out of the stereomicroscope creates a diminished image on the screen. The leaning screen has many adjustment screws by

which its position and tilting can be adjusted so that a sharp image on the screen can be ensured. The position of the screen can be adjusted back and forth on a rail and this enables the focusing. The substrate coated with photoresist is fixed on the screen by using small magnets and it offers temporary fixing until the completion of one exposure. Substrates of different thicknesses can be fixed on the screen using the magnets. All the component devices of MED are arranged on an aluminium platform.

Preliminary exposure experiments were carried out by applying the photoresist SU-8 on a silicon substrate and two layouts were tested. A 12 electrode configuration with big circles was imprinted to a 9.5 mm x 5.8 mm area on the silicon. The processes which followed produced electrode lines with 40 μm width and circles with 250 μm diameter. In the second layout horizontal, vertical and diagonal lines and English letters were included and it provided a resolution down to 10 μm . In order to examine the possibilities of positive and negative photomasks, bright field and dark field layouts were used in exposures. Even though there were variations in the quality of patterns produced, both bright and dark field exposures were carried out by the MED. All the developed patterns were verified by the inspection microscope in the cleanroom of the Department of Automation Science and Engineering and a few samples were taken for the topographic analysis by the profilometer. The x-y profile analysis confirmed the results once again.

The minute thickness variations caused by the unequal distribution of intensity due to various misalignments were corrected by software methods. The exposures, after the software correction imparted extremely nice results. The competitiveness of developed images in etching solution was also tested immediately after certain exposures. The random trial and error experiments proved that MED with blue light could definitely work as a software mask instead of hard photomasks. Positive tone photoresist ma-P 1225 was also used, and the optimal exposure time, developing time and the most suitable intensity of blue were finalised on making use of ma-P 1225. The intensity of blue, set in computer to values in between 120 and 140 (In graphic softwares', intensity is quantified in 0-255 range) along with half a minute exposure time can provide sharp patterns. The size of the image on the substrate surface can be adjusted from a higher area to 6 different values, and in each case the pixel size is automatically reduced to smaller values.

All the instructions for the proper operation of the MED are also presented here. The detailed step by step instructions allow the user to operate the device without too many complications. In many practical microscaled situations, multiple intensity exposures may also be required. To analyse the possibilities of multiple intensity exposure, a microelectrode array (MEA) containing 256 (16 x 16) electrodes was also tested. The MEA layout was split into two parts as one central small part containing thinner lines and another big surrounding part containing thicker lines. The thinner lines were

imprinted with blue light with less intensity while the thicker lines were imprinted with the same blue light but with higher intensity. Logically this can be concluded as, the reduction of image area on the substrate surface increases the quantity of light available on that area and therefore to compensate this increased light, the intensity of the light is set to smaller values.

Initially the MED is exclusively planned to be used in a project named Stemfunc for stemcell research financed by the Academy of Finland. However the device can be used in research and development applications in MEMS production, microfluidic systems, semiconductor and biosensor designs, patterning of cell culture substrates, electrode structures etc. Research on design of microsensors and microactuators could be confronted extremely cost effectively with maximum time saving considerations.

9. REFERENCE

- [1] Semiconductor fabrication: Photolithography.[www]
[Date 22.1.2008]. Available at :
<http://britneyspears.ac/physics/fabrication/photolithography.htm>

- [2] Microfabrication R. B. Darling / EE-527.[www]
[Date 22.1.2008]. Available at :
<http://www.ee.washington.edu/research/microtech/cam/PROCESSES/PDF%20FILES/Photolithography.pdf>

- [3] Photolithography, Using light to cut wafers by Bill Wilson
[Date 22.1.2008]. Available at :
<http://cnx.org/content/m1037/latest/>

- [4] Jong Rak Park, Hyun Su Kim, Jin-Tae Kim, Moon-Gyu Sung, Won-Il Cho, Ji Hyun Choi, and Sung-Woon Choi, Laser Process Proximity Correction for Improvement of Critical Dimension Linearity on a Photomask , ETRI Journal, April 2005, pp 188-194

- [5] Hank Hogan, Maskless Photolithography May Offer Cost Advantage, Technology World , December 2005, photonics

- [6] T. Walt, Directions in Maskless Lithography, Futurefab International, June 2005, pp 74-76, Issue 19

- [7] Menon, R., Patel, A., Dario Gil and Henry I. Smith, Maskless lithography. Materialstoday, February 2005, pp 26-33

- [8] P. Kruit, The role of MEMS in maskless lithography, Microelectronic Engineering, February 2007. pp 1027–1032.

- [9] Su E. Chung, Wook Park, Hyunsung Park, Kyoungsik Yu, Namkyoo Park, and Sunghoon Kwon, Optofluidic Maskless Lithography System, Transducers and Eurosensors 07-IEEE, pp 1569-1572.

- [10] C. Sun, N. Fang, D.M. Wu, X. Zhang, Projection micro-stereolithography using digital micro-mirror dynamic mask, *Sensors and Actuators*, March 2005 pp 113–120
- [11] D. Fries, G. Steimle, S. Natarajan, S. Ivanov, H. Broadbent, T. Weller, Maskless Lithographic PCB/Laminate MEMS for a Salinity Sensing System, *Intelligent MP [www]* [Date 22.1.2008]. Available at : <http://www.intelligentmp.com/Downloads/Technical%20Papers/PCBMEMS.pdf>
- [12] F. Carolyn, F. David, B. Heather, S. George, K. Eric, S. Jay
Direct Write Patterning of Microchannels, First International Conference on Microchannels and Minichannels April 2003
- [13] Jia-Chang Wang , Ming-Zhe Hsieh, Applying the one-column, many pencil local scanning maskless lithography technology to micro-RP system, *Int. Journal on Advanced Manufacturing Technologies*, April 2008.
- [14] J.kochl, E.Fadeeva, M. Engelbrecht, C. Ruffert, H.H.Ggatzten, A. Ostendorf, B.N. Chichkov. Maskless nonlinear lithography with femtosecond laser pulses, *Materials Science & Processing*, 2006 pp 23–26
- [15] Itoga, K. Kobayashi, J. Tsuda, Y. Yamato, M. Kikuchi, A. Okano, T.
Development of the Maskless Exposure Device equipped with a LCD-Projector for Fabrication of Micropatterned Surfaces and Microfluidic Channels
IEEE, Nov. 2007, pp 169-172
- [16] J. David Musgraves, Brett T. Close, and David M. Tanenbaum, A maskless photolithographic prototyping system using a low-cost consumer projector and a microscope, *American Journal of Physics*, October 2005. pp 980 – 990.
- [17] Fundamentals of microfabrication by Marc Madou, Book, Published: Boca Raton (FL) : CRC Press , 1997
- [18] Photomask [www]
[Date 7.1.2008]. Available at : <http://en.wikipedia.org/wiki/Photomask>
- [19] Photomask Costs [www]
[Date 7.1.2008]. Available at : http://www.future-fab.com/documents.asp?grID=213&d_ID=2617

- [20] Technical Information on commercial mask production and cost [www]
 [Date 7.1.2008]. Available at :
http://www.euva.or.jp/technical_info/technical_list.html#1
- [21] Formula for Mask cost calculation [www]
 [Date 7.1.2008]. Available at :
http://www.euva.or.jp/images/technical_info/pdf/MaskCost_d.pdf
- [22] Mask costs for various lithography methods [www]
 [Date 7.1.2008]. Available at :
http://www.euva.or.jp/images/technical_info/pdf/MaskCost_x02.pdf
- [23] Hyoung-Hee Kim, Ji-Yong Yoo, Seung -Wook Park, Young-Keun Kwon, Ilsin An, Hye-Keun Oh, A Practical Method of Extracting the Photoresist Exposure Parameters by Using a Dose-to-Clear Swing Curve, Journal of Korean Physics Society, February 2003, pp 280-284.
- [24] Modeling of conventional resists
 [Date 15.2.2008]. Available at :
<http://www.iue.tuwien.ac.at/phd/kirchauer/node69.html>
- [25] Fundamentals of microfabrication by Marc Madou, Book, Published: Boca Raton (FL) : CRC Press , 1997
- [26] Wet etching [www]
 [Date 7.1.2008]. Available at :
<http://www.memsnet.org/mems/processes/etch.html>
- [27] Lectures on Microsensors by Dr.Jukka Lekkala [www]
 [Date 7.1.2008]. Available at :
<http://www.mit.tut.fi/MIT-4030/Lecture%20material/6.%20Etching.pdf>
- [28] Introduction to Microfabrication by Sami Franssila. Publisher: Wiley; 1 edition (May 13 2004)
- [29] Digital Micromirror Devices
 [Date 24.5.2008]. Available at :
http://www.bccrc.ca/ci/qm01_microtomography.html

- [30] Digital Light Processing, Texas Instruments. [www]
[Date 14.5.2008]. Available at :
http://www.dlp.com/includes/demo_flash.aspx
- [31] Mediachance, DVD Lab [www]
[Date 14.5.2008]. Available at :
<http://www.mediachance.com/dvdlab/cinema/index2.html>
- [32] Operation Manual of microscope SMZ-168-BL-TL [www]
[Date 7.1.2008]. Available at :
<http://www.m-r-c.co.il/data/assets/OPERATION%20MANUAL/SMZ168-BL-TL.pdf>
- [33] SMZ-168 SERIES ADVANCED ZOOM STEREO MICROSCOPES [www]
[Date 7.1.2008]. Available at :
http://www.lukasmicroscope.com/Motic_Microscopes/SMZ-168_Stereo/smz-168_stereo.html
- [34] Microscope Ray Diagram [www]
[Date 7.1.2008]. Available at :
<http://www.freepatentsonline.com/6985287-0-large.jpg>
- [35] Microscopy [www]
[Date 7.1.2008]. Available at :
<http://www.microscopy-uk.org.uk/mag/indexmag.html?http://www.microscopy-uk.org.uk/mag/artfeb04/pjcollim.html>
- [36] [tyu] Material safety Data Sheet, SU-8 2000 Series Resists
[Date 7.1.2008]. Available at :
\\Mit\\intra\\Download\\Puhdastila\\Kayttoturvallisuustiedotteet,
File name : SU-8 2000 SERIES RESISTS 2.DOC.
- [37] Lectures on Lithography and Pattern Transfer by Dr. Alan Doolittle in Georgia Tech. [www] [Date 7.1.2008]. Available at :
<http://users.ece.gatech.edu/~alan/ECE6450/Lectures/ECE6450L7-Optical%20Lithography.pdf>
- [38] Brochure on Photoresist ma-P_1200 processing guidelines. [www]
[Date 7.1.2008]. Available at :
\\Mit\\intra\\Download\\Puhdastila\\Kayttoohjeet,
File name : ma-P_1200_processing_guidelines.pdf

- [39] A maskless exposure device for rapid photolithographic prototyping of sensor and microstructure layouts, D. Kattipparambil Rajan, J. Leikkala, Procedia Engineering, Volume 5, 2010, Pages 331-334, ISSN 1877-7058, <https://doi.org/10.1016/j.proeng.2010.09.115>.
- [40] Novel method for intensity correction using a simple maskless lithography device, D. Kattipparambil Rajan, J.-P. Raunio, M. T. Karjalainen, T. Ryyänen, and J. Leikkala, Sensors and Actuators A: Physical, Volume 194, 2013, Pages 40-46, ISSN 0924-4247, <https://doi.org/10.1016/j.sna.2013.01.024>.
- [41] T. Ryyänen, D. Kattipparambil Rajan, Jukka Leikkala, Concept for Low-cost Rapid Prototyping of New MEA Designs, Proceedings of the 2009 Symposium on Microelectrode Arrays in Tissue Engineering, p 26–28 <https://doi.org/10.6084/m9.figshare.12613850>